SELF-CONSOLIDATING CONCRETE CONSTRUCTION FOR MODULAR UNITS

DE-NE0000667 NEET

Final REPORT

(1 February 14 through 30 April 2016)

Prepared by:

Dr. Russell Gentry (PI) russell.gentry@coa.gatech.edu
Dr. Lawrence Kahn (Co-PI) lawrence.kahn@ce.gatech.edu
Dr. Kimberly E. Kurtis (Co-PI) kimberly.kurtis@ce.gatech.edu
Dr. Bojan Petrovic (Co-PI) Bojan.petrovic@gatech.edu
Dr. Giovanni Loreto (Researcher) giovanni.loreto@ce.gatech.edu

School of Civil and Environmental Engineering
Georgia Institute of Technology
790 Atlantic Drive, Atlanta, GA 30332

Jurie van Wyk vanwykjj@westinghouse.com
Carlos Cantarero-Leal

Westinghouse Electric Company LLC,
1000 Westinghouse Drive
Cranberry Township, PA 16066

29 July 2016

(This page intentionally left black)

Disclaimer

Authors' Disclaimer: This report was prepared as an account of work sponsored by an agency of the United States Government. Neither the United States Government nor any agency thereof, nor any of their employees, makes any warranty, express or implied, or assumes any legal liability or responsibility for the accuracy, completeness, or usefulness of any information, apparatus, product, or process disclosed, or represents that its use would not infringe privately owned rights. Reference herein to any specific commercial product, process, or service by trade name, trademark, manufacturer, or otherwise does not necessarily constitute or imply its endorsement, recommendation, or favoring by the United States Government or any agency thereof. The views and opinions of authors expressed herein do not necessarily state or reflect those of the United States Government or any agency thereof.

Acknowledgments

Table of Contents

List of Figures

List of Tables

(This page intentionally left black)

1 Executive Summary

Two needs were identified in the Department of Energy Nuclear Energy Enabling Technologies (DOE-NEET) program: (1) Assembly and material innovation to enhance modular building techniques such as advances in high strength concrete and rebar, inspection equipment, and pre-assembled rebar systems; and (2) Advances in modular construction to include improved design codes, improved methods for transport and delivery and advancements in integrated prefabrication.

This report focuses on work completed on DE-NE0000667, Self-Consolidating Concrete for Modular Units. This project was undertaken in the School of Civil and Environmental Engineering at the Georgia Institute of Technology, with Westinghouse Corporation as the industrial partner from February 1, 2014 through April 30, 2016. The primary objective of this project was to develop self-consolidating concrete (also termed "self-compacting concrete" or SCC) mixtures so that concrete placement can be made into steel plate composite (SC) modular structures without the need for continuous concrete placement. As part of the research, SCC mixtures were developed and validated to ensure sufficient shear capacity across cold-joints, while minimizing shrinkage and temperature increase during curing to enhance concrete bonding with the steel plate construction found in modular units.

SCC mixtures developed were able to carry shearing forces across the cold-joint boundaries. This "self-roughening" was achieved by adding a tailored fraction of lightweight aggregate (LWA) to the concrete mix, some of which raised to the surface during curing, forming a rough surface on which subsequent concrete placements were bond. The desired properties of a self-roughening SCC concrete mix design for the construction of modular units are reported below:

1. Self-consolidating concrete (or SCC) mixes demonstrated very high slumps to facilitate concrete placement in the field without internal vibration. The slumps of SCC relative to typical concrete mixes range between 21 in. (530 mm) and 26 in. (660 mm), where the minimum value is set to achieve flowability and the maximum to reduce possible segregation.

2. SCC mixes maintained said slump for a sufficient period of time to allow for in-situ concrete placement operations. Times between 45 min and 60 min were considered an average in which regular concrete mix ensure their fresh properties. This aspect of the concrete mixes was assessed primarily during Tasks 3 and 4, when medium-scale (Task 3) and full-scale (Task 4) specimens were produced.

3. The SCC mixes also demonstrated cohesive properties, so that the mixture remained in a consistent state during concrete placement. This was a particular challenge in the self-roughening concrete because it was necessary that some fraction of the lightweight aggregate raised through the mix (and thus segregate) to form the rough surface, but the remaining portion of the mix, including the normal weight aggregates and fines, remained cohesive.

4. The SCC mix demonstrated ability to control heat generation in mass concrete placements due to the exothermic heat generation in high-cement fraction SCC concrete mixes. By using a relatively high percentage of fly ash as a supplementary cementitious material (SCM) better performances in terms of heat generation were achieved while also improving fluidity and cohesiveness. Concrete heat development was monitored during Task 3 when mass concrete elements were cast.

5. Because of the high cement fraction in SCC mixes, shrinkage was also monitored. High volumes of fly ash used to produce SCC helped to reduce phenomena related to drying shrinkage.

6. Finally, the development of the self-roughening surface during concrete placement and consolidation was the most important aspect of the self-roughening SCC mixes and was the focus of the research.

2 Project Background

The concept of shear friction in the behavior of concrete structures describes the ability to transmit shear across a given boundary, typically between two separate placements of concrete – sometimes called a "pour joint" or "cold joint". In conventional reinforced concrete internal reinforcements provides a tension tie that prevents the concrete placements from moving perpendicular to the boundary. The friction of the surface, which is considered by ACI 318 to be a function of the surface roughness, prevents the placements from moving parallel to the boundary. The normal force comes from the tensile strength of the steel and the coefficient of friction comes from the boundary, thus "shear friction".

In the construction of modular units, no internal reinforcement is used. Instead two external steel plates, one per each side of the unit, are employed in order to increase the confinement action. Steel plates are bonded to concrete by stud connectors, which provide force transfer between concrete and steel plate. The project main focus was to advance the technology in high strength/high performance concrete materials and SC structures. The goal was to improve the construction and economy of modular systems by facilitating the concrete construction while assuring high quality bonding of concrete and composite steel elements. An innovative approach was taken in the composition and properties of SCC. Mixtures and processes were optimized to overcome challenges of cold-joint shear capacities, while also addressing heat generation and shrinkage, factors which have constrained construction operations employing modular steel plate composite structure until now. In addition, the capability to perform intermittent SCC pouring into modular SC structures provides more construction flexibility, reduces risk, and reduces critical path schedule duration.

2.1 Report organization

The chapters of the report follow the order of the five tasks that were completed during the project. In particular, each chapter is dedicated to one specific task:

- *Chapter 3: Task 1 – Development of SCC with Shear-Friction Capacity for Mass Placement.* This Task focuses on the development and assessment of SCC concrete mixes that are both suitable for mass placement and capable of the self-generation of rough surfaces across horizontal cold joints. The self-roughening aspect of the concrete mix is generated by the addition of a tailored fraction of lightweight aggregate to the SCC concrete mix. During concrete placement, a portion of the lightweight aggregate "floats" to the surface of the concrete, providing the roughness required to develop shear friction across the cold-joint boundary.
- *Chapter 4: Task 2 – Assessment of Cold Joint Shear-Friction Capacity.* The shear friction of self-roughening concrete (SRC) joints in small-scale experiments, named shear-friction or push-off specimens, were the focus of Task 2. The test program was designed to experimentally evaluate shear friction behavior in specimens created using SRC. The mix was selected among the ones developed in Task 1. Two percentages of lightweight aggregates (LWA), 5% and 15%, were examined for their potential to provide increased bond – higher friction factors. Both reinforcing bars and the composite plates with studs were examined and compared for providing the shear-friction reinforcement.
- *Chapter 5: Task 3 – Assessment of Shear and Flexural Performance.* Using SCC identified through Tasks 1 and 2, mid-scale experiments, three 11 ft (335cm) long and squared cross section with sides of 18in (45cm) were constructed in a vertical orientation with horizontal cold joints

and tested as a horizontal beam in flexure to examine shear and flexural performance. The results were compared to a module made with no cold joints.

- *Chapter 6: Task 4 – Validation through Full-Scale Testing and Modeling.* Task 4 specimens was essentially a validation phase, where the shear-dominated specimens from Task 2 were replaced by a full scale beam specimens used to assess the force transfer of the steel plates across boundaries in both shear and flexure.

- *Chapter 7: Task 5 – Draft Code Requirement for Shear Friction Design of Cold Joints.* The goal of this task was to develop shear friction provisions that are proposed as an additional section on out-of-plane shear in AISC N690-12 Appendix N9 [2015]. Equations for prediction were determined based on the results of the push-off and beam cold-joint shear tests.

2.2 Main developments, results, and findings

In the section below we identify key findings of the project.

2.2.1 Development of SRC

The self-roughening, self-consolidating concrete, or SRC, is formed when a fraction of the dense, normal-weight coarse aggregate in an SCC mix is replaced with expanded shale aggregate. The project shows replacements in the 10% to 15% range by volume are sufficient to achieve a roughened surface. The SRC mixes worked best when a slump flow test (ASTM C1611) of 23 to 25 inches is maintained in the mix. As in most SCC mixes, the slump flow of SRC tends to decrease with time, and self-roughening properties are attenuated when slumps fall below 23 in. In addition, the best performance with this mix was found when the lightweight aggregate (LWA) was added to the mix at the end of the batching cycle.

2.2.2 Shear friction behavior across cold-joints

Irrespective to the amount of LWA, all of the Task 2 cold-joint specimens had higher capacity than predicted by the ACI shear friction equation. This conclusion holds for concretes with lightweight aggregate percentages substitutions between 5% and 15% and demonstrates that SRC surfaces are sufficient to develop shear transfer across the interface between layers of concrete. The shear friction coefficient for intentionally-roughened cold joints in SC construction may be taken as 1.35.

2.2.3 Behavior of cold-joints in flexure and shear

The Task 3 specimens were tested in both in-plane and out-of-plane bending, where in-plane bending implies that the steel plates are bending in flexure and out-of-plane bending implies that the steel plates are in either tension or compression. The Task 4 validation test was tested in out-of-plane bending.

All of in-plane experiments show higher strengths than the AISC N690 Appendix N9 prediction. This means that the beam at an SRC cold joint was stronger than the code prediction *with no cold joint.* This is a significant and positive test result. For Task 3, the monolithic specimen without cold joint, MO-IP, shows the highest strength and ductility. The specimens with cold-joints are somewhat less strong than the monolithic specimen but still exceed N690 strength predictions.

The out-of-plane behavior the flexural specimens was also acceptable. The first Task 3 cold-joint specimen, CJ-OOP-1, demonstrated excellent behavior, with a capacity greater than predicted by AISC N690 N9 and by the analytical model along with good ductility. The Task 3 mid-scale beam specimens confirmed the ability SC modular construction to resist shear and flexural failure at cold joints. The cold-joint capacity and ductility was clearly increased when SRC was used. One of the Task 3 cold-joint specimens did not perform as well, demonstrating a high strength but little ductility. Forensic examination of the cold-joint in this specimen showed that it was almost completely slick (reasons for this are discussed in detail in Chapter 5 of the report). This specimen inadvertently demonstrated the efficacy of the self-roughened cold-joint, by highlighting the deficiency of a slick cold-joint.

3 Task 1 – Development of Self-Roughening (SR) Concrete Mix Design

The primary objective of Task 1 was to optimize a self-consolidating concrete (SCC) mixtures so that concrete placement could be made into steel plate composite (SC) modular structures without the need for continuous concrete placement. Task 1 focused on the design and resulting properties of SCC mix design to ensure that sufficient shear capacity across cold-joints was achieved by incorporating or "seeding" a relatively small fraction of light-weight coarse aggregate (LWA). The LWA provided an internal source of surface roughening; because of its low density, it rises to the surface and produces required roughness amplitude (Figure 3-1).

The attributes of an appropriate SCC mixtures were selected as follows: (1) high spread to facilitate concrete placement in the field without internal vibration, (2) cohesive concrete mixture to prevent segregation of the normal weight aggregates from the cement paste during concrete placement, and (3) low viscosity of the SCC so that the LWA would float. A SCC mix design that respected all these characteristics was referred as self-roughening concrete (SRC). In order to limit shrinkage and heat development associated with cement hydration, improve durability, and to provide the desired self-consolidating behavior, the use of relatively high substitution of fly ash (>35%) for cement was included in designing the mixtures. The SRC mix was designed using materials readily available to concrete producers in Georgia. At first, a number of trials were tested for fresh properties. During this phase fresh concrete properties such as slump spread and segregation resistance were evaluated. The effects of LWA size and dosage rate on surface roughness were also qualitatively assessed in Task 1.

The following sections discuss the methodology used in designing SRC mixtures: selection of material constituents, optimization of the mixtures, and evaluation of fresh and hardened properties.

3.1 Concrete constituents

Concrete typically contains four main ingredients: coarse aggregate, fine aggregate, cement, and water. Additionally, mineral and chemical admixtures such as fly ash and super-plasticizers are used to modify the plastic and/or hardened state properties. SCC mixes generally uses a higher volume of fine aggregates and employ super-plasticizers and water-reducers to achieve their increased workability. The SRC mix developed in this project contained coarse and fine aggregates, cement, supplementary cementitious materials (SCM) such as fly ash, water and high-range water reducer as admixture.

3.1.1 Aggregates

The coarse aggregate used were crushed granite from the Vulcan Materials quarry in Lithia Springs, GA. Both #67 and #89 stones were used in these mixes. As a fine aggregate, a blend of 50% manufactured (e.g., fractured granite) sand and 50% alluvial sand was used in order to enhance better performances during the fresh state. Both type of sand were locally available and, overall, the materials could be considered very accessible to regional concrete producers.

The aggregates were characterized using ASTM standards. Density and specific gravity were determined as per ASTM C29 and ASTM C127, respectively. In addition the absorption in saturated surface dry condition was also computed as per ASTM C127. Gradation curves were generated in accordance to the ASTM C33, which fully respected the upper and lower limits of the ASTM specifications.

Results were collected into material data sheets and reported in Appendix A.

The LWA used to generate surface roughness was an expanded slate aggregate supplied by Stalite Company (Salisbury, NC), which produced the aggregate by a rotary kiln process. The physical and mechanical properties provided by the manufacturer were also reported in Appendix A.

All aggregates were stored in a dry condition using large metal storage bins located in the lab where the temperature is constantly maintained around 73.5 ± 3.5 °F (23 ± 2 °C).

3.1.2 Cementitious materials

The cement used for the laboratory mixes was an ASTM C150 Type I/II Portland cement. Argos USA (Atlanta, GA) supplied the cement in 80 lb. (36 kg) bags. The cement was also stored in the lab and kept sealed in the large steel drums to minimize any pre-hydration or carbonation of the cement particles.

The only supplementary cementitious material used in combination with cement was fly ash. The fly ash was provided by Boral Material Technologies LLC, United States, and conformed to ASTM C618 specifications for Class F.

3.1.3 Admixture

The chemical admixtures used was the Sika ViscoCrete 2100, a high range water reducing and superplasticizing admixture supplied by Sika. Dosage rates vary according to materials, environmental conditions and requirements of a specific project. For lab condition the recommended dosage was between 5 fl. oz. and 12 fl. oz. per 100 lbs. (145-390 ml/100 kg) of cementitious materials. Sika ViscoCrete 2100 was added at the end of the batching cycle directly to freshly mixed concrete in the concrete mixer.

3.2 Laboratory mix design matrix

The development of the mix design included researching SCC mixes with similar materials and adjusting those mixes until the desired characteristics were achieved. At the beginning some design parameters were set in order to quantify and qualify the concrete. The first properties of concern were at SCC fresh state and included flowability and resistance to segregation. In order for the fresh concrete to qualify as an adequate mix, the slump flow was limited to 23 ± 2 in. (584 ± 51 mm). If the mix passed the slump flow test, then it would be considered for the "S" groove test and the visual stability index (VSI) were used to rate the quality of the mix as it pertains to segregation resistance. These tests will be fully described in the following sections.

If the mix passed these qualifications, 4x8 in. (102x203 mm) concrete cylinders would be made to investigate on the concrete compressive strength.

The SCC mixes that better performed at their fresh state were selected for a second cast in which the original mix proportions were conserved while substituting 5%, 10% or 15% in volume of LWA to the #67. The inclusion of LWA into the mix led to the formation of a rough surface. When a SRC were cast, 6x12 in. (152x559 mm) cylinders were used for surface characterization in addition to 4x8 in. (102x203 mm) cylinders for concrete compressive strength. Figure 3-2 compares a SCC and a SRC mix design during their fresh state.

Using standard test methods, SCC flow and viscosity (ASTM C1611 "standard test method for slum flow of self-consolidating concrete") as well as drying and autogenous shrinkage (ASTM C157 "standard test method for length change of hardened hydraulic-cement mortar and concrete") and strength (ASTM C39 "standard test method for compressive strength of cylindrical concrete specimens") were measured for the selected mix design; those which achieved targets were identified, and mix designs will be further improved.

All mixes were cast in accordance with ASTM C 192 (standard practice for making and curing concrete test specimens in the laboratory). During the mixing, dry sand was used while coarse aggregates were used in the saturated surface-dry (SSD) condition. LWA were pre-soaked in water for 24 hours and then brought to SSD condition before their use. The design quantities considered in the mix design proportions were:

- Total Cement, lb/yd^3 (kg/m^3)
- Fly Ash, lb/yd^3 (kg/m^3)
- Coarse Aggregate - #67 - lb/yd^3 (kg/m^3)
- Coarse Aggregate - #89 - lb/yd^3 (kg/m^3)
- Coarse LWA - #7 – 5%, 10% and 15% in volume of #67
- Water Cement (w/c) ratio
- Chemical admixtures fl oz/yd^3 (ml/m^3)

A total of thirty-five trial mixes were cast. Table 3-1 and Table 3-2 report on some of the mixes that passed the first qualification protocol. These included the mixes with 5%, 10% and 15% of LWA. The batches reported in Table 3-1 and Table 3-2 were chosen for several reasons: adequate slump flow ranging from 21 in. to 25 in. (533 – 635 mm), comparable performances using slightly different amount of HRWR, differences in the aggregate gradation (i.e. trial 07 23 – 2 contained the two sizes of crushed granite, #67 and #89, giving a much more "well-graded" aggregate curve for the mix since #89 stone fills the gaps between the sand and the large #67 stone and separates the larger aggregates).

Mixing was conducted in a 2.5 cu. ft. (0.07 cu. m) countercurrent, high shear manufactured by Eirich (Figure 3-3). The first step was to ensure that the mixer was clean and free of leftover chemical admixtures that could affect the outcome of the mix. Once the mixer was thoroughly cleaned, excess water was removed leaving only a small film of water inside. This ensured that the mixer was not absorbing any water intended for the mix.

Another concern was the timing of the high-range water reducer addition. It was decided to add the HRWR after the addition of the mixing water. This procedure allows to assess the water demand of the cement and aggregates and adjust the HRWR dosage if needed.

The final mixing procedure was as follows:
1. The coarse and fine aggregates were added next to the mixer.
2. Mixing took place for approximately two minutes.
3. The cementitious materials and water were added next.
4. Mixing took place for approximately four minutes.
5. The super-plasticizer was added to the mixer.
6. Mixing took place for two minutes.
7. If required, more super-plasticizer was added.
8. Mixing took place for an additional two minutes.
9. Slump flow readings were taken at this point.
10. If the mix passed the slump flow test, "S" groove test and VSI were performed.
11. If the mix passed the "S" groove test and the VSI, specimens were cast for hardened state property testing.

3.3 Fresh properties

As for SCC, self-roughening ability depends entirely on its fresh properties; therefore, a successful SRC mix must have high fluidity, deformability, good filling ability, and adequate resistance to segregation. Additionally, aggregate particles have to be uniformly distributed throughout the mix to avoid uncontrolled segregation at all times especially during transportation and placement. In general, SCC with a slump flow less than 17 in. (432 mm) will not have self-compacting properties; on the other hand SCC with a slump flow over 26 in. (660 mm) may experience severe segregation and bleeding. Evaluation of the fresh properties for SRC was essentially carried out in the same way as for SCC. The slump flow tests in conjunction with the visual stability index (VSI) are effective in evaluating the workability of the mix on-site. The data collected using these tests appeared to be adequate for quantifying the rheological

properties of the SCC. A sufficient understanding of the quality of SRC in its plastic state was achieved by visual observations of the floating LWA during mixing.

3.3.1 Flow slump test

The slump flow method is the oldest and most widely used test in concrete technology. The simplicity of the procedure and apparatus used makes it suitable for every-day practice and field application (Figure 3-4). Mainly the test measures the fluidity or filling ability of the concrete paste. To determine the slump flow, an Abrams cone is placed on a non-absorptive surface and filled with fresh concrete without any tampering. The cone is lifted and the concrete flows out under its own weight (Figure 3-5). Two perpendicular measurements of what appears to be the maximum diameter are taken across the spread of concrete and the average is reported. The final flow time, from cone removing to flowing completion is recorded, as well as the T20 flow time, which is the time needed by the paste to spread up to 20 in. (50 mm). Slump flow spread diameter values of 23 ± 2 in. (584 ± 51 mm) were considered satisfactory with test results ranging from 21 in. to 25 in. (533 – 635 mm). T20 values were spanning from 3 sec. to 5 sec. and they were inversely proportionated to the slump flow diameter. A complete overview of data is reported in Table 3-1 and Table 3-2.

3.3.2 "S" groove test – Resistant to segregation

The "S" groove test is a simple and effective method of determining the stability and self-healing ability of fresh SRC. Using a finger or a tamping rod, an "S" is drawn into the concrete on the slump flow board (Figure 3-6). If the mix is stable, the concrete will rapidly fill the 'S' groove and the stability of the concrete is good, as seen in Figure 3-7a; otherwise a layer of paste or bleed will fill in the groove essentially showing the segregation of the coarse aggregate within the mix (Figure 3-7b). An empirical range of values spanning from 0 to 5 was used (0 being highly stable and 5 highly unstable) was associated to the test in order to better characterize the behavior. Numerical data are reported in Table 3-1 and Table 3-2 whereas pictures taken at the sample after test are reported in Figure 3-8 and Figure 3-9.

3.3.3 Visual stability index

The resistance to segregation of SCC can be visually evaluated in a lesser or greater degree in almost every test mentioned above. The VSI test is recommended to be implemented with the slump flow test; although, the parameters evaluated in the VSI test can be found in every test that allows the observation of a significant volume of SCC. The range of values for the VSI is 0 through 3, with zero being a highly stable mix, and 3 designates a highly unstable mix. The parameters for determining the VSI number of a given mix are mortar halos, bleed, air bubbles, and aggregate pile-up. Table 3-3 presents the different criteria for VSI numbers. Mortar halos result from the segregation of the paste from the concrete due to too much water or coarse aggregate in a mix. An unstable mix may contain a mortar halo less than 0.4 in. (10 mm); larger halos result in highly unstable concrete mixes. Slight bleed and few air bubbles surfacing are allowed for stable mixes, but not highly stable. Figure 3-10 displays example of the different VSI, whereas data are reported in Table 3-1 and Table 3-2. Pictures taken at the sample after test are reported in Figure 3-8 and Figure 3-9.

3.3.4 Rheology

SCC mixtures are much more fluid than conventional concrete mixture. The yield stress (τ_0) of SCC is considerably lower than ordinary concrete and the viscosity (μ) relationship, defined from shear stress-shear strain rate (γ) behavior, and usually shows a shear-thickening behavior. Therefore, the rheological behavior of a subset of SRC mixes was measured in order to provide useful information of these mixtures during their fresh stage. Numerous rheological models and tools to measure rheological proprieties exist. In terms of models, a Bingham model modified to include a 2nd-order term and parameter, as reported in equation 3.1, can describe SCC rheology.

$$\tau = \tau_0 + \mu\dot{\gamma} + c\dot{\gamma}^2 \tag{3.1}$$

This model proposes two constants defining the flow of the material: the yield stress, which is defined as the amount of force required to initiate the concrete flow, and the plastic viscosity, defined as the concrete internal resistance to flow.

In terms of tools, a compact rheometer as shown in Figure 3-11, was used to determinate yields stress and relative viscosity. A sample of test material was placed in a sample container. The rheometer was fixed in the middle of the container and turned one round by hand. An internal processor monitored the measuring data (i.e. the momentum on the three probes and the angular velocity). On completion of the measurement the readings was wireless transferred and displayed for post processing. The rheometer measured torque (T) versus rotation speed (N). To compute relative units, a straight line was use to fit T vs. N data. The intercept of this line is named the "g-value" and the slope is referred to as the "h-value." It is assumed that the g-value is related to yield stress and the h-value to plastic viscosity. These measurements were taken an interval of 15 minutes. In parallel, flow slump test were perform to correlate the loss in flowability with the rheological measurements.

As expected, Figure 3-12 shows how the SRC yield stress is inversely proportionated to the slump of the concrete. In addition, the self-roughening characteristics of the mixtures, were held for a period of time between 30 and 45 minute. After that, the mixtures, even if preserving characteristics of a SCC mix, were not able to produce a controlled surface roughness.

3.4   Hardened properties

Preliminary hardened properties were measured for some mixes in which free shrinkage under controlled laboratory conditions, compression capacity and surface roughness were studied. The following sections present the procedures followed for each test. Further analyses will be conducted in order to characterize the SRC used during Task 2.

3.4.1   Curing procedures

All specimens were cured following the ASTM C192 (Making and curing concrete test specimens in the laboratory) prescriptions. Specimens were stored in a controlled environment (fog room) with monitored temperature and humidity levels of 73.5 ± 3.5 °F (23 ± 2 °C) and >95%, respectively.

3.4.2   Long term property – Drying and autogenous shrinkage

Drying shrinkage tests were performed following the ASHTOO T160 (Length Change of Hardened Hydraulic Cement Mortar and Concrete) and Alabama DOT (Standard Specification for Highway Construction) specifications. In addition autogenous shrinkage tests on the 1104-1 mix design were also performed following the ASTM C157 (Standard Test Method for Length Change of Hardened Hydraulic-Cement Mortar and Concrete).

For drying shrinkage two sets of three specimens were cast in prism molds (75x75x285 mm - 3x3x11.25 in.), coated in advance with an oil-based form release agent, with gage studs inserted into their ends. SCC was cast using the proportion of the 0625-1 mix. Freshly mixed concrete was placed in one lift. Excess was struck off. Concrete specimens were covered with a polyethylene sheet and wet towels to avoid moisture loss during the first 24 hours, demolded after one day, and placed in the environment chamber 73.5 ± 3.5 °F (23 ± 2 °C) and >95% RH after measuring the initial length.

Following the Alabama DOT specification, a first set of specimens (0625-1a, 0625-1b and 0625-1c) was cured in these conditions for seven days, whereas the remaining specimens (0625-1d, 0625-1e and 0625-1f) were left curing for 28 days in accordance to AASHTO T160. Upon the end of curing duration, the specimens were moved to an environmental chamber with control drying condition of 73.5 ± 3.5 °F (23 ± 2 °C) and 50 ± 4 % RH. During drying, the length was monitored by a length comparator, which was kept in the same temperature chamber to avoid any variations due to temperature change according to ASTM

C 157 (the standard test method for length change of hardened hydraulic-cement mortar and concrete). Measurements were taken at the ages of 3, 7, 14, 21, 28, 35, 42, 49, and 56 days. The following procedure was used for each shrinkage measurement:

- Recorded the length of the reference bar.
- Reset the measuring gauge to zero and removed the reference bar.
- Placed the sample in the dilatometer bench and recorded the gauge reading.
- At the early age, soft samples were handled carefully, using both hands to carry them, to avoid any damage. To obtain accurate results, it was important to place the reference bar and all samples in the same orientation. A line mark helped to keep all samples at the same position after each measurement.

The shrinkage values were calculated as the percent change in length from the time the specimen was removed from curing. Results were plotted in two graphs throughout time and reported in Figure 3-13. For both sets, the average measured drying shrinkage was less than 250 $\mu\varepsilon$, which was below the limit of 400 $\mu\varepsilon$ reported in the Alabama DOT specification.

For the autogenous shrinkage one set of three specimens were cast in prism molds (75x75x285 mm - 3x3x11.25 in.). In making the specimen the same procedure described for the drying shrinkage specimens was adopted, however, after being de-molded the specimens were immediately double-wrapped with a self-sealing polythene film and sealed in aluminum tape to minimize any moisture loss. After being sealed, the specimens were stored in an environment chamber at a constant 73.5 ± 3.5 °F (23 ± 2 °C) and >95% RH after measuring the initial length, until further testing. Also in this case the shrinkage values were calculated as the percent change in length from the time the specimen was removed from curing. Figure 3-14 shows the 28days results of 1121-1a specimens in which autogenous shrinkage reached the value approximately 200 $\mu\varepsilon$.

3.4.3 Compressive strength

Compression tests were conducted as per ASTM C39 using 4x8 in. (100x200 mm) cylinders. Five cylinders were cast for every mix, de-molded after 24 hours and stored in a fog room where they were kept until testing. The fog room held a constant temperature of 73°F (23°C) and 100% humidity. Specimens were cured for 28 days before testing. Results are reported in Table 3-1 and Table 3-2 along with their standard deviations.

3.4.4 Measurements of surface roughness

One of the main objective in Task 1 was to generate the appropriate surface roughness essential to facilitate shear interlock between the existing substrate of concrete and the overlay at a cold joint. The ACI 318 shear friction concept is that shear forces are transferred across a joint by friction between the surfaces. The frictional force is a function of the normal force applied and the coefficient of friction, μ, between the surfaces. By incorporating a small fraction of LWA (5%, 10% and 15% in volume,) in the SCC mix designs, the SCC was able to generate a rough surface so that roughening by raking or other means may not be necessary (Figure 3-15). Surface roughness was measured using two methodologies: (1) International Concrete Repair Institute's (ICRI's) standard concrete surface profiles (CSPs) (qualitative assessment) and (2) a quantitative assessment.

ICRI's CSPs are benchmarks used to establish industry acceptable specifications and represent varying degrees of concrete roughness and texture. Nine rubber profiles represent varying degrees of concrete roughness, with CSP 1 being thought to represent the least rough (smoothest), while CSP 9 being the most rough (Figure 3-16). Comparing the concrete surface to the CSPs, a qualitative assessment of the surface roughness was performed by visual inspection.

In addition to the CSP molds, a quantitative assessment of concrete surface condition was also performed. Using 152x559 mm (6x12 in.) concrete cylinders, the amplitude of surface roughness was determined by measuring the distance between the top of the exposed aggregate and its junction with the paste (distance A) using a caliper as shown in Figure 3-17. A coefficient of surface roughness, Sa, was then calculated considering that roughness is directly proportioned to the number of LWA particles present on the surface and their average amplitude, whereas it is inversely proportional to the surface area. These consideration and the device used for measuring the average amplitude led to the following equation:

$$S_a = \frac{n \cdot \sum_1^n A_n}{S}$$
(3.2)

where: n is the number of LWA particles present on the surface, A_n represents the average amplitude and S is the nominal surface area of the concrete specimen. Results of both methodologies are reported in the last two rows of Table 3-1 and Table 3-2.

3.5 Measurements of temperature

All concretes generate heat as the cementitious materials hydrate and an exothermic reaction occurs. Most of this heat generation occurs in the first few days after placement. For thin structural elements such as pavements, slabs and walls, the heat dissipates almost as quickly as it is generated. However, for thicker concrete sections (considered "mass concrete", as is the case in many SC modular structures), heat dissipates more slowly than it is generated and the temperature of the mass concrete increases – often reaching an upper bound where the durability of the concrete can be compromised.

There are various factors which effect heat of hydration like cement content, cement type, size of concrete pour, type of formwork, concrete temperature, thermal coefficient of aggregates and ambient temperature. Generally higher the cement content, the more will be heat of hydration. In case of SCC concrete, due to the higher level of paste fraction required to meet slump flow characteristics, temperature needs to be controlled in order to prevent damage, minimize delays and meet specifications.

To assess the thermal generation in the SRC, one-cubic yard of concrete (0.75 m³) was cast into a cube of 3ft. (90 cm) of side as shown in Figure 3-18. Internal vibrating wire sensors measuring both temperature and strain were installed in the several locations within the cube and monitored during the first two weeks of curing.

Figure 3-19 shows the temperature profile for the concrete cube case using the mix design 06 24-1 reported in Table 3-1. Despite the high level of cementitious materials in the mixture, the max temperature measured in the center of the cube were well below the threshold value of 155 °F (68 °C). This behavior was possible due to the present of a high level of fly ash, indicating that our SRC mixes are suitable for mass concrete applications.

Table 3-1: Trial mixes 1 of 2.

Mix Component	05 28 - 2	05 30 - 2	06 05 – 3	06 10 - 1	06 23 - 1	06 24 - 1
Cementitious	lb/yd³	lb/yd³	lb/yd³	lb/yd³	lb/yd³	lb/yd³
Cement Type I/II	808	808	770	770	617	617
Fly Ash, Class F	161	161	306	153	459	459
Water	315	315	350	329	343	343
w/cm	*0.326*	*0.326*	*0.325*	*0.356*	*0.318*	*0.318*
Coarse Aggregates						
# 67	1510	1510	1286	1439	1286	1286
# 89	-	-	-	-	-	-
LWA	-	10%	-	-	-	15%
Fine Aggregates						
Natural sand	712	712	678.5	678.5	678.5	678.5
Manufactured sand	712	712	678.5	678.5	678.5	678.5
Admixtures (fl oz./cwt)						
HRWR	5.65	5.65	5.09	7.42	5.94	6.36
Flow Slump (in.)	23	23	21	25	21	23
T20 (sec)	4	4	5	3	4.5	3
"S" groove (0-5)	1	0.5	2	0	1	0
VSI (0-3)	0.5	0.5	1	0	0	0
Compression (psi)	-	8682	9208	9602	9942	11347
Std. dev.	-	352	305	818	671	396
Unit weight (pcf)	156.3	156.3	150.7	149.9	150.4	150.4
CPS Roughness (1-9)	-	8	-	-	-	9
S_a, (in^{-1})	-	0.789	-	-	-	1.071

Table 3-2: Trial mixes 2 of 2.

Mix Component	06 25 - 1	07 08 - 1	07 23 - 1	07 23 - 2	11 04 – 1	12 16 – 1
Cementitious	lb/yd^3	lb/yd^3	lb/yd^3	lb/yd^3	lb/yd^3	lb/yd^3
Cement Type I&II	617	617	617	617	617	510
Fly Ash, Class F	459	459	459	306	459	340
Water	343	343	343	294	343	271
w/cm	*0.318*	*0.318*	*0.319*	*0.319*	*0.319*	*0.319*
Coarse Aggregates						
# 67	1286	1286	1286	1136	705	1512
# 89	-	-	-	306	459	
LWA	15%	5%	-	-	15%	-
Fine Aggregates						
Natural sand	678.5	678.5	678.5	678.5	678.5	950
Manufactured sand	678.5	678.5	678.5	678.5	678.5	407
Admixtures (fl oz./cwt)						
HRWR	6.79	6.36	6.36	7.42	6.8	6.44
Flow Slump (in.)	21	25	23.5	23.5	26	29.5
T20 (sec)	5	4	4	4	3	4
"S" groove (0-5)	1.5	1	0.5	0.5	0	0
VSI (0-3)	0	0.5	0.5	1	0	2
Compression (psi)	9755	9834	10575	9186	8233	
Std. dev.	689	1035	1076	672	450	
Unit weight (pcf)	150.4	150.4	150.4	137.4	145.9	147.4
CSP Roughness (1-9)	9	7	-	-	-	-
S_a, (in^{-1})	1.052	0.448	-	-	-	-

Table 3-3: Visual stability index

Rating	Number	Criteria
Highly Stable	0	No evidence of slump segregation
	0.5	Very slight evidence of bleed and air popping
Stable	1	No mortar halo No aggregate pile-up Slight bleed and air popping
	1.5	Just noticeable mortar halo and aggregate pile- up
Unstable	2	Slight mortar halo, less than 0.4 in. (10mm) Slight aggregate pile-up Noticeable bleed
Highly Unstable	3	Large mortar halo greater than 0.4 in. (10mm)

a. LWA during mix   b. LWA after casting

Figure 3-1: Generation of a rough surface by incorporating LWA into the mix.

a.   b.

Figure 3-2: Comparison between SCC (a) and SRC (b).

Figure 3-3: EIRICH concrete mixer.
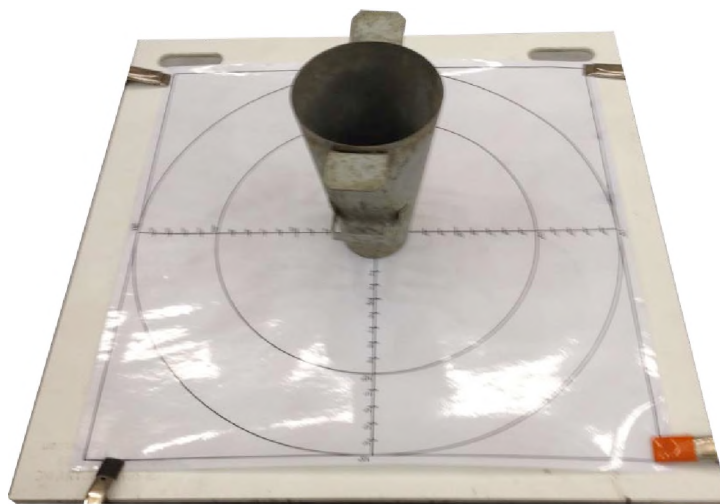
Figure 3-4: Flow test apparatus – Abram cone and flow table.

a. 0 sec   b. 1 sec   c. 2 sec   d. 4 sec (T20)   e. End of test
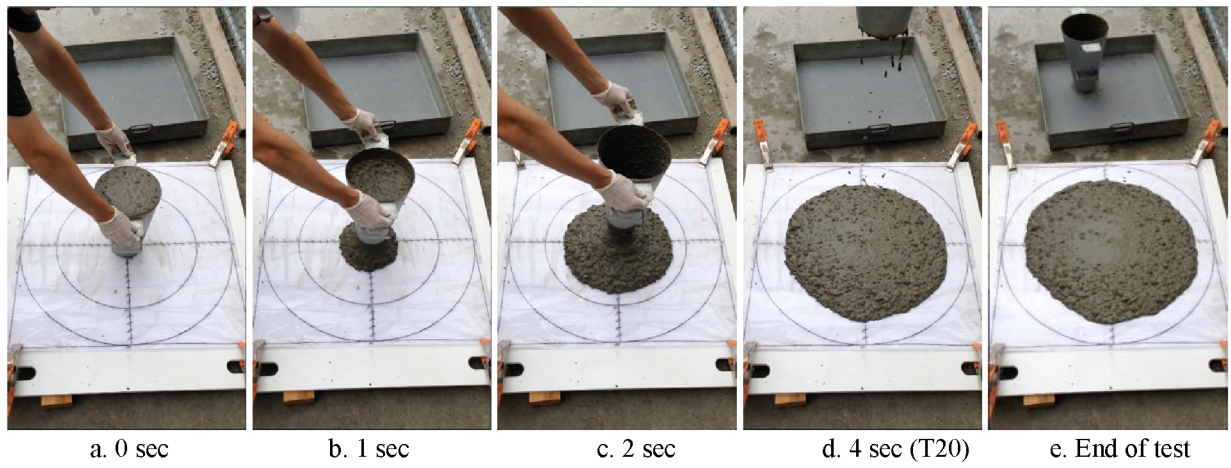
Figure 3-5: Performing a flow slump test.

a.   b.   c.   d.   e.
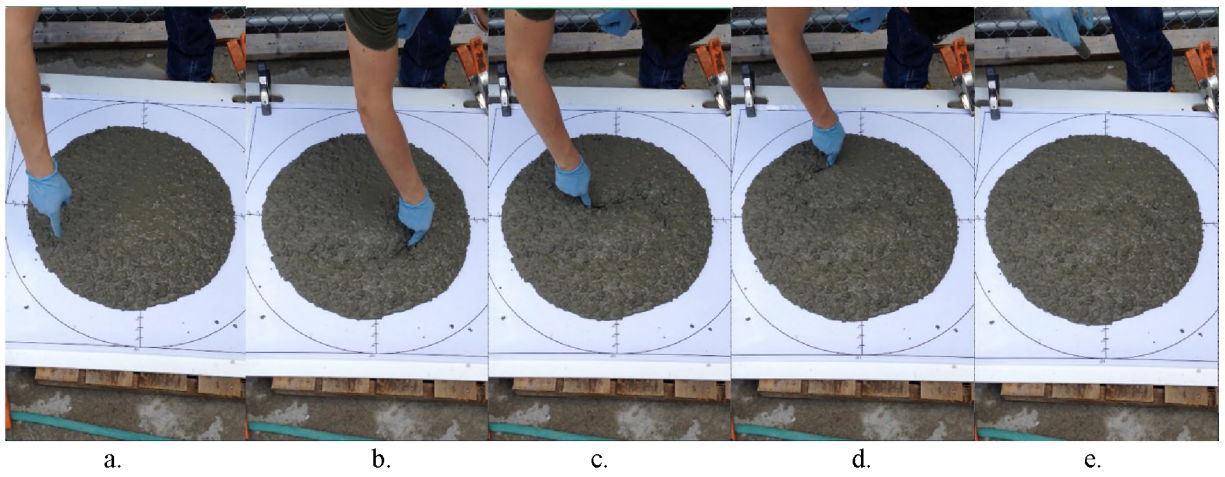
Figure 3-6: Performing "S" groove test.

a.   b.

Figure 3-7: "S" groove test good (a) and poor (b) performances.
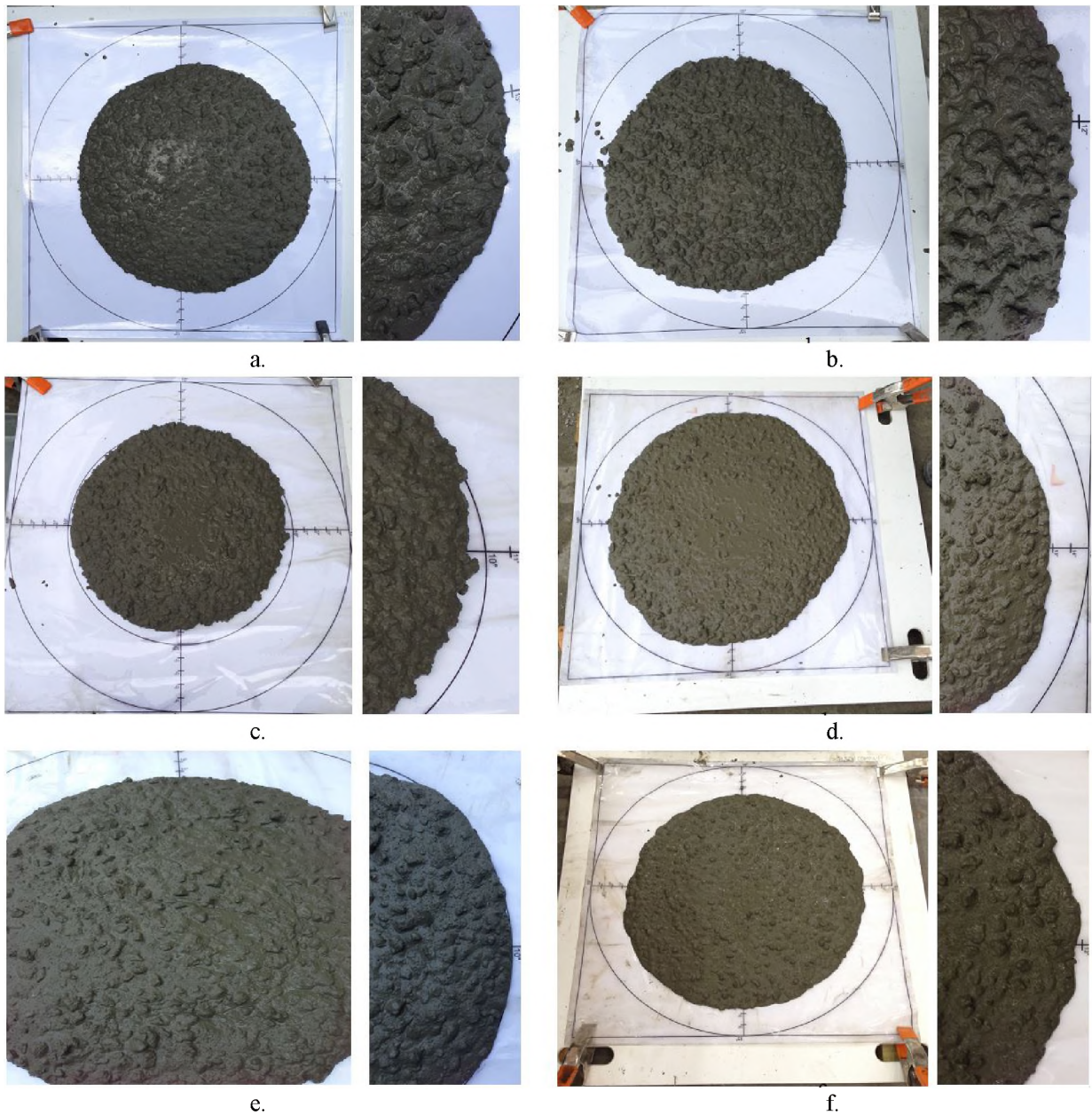
Figure 3-8: Samples after "S" groove test and VSI, part A. (a. 0528-1, b. 0530-2 c.0605-3, d. 0610-1, e. 0623-1, f. 0624-1).
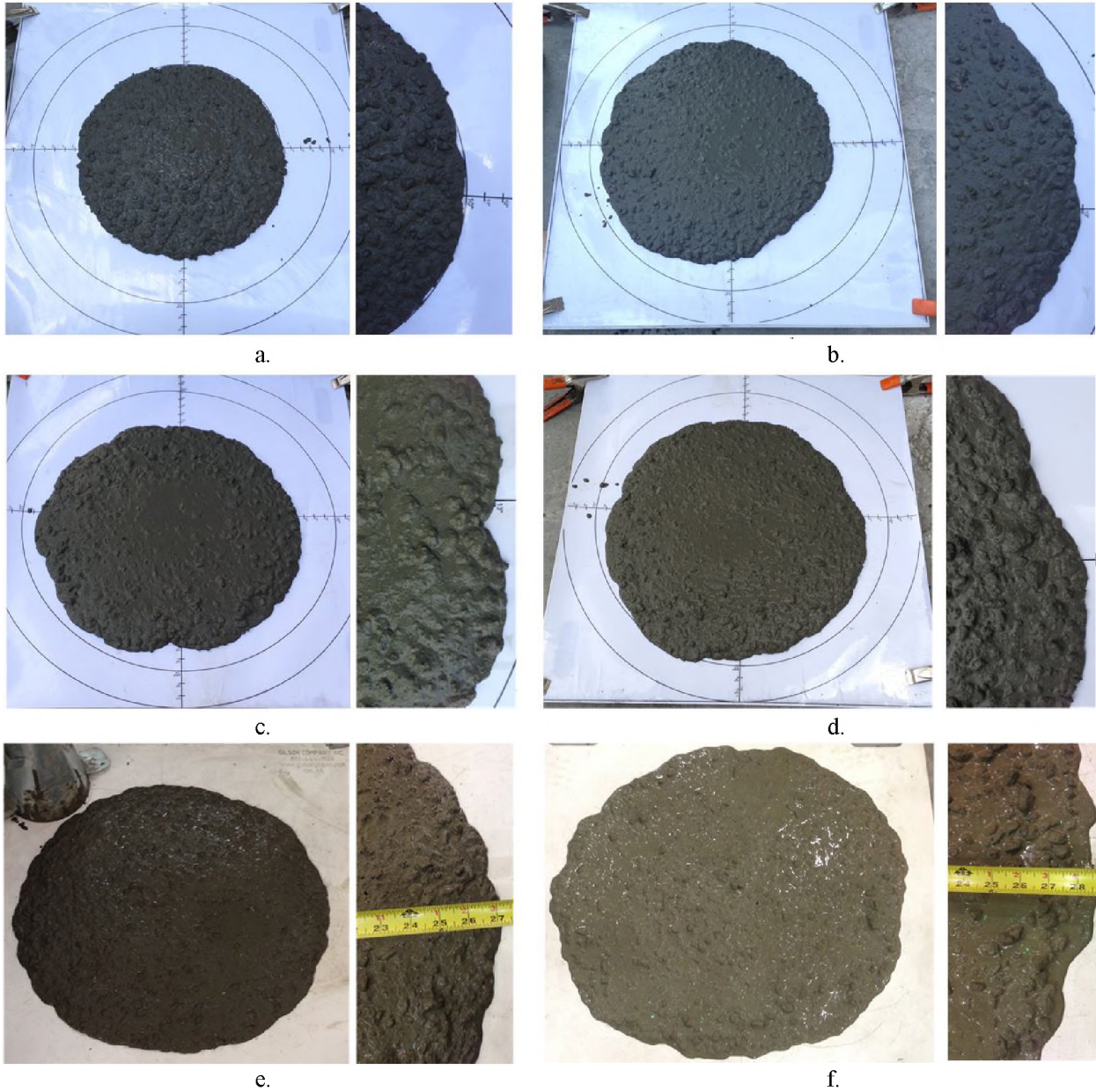
Figure 3-9: Samples after "S" groove test and VSI, part B. (a. 0625-1, b. 0708-1, c. 0723-1, d. 0723-2, e. 1104-1, f 1216-1).

Figure 3-10: Visual stability index examples for various slump flow test
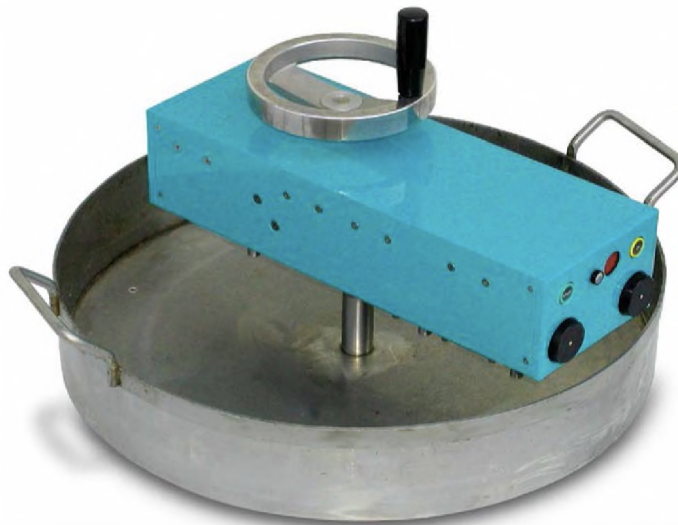
Figure 3-11: SCC concrete rheometer BT2 with hand drive and small vessel
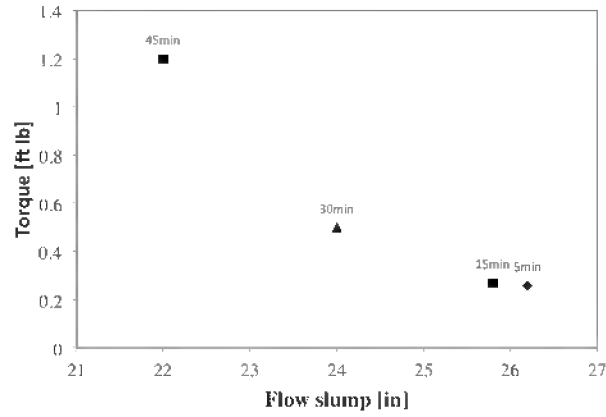
Figure 3-12: G-value versus SRC flow slump
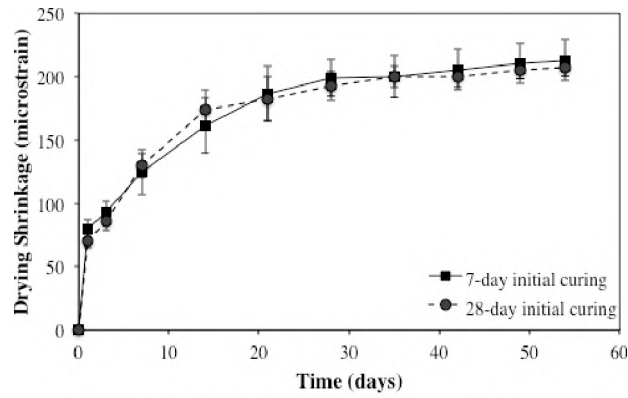
Figure 3-13: Free Shrinkage test result
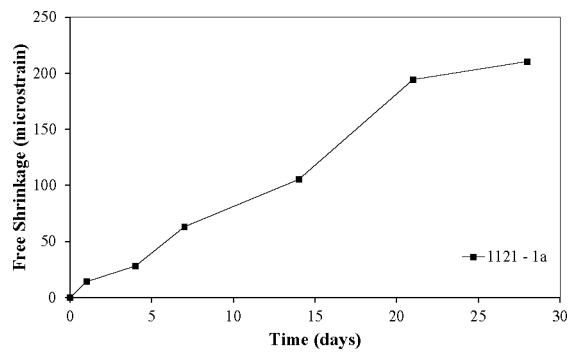
Figure 3-14: 28 days autogenous shrinkage test results.
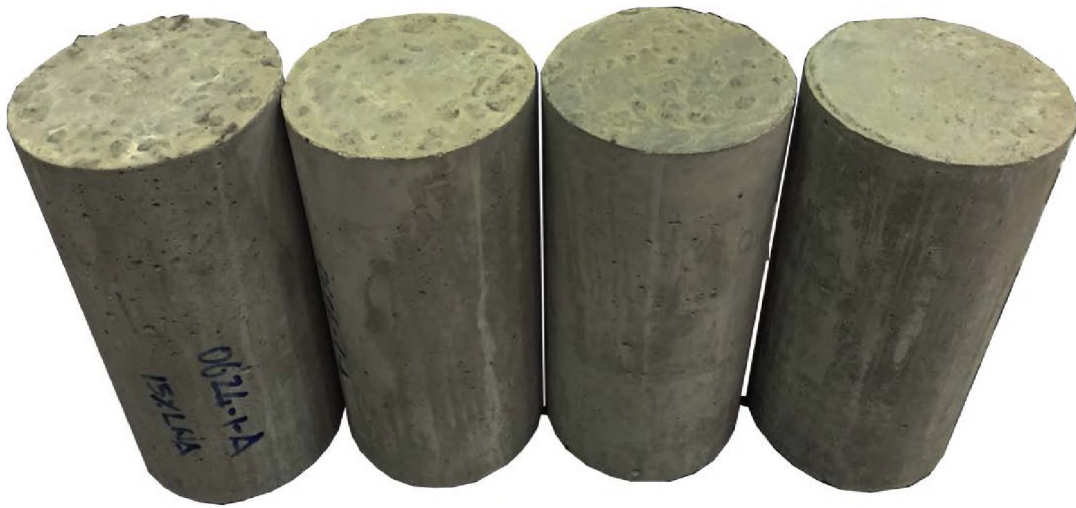
Figure 3-15: From left to right, concrete cylinders with 15%, 10%, 5% and no-LWA substitution.

Figure 3-16: ICRI's standard CSPs

Figure 3-17: Roughness quantitative measurements

a)   b)
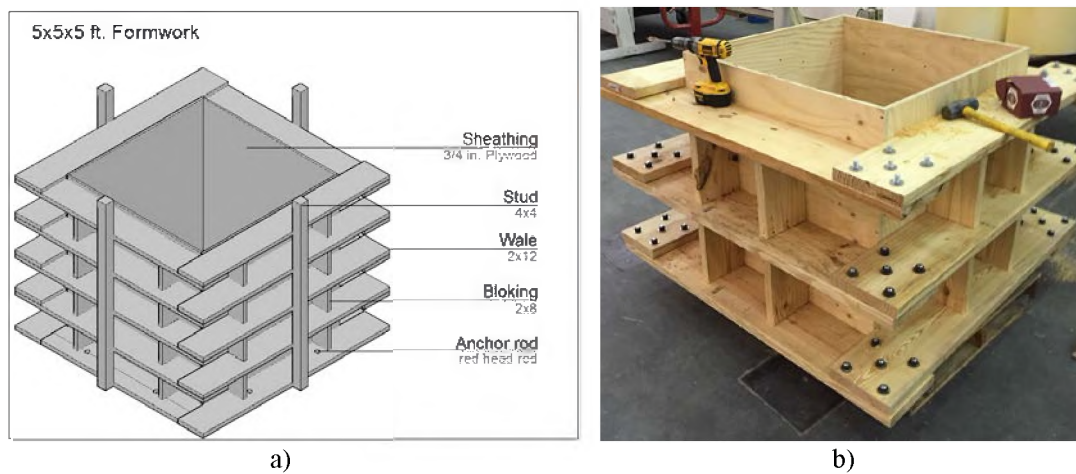
Figure 3-18. Mass concrete formwork: a) design, b) fabrication
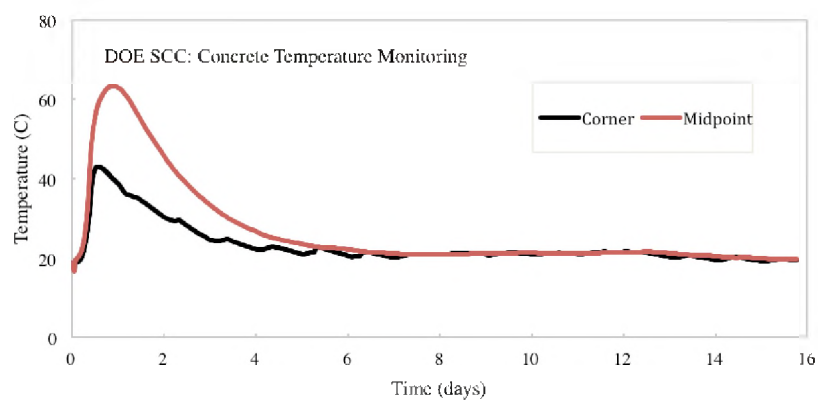
Figure 3-19. Concrete temperature monitoring

4   Task 2 – Assessment of Cold Joint Shear Capacity

The shear friction of Self-Roughening Concrete (SRC) joints in small-scale experiments in Task 2 were used to optimize mixtures prior to full-scale shear-friction experiments (Task 3). Historically push-off tests have been the primary test specimen used to evaluate shear friction; in fact they can be fabricated with a cold-joint to simulate the interface of two layers of concrete cast in different times. The test program was designed to experimentally evaluate shear friction behavior in specimens created by using SRC. The mix was selected among the ones developed in Task 1. Two percentages of lightweight aggregates (LWA), 5% and 15%, are examined for their potential to provide increased bond – higher friction factors. Both reinforcing bars and the composite plates with studs are examined and compared for providing the shear friction reinforcement.

4.1   Shear friction test design

The specimens were designed similar to typical specimens from previous research. This allowed the shear friction data to be directly extended and compared to other tests. The specimens were divided into three groups based on the two joint conditions and the shear reinforcement location:

- Type 1, monolithic pre-cracked push-off specimen.
- Type 2, cold-joint specimen to simulate the behavior that occurs at the interface between two consecutive layers in a concrete wall. The cold-joint surface condition is left as-cast in an unaltered condition. The surface is characterized by a roughness amplitude of 1/4 in. qualifying it as a rough interface.
- Type 3a and 3b, cold-joint specimen to study the effect of traversing the failure surface with steel plate reinforcement as shear-friction reinforcement anchored to concrete through using shear studs rather than reinforcing bars.

4.2   Test matrix

Design data for the 27 push-off test specimens are listed in Table 4-1. The table indicates the joint condition of each specimen, the area and type of steel crossing the shear plane, the reinforcement ratio (ρ), the amount of LWA and the number of repetition.

The general push-off specimen (Type 1 and 2) is illustrated in Figure 4-1. The shear plane is rectangular with dimensions of 12 in. (305 mm) long by 7.5 in. (190 mm) wide. The amount of stirrup reinforcement crossing the shear plane is 3#3 stirrups with a reinforcement ratio equal to 0.75%. Shear stirrups are equally distributed across the shear plane.

Type 3a and 3b push-off specimen are illustrated in Figure 4-2. While the shear plane remains the same, the reinforcement is now located on the outside and anchored to the specimen using shear studs. Different configuration of the steel plate and reinforcement ratio are considered as reported in Table 4-1. Indicating with A_s the area of steel reinforcement transverse to the shear friction plane and f_y its corresponded yielding capacity, steel plate thicknesses were calculated using an $A_s f_y$ type of analysis in order to obtain Type 3a and 3b specimens with comparable reinforcement ratio of Type 2 specimens. An example of this analysis is reported in Appendix B.

4.3   Materials

The SRC mixtures developed in Task 1 contained coarse and fine aggregates, cement, and supplementary cementitious materials (SCM) such as fly ash, water and high-range water reducer as admixture. In addition, a percentage of LWA was substitute in volume to the coarse aggregate in order to provide self-roughening properties typical of a SRC. The mix design used in Task 2 reflected the developments made

during Task 1 and uses the same materials. Aggregate properties of the concrete mixture are summarized in Appendix A. The concrete mixture is described in greater details in Section 4.3.1, and reinforcing steel bars and plates' properties are reported in Section 4.3.2.

4.3.1 Concrete Mixtures.

The concrete mixture used in specimen construction was selected among the trials reported in Task 1. SRC mixtures contained Portland cement type 1-2, water, #67 granite coarse aggregates, a blend of 50% manufactured sand and 50% natural sand, and high range water reducers (HRWR). Mixture proportions are provided in Table 4-2. Aggregates used in the production of concrete met or exceeded ASTM C33 specification requirements. Similarly, LWA met or exceeded the requirements set forth by ASTM C330. All concrete was batched, mixed, and cast in the Structural Laboratory of Georgia Tech using a 5 cubic feet rotary drum mixer.

At the end of each batch, fresh concrete unit weight was determined in accordance with ASTM C138, whereas flow and viscosity were determined in accordance with ASTM C157. Also, five 4x8 in. (100x200 mm) cylinders were cast for every mix along with the corresponding specimens. Cylinders were demolded after 24 hours and stored in a fog room where they were kept for 28 days. Compression tests were conducted as per ASTM C39 and results were used to predict the shear friction capacity.

4.3.2 Reinforcing Steel Bars

All reinforcing steel bars used in this experimental program were ASTM A615 Grade 60 provided by Gerdau SA. Properties reported by the manufacturer were verified by conducting tensile tests of representative samples. Reinforcing bar testing was performed in accordance with ASTM A370. A typical stress-strain plots for the tensile tests is shown in Figure 4-3, in which values of stress were the applied force divided by the nominal cross sectional area of the bar. Values of strain were measured using a 4.0 in. extensometer attached to the reinforcing bar, which was removed upon yielding of the specimen. A summary of the measured results is provided in Table 4-3.

The Grade 60 No. 3 reinforcing bars used for all closed stirrup transverse reinforcement had an average yield stress of 92.3 ksi (636 MPa); however, the ACI-318 recommended maximum f_y of 60 ksi (414 MPa) was used in the calculations of predicted shear stress values.

4.3.3 Steel Studs

Steel studs used for the Task 2 specimens were provided by the Nelson Stud Welding Company and were attached to the steel plates using a Nelweld Model 6000 stud welder. The studs were nominal 0.25 in. (6 mm) diameter, 2.75 in. (70 mm) long with a tensile yield stress of 51,000 psi (350 MPa). The number and spacing of studs for each plate was computed to overcome the shear friction capacity of the cold-joint and to avoid any local failure within the stud. To aid in the installation, a guide plate was created in order to facilitate the stud installation and to ensure consistency (see Figure 4-4).

4.3.4 Steel Plates

The steel plate thicknesses were computed using an $A_s f_y$ analysis reported in Appendix B. Three different thicknesses were selected, 13, 16 and 22 gauge, which correspond to a reinforcement ratio of 0.75%, 0.50% and 0.25%, respectively. Tensile test were performed on 1 in. by 8 in. (25.4x203.2 mm) coupons in order to characterize the tensile strength. A summary of the measured results is provided in Table 4-4.

Steel plates are bonded to concrete through headed anchors welded to the steel plates using a Nelson Stud Welding system composed of a power supply with a transformer rating of 7600 amps and standard welding gun. Equipment settings vary based on the steel plate thickness and different trials were performed to optimize the equipment configuration. During the trials, a visual inspection was performed to ensure the formation of a full 360 degree weld fillet around the circumference of the stud. In addition,

test on the welded stud was performed by bending the stud in any direction to a 30 degree angle from weld position. For 13 and 16 gauge steel plates the test was easily satisfied (Figure 4-5).

At first it was impossible to successfully attach studs to the 22 gauge steel plate. Even with reduced welding settings (amperage and time), the energy release from the stud gun created a large hole in the thin plate with the stud remaining unattached. A number of strategies were developed to aid in the attachment of the plate. A simple 1 in. square backing plate of 16 gage steel did not remedy the problem, as the stud would attach to the backing plate but would leave a circular damage zone around the 22 gage main plate and thus the stud was attached to the backing plate but not the primary plate. In the end, a novel solution was developed. A series of holes, of 0.2 in. (5 mm) diameter were waterjet cut in the 22 gage steel plates. The 16 gage steel backing plate was used under the point of application of the stud to avoid the penetration of the stud through the plate. The hole allowed the stud to be welded to the support while forming a complete weld fillet on both steel plates. This configuration successfully passed the 30 degree angle test as shown in Figure 4-6.

4.4   Specimen preparation
Two methods were used to fabricate the push-off specimens; though the final result are the same except for the surface condition at the cold joint location.

The monolithic specimens were cast on their sides compared to the testing position with the shear plane oriented vertically. A picture of the monolithic specimen forms prior to casting is shown in Figure 4-7.

The cold-joint specimens (Type 2, 3a and 3b) were cast in two stages with the shear interface surface horizontal, so that it could set as an as-cast surface. In order to achieve that, one half of the rebar cage with all the stirrups is tied separately from the other half. Each Type 2 specimen includes three No. 3 closed tie stirrups placed normal to the shear plane. The so formed cage was placed in a separate reusable forming designed to produce half a specimen with the stirrups protruding from the surface after casting. Minimum cover of 0.5 in. (12.7 mm) was provided at the intended shear plane, and 0.75 in. (19.1 mm) was provided in the remainder of the specimen. The cold-joint specimens were left to set with an as-cast surface at the shear plane generated from the SRC. After adequate hardening of the concrete, the forms were removed and the surface cleaned of any impurities. The other half of the specimen was formed and cast on top of a moist interface. Schematic steps of the construction process are illustrated in Figure 4-8 whereas the fabrication process is shown in Figure 4-9.

Similarly to Task 1, the surface roughness was measured using two methods: (1) International Concrete Repair Institute's (ICRI's) standard concrete surface profiles (CSPs) (qualitative assessment) or (2) profilometry (quantitative assessment).

Table 4-5 summarizes the details. The first two letters reported in the ID classification of Table 4-5 represent the type of specimen (MO for monolithic, CJ for cold-joint, SP for steel plate, ST for strips), the first two numbers indicate the interface type characterized by the amount of LWA (5% and 15%), and the following two numbers indicate the reinforcement ratio (0.25, 0.50 and 0.75).

4.5   Test Setup
The monolithic pre-cracked specimens were prepared by placing a specimen on its front side while aligning a knife-edge plate perpendicular to the shear plane as shown in Figure 4-10.

All push-off specimens were tested using the set up illustrated in Figure 4-11. Testing was performed using a screw-driven hydraulic testing machine with a maximum capacity of 400 kip (1,780 kN). Applied load was recorded using a 200 kip load cell placed at one of the supports. Relative slip movement across the interface was measured by two linear voltage displacement transformer (LVDT) located on both front

and back of the specimen. In the case of specimens reinforced using steel face plates, strain measurements were recorded using two strain gauges, one horizontal and one vertical, located at the mid-height of the specimen. Experimental data were gathered using a National Instruments data acquisition system running Lab VIEW software. Load was applied at a rate of 500 lb/s (2,224 N/s). Specimens were tested until one of the following conditions occurred: a target slip of 0.3 in. was reached, or a sudden and significant drop in applied load occurred. Prior to testing, the width and height of the interface shear surface were measured and recorded for determining interface shear stress.

4.6   Test results

This section outlines results obtained during Task 2 test campaign. Critical values recorded for each specimen includes peak applied load (V_u) and slip at peak load and data are presented in Table 4-6 along with the predicted capacities. In addition, force-slip diagram for each specimen is reported in Figure 4-16.

The load-slip curves for the pre-cracked specimens (MO-1) are not presented as they showed an initial slope of the curve less than the slope for cold-joint specimens. No peak load was observed because the load increased through the entire displacement and due to the application of a larger load then needed during the cracking of the specimens.

All specimens with internal (rebars) reinforcement behaved similarly. Initial cracks were observed at loads between 20% and 65% of the peak ultimate capacity and were only visible when alcohol was applied. These cracks were between 1 to 4 in (25 to 102 mm) long and oriented diagonally between 0 to 30 degrees to the shear plane from top and bottom. The pre-cracked specimen showed a plateau when slip was around 0.2 in. After that point the load transferred from the concrete to the rebar, which were resisting to shear thought the formation of dowel mechanism.

The cold-joint specimen with external reinforcement (steel plate bonded through headed studs) tended to have more gradual changes to the slope of the load-slip curve than did the cold-joint specimen with internal reinforcement even though they exhibited a higher stiffness before reaching the peak load. This could be due to a more gradual transfer of force from cohesion to shear friction.

The specimens with external reinforcement exhibited much more ductile failures than the ones with internal reinforcement with a load carrying capacity comparable to cold joint specimens with internal reinforcement. However, failure mode where governed by the different reinforcement configuration. Sudden and brittle was the failure showed by the cold-joint specimens with internal reinforcement where cracks started to propagate after reaching an approximated value of slip of 0.05 in. Although the obvious increase in terms of ductility, the specimens with external reinforcement failed due to local buckling of the steel plate between the studs. This type of failure is typical in steel composite (SC) structures and it is governed by geometry of the stud system and the thickness of the steel plate (Figure 4-17).

Figure 4-18a and Figure 4-18b show the comparisons among specimens with different types of reinforcement, internal and external, and different levels of reinforcement ratio, ρ (from 0.25% up to 0.75%). As expected, V_u increases as ρ becomes larger. A smaller increase in the peak load can be also noted by comparing the curves that have the same reinforcement ratio but different amount of LWA (5% and 15%). However, in this last case, the level of ductility and the ultimate displacements remain essentially the same proving that an amount between 5% and 15% is enough to generate similar shear friction capacity. Last consideration can be noted by looking at specimens with internal and external reinforcement but with similar reinforcing ratio, ρ. In this cases, V_u reaches higher value when applied as external steel plate rather than internal reinforcing bars, providing also a higher ductility to the specimen behavior.

4.7 Comparison with code equations

The purpose of Task 2 was to determine if code equations for shear friction developed for regular reinforced concrete structures are applicable for SRC mixtures and for cold joints between and cast-in-place concrete layers in SC modular structures. The concept of shear friction uses the idea of a coefficient of friction to quantify shear transfer across a given plane, especially at a cold joint or at an existing or potential crack. The current ACI shear friction equations is:

$$V_n = \mu \, A_v f_y \qquad (4\text{-}1)$$

but not greater than the smaller of:

- $0.2 f_c' A_c$,

- $(480 + 0.08 f_c') A_c$,

- or $1600 A_c$

where μ is the coefficient of friction, A_v is the area of steel crossing interface, f_y is the yield stress of steel, f_c' is the concrete compressive strength and A_c is the area of concrete contact across interface. Using Equation 4-1, shear stress is calculated by dividing nominal shear strength by the area of the concrete engaged in shear transfer as follows in Equation 4-2

$$v_n = \mu \, \rho \, f_y \qquad (4\text{-}2)$$

where ρ is the interface shear reinforcement ratio. The current ACI code provision needs to be validated in order to determine if can be used for SRC shear resistance. This particular aspect will be addressed in Chapter 7.

Figure 4-19 (a), (b), (c), (d) and (e) show the ultimate shear stress, v_u, as a function of a ω ratio defined as ρ (f_y/f'_c), which takes into account the different specimen configurations, steel yield stress and concrete strengths. The solid lines in the figure represent Equation 4-1 with coefficient of friction, μ, of 1.0.

Irrespective to the amount of LWA, all shear stresses were greater than those predicted by equation 4-1, proving that SRC with lightweight aggregate percentages substitutions between 5% and 15% is enough to develop shear transfer across the interface between layers of concrete. The only exemption is represented from ST specimens. This was due to the nature of the reinforcement and studs configuration. In a strip form, the steel is not able to transfer shear across the plates allowing a relative rotation of the strips around the point of application of the studs.

4.8 Analytical Modeling of Task 2 Specimens

From Task 2 test results, it is clear that the specimens with external steel plates are capable of carrying a significant load across the cold joint – and that the capacity of the specimen is comparable to that of similar internally-reinforced shear friction specimen. For specimens with thin steel plates, the onset of failure is characterized by yielding and subsequent shear buckling of the steel plate (see Figure 4-20). The propagation of the shear buckling is constrained by the studs and the specimen demonstrates a flat force-displacement curve post-buckling, indicating significant energy dissipation and continued load capacity. It is critical that we be able to capture and model this behavior analytically, so as to predict the behavior of the more complex specimens such as those tested in Task 3 and Task 4 and provide guidance for cold-joints in our proposed updates to AISC N690-12 Appendix N9. The analytical model is described below.

This analytical model depicts the steel plate on one size of the Task 2 specimen. The steel plate is subject to in-plane loading that is transferred to the steel plate through the Nelson studs on each side of the cold joint boundary. In Figure 4-21, the analytical model for the Nelson studs is depicted. The concrete is not

modeled, but rather the point of fixity of the stud inside of the concrete is estimated, and the stud cantilevers off of this boundary. This model only captures the "web shear" capacity of the steel plate, as the concrete shear friction is not included. This is considered useful because it provides a means for separating the web shear behavior from the shear friction behavior in the experimental data.

The finite element model is developed in LS-DYNA explicit and considers both material and geometric non-linearities. A monotonically increasing displacement across the cold-joint boundary is applied to the model, with the displacement being applied to the plate by the moving shear studs on one side of the cold-joint boundary, while the studs on the opposite side are fixed. The concrete in the Task 2 specimen is not modeled, but a contact surface is applied to the stud-side of the steel plate to prevent the plate from buckling into the concrete surface.

The behavior of the steel plates as the load is applied is shown in Figure 4-22. Initially the load is carried as uniform shear in the plane of the steel plate. As the displacement increases, the actions of the studs in anchoring the plates becomes clear. The post-yield buckling behavior is captured by the model.

In Figure 4-23 a comparison of the load-displacement behavior of the Task 2 specimens SP xx 25 and the analytical model are depicted. The experiments are much stiffer at the start, with no detectable slip until the load reaches 20 kips. At this point, the specimen shows slip along the shear-friction boundary. The analytical model does not capture the concrete interlock, and is thus more flexible than the experiment. The analytical model does capture the capacity of the connections, and makes a relatively good prediction of the ductility of the connection. In the model, as well as in the experiments, the final failure model is the shearing of one or more of the studs.
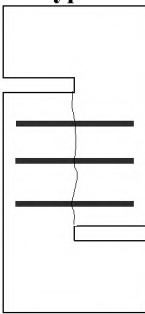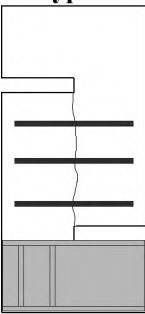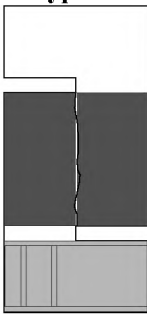
Table 4-1: Push-off test matrix

	Type 1	Type 2	Type 3a		Type 3b	
Cold joint	No	Yes	Yes	Yes	Yes	Yes
Reinforcement ratio - ρ (%)	0.75	0.75	0.25	0.50	0.75	0.75
#3 shear reinforcement	Yes	Yes	No	No	No	No
Steel plate (thickness)	No	No	0.03125 in. (22 gauge)	0.0625 in. (16 gauge)	0.09375 in. (13 gauge)	0.375 in. (00 gauge) h= 1.0 in.
5% LWA	n/a	2	2	2	2	2
15% LWA	n/a	3	3	3	3	3
N. of repetitions	2	5	5	5	5	5

Table 4-2. Concrete mix design for Task 2 specimens

Mix Component	06 25 - 1
Cementitious	**lb/yd^3**
Cement Type I&II	617
Fly Ash, Class F	459
Water	343
w/cm	*0.318*
Coarse Aggregates	
# 67	1286
# 89	-
LWA	15%
Fine Aggregates	
Natural sand	678.5
Manufactured sand	678.5
Admixtures (fl oz./cwt)	
HRWR	6.79

Table 4-3. Reinforcing steel bar properties

Specimen ID*	Nominal Diameter	Yield Stress (kip/in²)	Modulus of Elasticity** (kip/in²)	% Elongation at Break
60-3 – 1	No 3	110	25,000	10.75
60-3 – 2	No 3	85	26,700	8.75
60-3 – 3	No 3	83	26,400	8.75
Average		92.7	26,100	9.42
Standard Deviation		12.3	758	0.94

*Specimen ID notation; first indicates grade, second bar nominal size, and third specimen number.
**Slip of extensometer on small-diameter bars led to lower than anticipated modulus values.

Table 4-4. Steel plate properties

Specimen ID*	Width (in.)	Thickness (in.)	Yield Stress (kip/in²)	Modulus of Elasticity (kip/in²)
36-13 – 1	1.019	0.087	31.5	27,800
36-13 – 2	1.018	0.087	31.0	24,900
36-13 – 3	1.018	0.087	31.6	32,800
Average	*1.018*	*0.087*	*31.4*	*28,500*
Standard Deviation	*0.0005*	*0.00*	*0.24*	*3,229*
36-16 – 1	1.019	0.063	46.1	30,500
36-16 – 2	1.017	0.063	44.7	29,700
36-16 – 3	1.019	0.063	45.7	32,300
Average	*1.018*	*0.063*	*45.5*	*30,800*
Standard Deviation	*0.0009*	*0.00*	*0.58*	*1,096*
36-22 – 1	1.008	0.031	48.8	28,500
36-22 – 2	1.013	0.030	47.5	29,700
36-22 – 3	1.011	0.030	47.9	27,800
Average	*1.011*	*0.030*	*48.1*	*28,600*
Standard Deviation	*0.0021*	*0.000*	*0.54*	*0.768*

*Specimen ID notation; first indicates grade, second bar gauge, and third specimen number.

Table 4-5. Specimen IDs, properties and test results

Specimen ID	Flow Slump [in]	t_{20} [sec]	S test [0-3]	VSI [0-5]	CSP Roughness	f'_c [psi]	f'_c(2nd) [psi]
MO - 1	24	3	0	0	n/a	7275	n/a
MO - 2	24	3	0	0	n/a	7377	n/a
CJ 15 75 - 1	23	5	0	0	9	9644	8121
CJ 15 75 - 2	23.5	4	0	0	9	9185	6556
CJ 15 75 - 3	23.5	4	0	0	8	9185	12949
CJ 05 75 - 1	26.5	3	0.5	1	7	10628	9175
CJ 05 75 - 2	26.5	3	0.5	1	8	10628	9175
SP 15 25 - 1	23	5	0	0	9	10529	12039
SP 15 25 - 2	23	5	0	0	9	10529	11519
SP 15 25 - 3	23	5	0	0	9	10529	11810
SP 05 25 - 1	23.5	4	0	0	9	10196	11519
SP 05 25 - 2	23.5	4	0	0	9	10196	12309
SP 15 50 - 1	22.5	6	0.5	0	8	8419	6653
SP 15 50 - 2	22.5	6	0.5	0	9	8419	6653
SP 15 50 - 3	22.5	6	0.5	0	7	8419	6653
SP 05 50 - 1	23	5	0	0	8	11214	12327
SP 05 50 - 2	23	5	0	0	9	11214	12327
SP 15 75 - 1	24	4	0	1	9	11253	11391
SP 15 75 - 2	24	4	0	1	9	11253	11810
SP 15 75 - 3	24	4	0	1	8	11253	11810
SP 05 75 - 1	23.5	5	0	0	9	11214	12636
SP 05 75 - 2	23.5	5	0	0	8	11214	12636
ST 15 75 - 1	23	5	0	0	9	9391	11519
ST 15 75 - 2	23	5	0	0	9	9391	11810
ST 15 75 - 3	24	3	0	0	9	9391	12039
ST 05 75 - 1	24	3	0	0	9	10196	11519
ST 05 75 - 2	24	3	0	0	8	10196	12039

Table 4-6. Test results and ACI predictions

| Specimen ID	V_u [kip]	v_u [psi]	V_n [kip]	v_n [psi]
MO - 1	69.29	769.9	39.740625	441.5625
MO - 2	68.88	765.3	39.740625	441.5625
CJ 15 75 - 1	51.24	569.3	39.740625	441.5625
CJ 15 75 - 2	53.99	599.9	39.740625	441.5625
CJ 15 75 - 3	51.30	570.0	39.740625	441.5625
CJ 05 75 - 1	54.24	602.7	39.740625	441.5625
CJ 05 75 - 2	43.66	485.1	39.740625	441.5625
SP 15 25 - 1	33.19	368.8	25.92	288
SP 15 25 - 2	30.11	334.5	25.92	288
SP 15 25 - 3	32.20	357.8	25.92	288
SP 05 25 - 1	29.90	332.2	25.92	288
SP 05 25 - 2	28.98	322.0	25.92	288
SP 15 50 - 1	55.40	615.6	54.432	604.8
SP 15 50 - 2	57.40	637.8	54.432	604.8
SP 15 50 - 3	56.70	630.0	54.432	604.8
SP 05 50 - 1	95.47	1060.7	54.432	604.8
SP 05 50 - 2	96.99	1077.7	54.432	604.8
SP 15 75 - 1	76.08	845.3	75.168	835.2
SP 15 75 - 2	105.80	1175.6	75.168	835.2
SP 15 75 - 3	102.78	1142.0	75.168	835.2
SP 05 75 - 1	85.82	953.6	75.168	835.2
SP 05 75 - 2	80.76	897.3	75.168	835.2
ST 15 75 - 1	36.78	408.7	324	3600
ST 15 75 - 2	35.10	390.0	324	3600
ST 15 75 - 3	34.80	386.7	324	3600
ST 05 75 - 1	38.65	429.4	324	3600
ST 05 75 - 2	31.55	350.6	324	3600
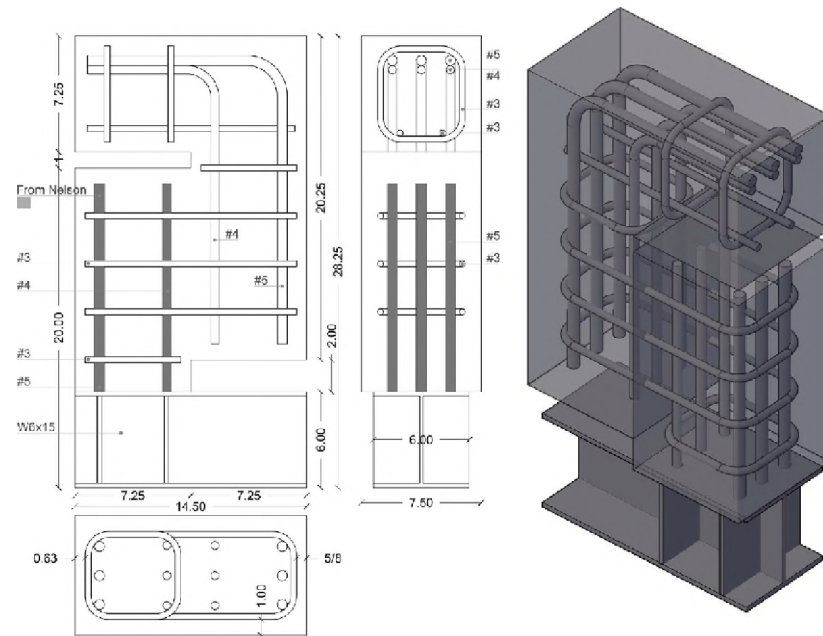
Figure 4-1: Type 2 push-off specimen design
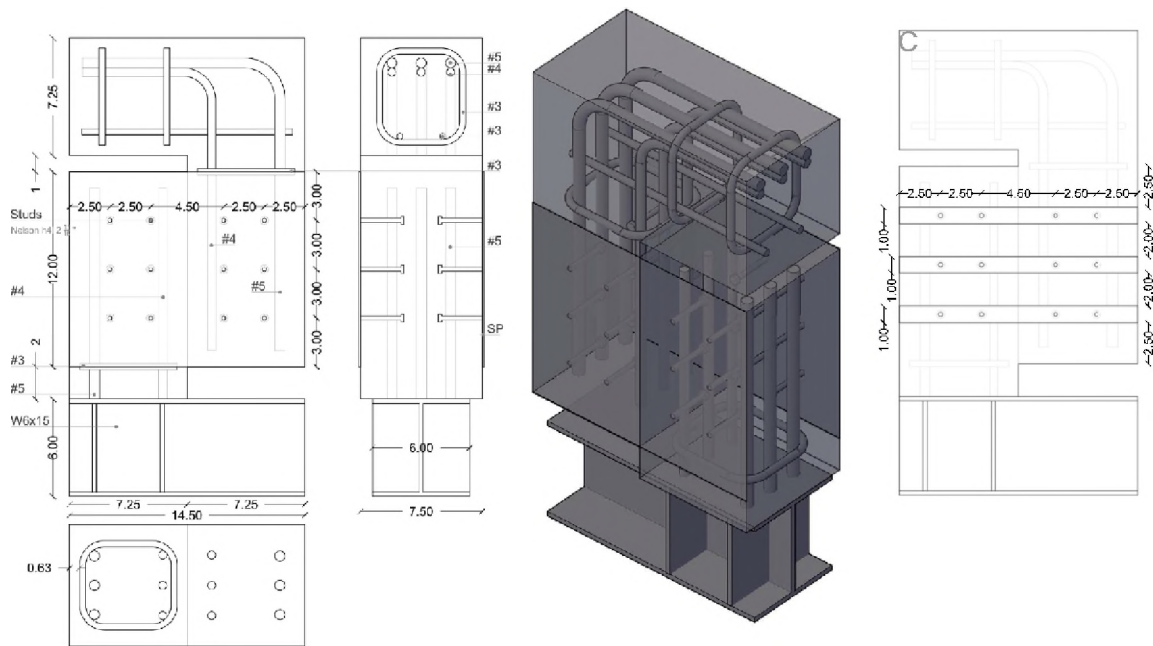
a.

b.

Figure 4-2: a. Type 3a push-off specimen design, Type 3b push-off specimen design
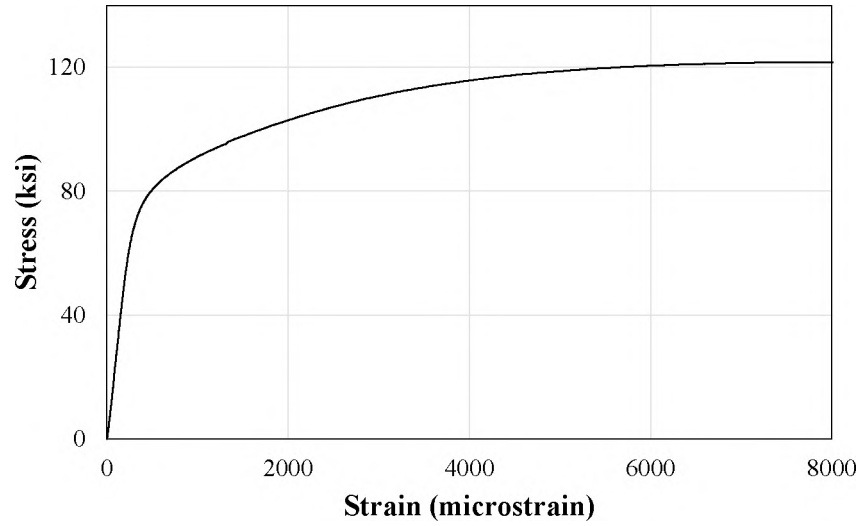
Figure 4-3. Typical stress vs. strain for reinforcing steel bar from tensile test.

Figure 4-4. Steel plate and stud matrix.

Figure 4-5. 30 degree angle test on welded studs:
a) Complete formation of fillet around stud circumference,
b) 30 degree angle test.

0.2 in. [5mm] hole in 22 gage plate allows stud to contact backing plate

Sound weld to both main plate and backing plate
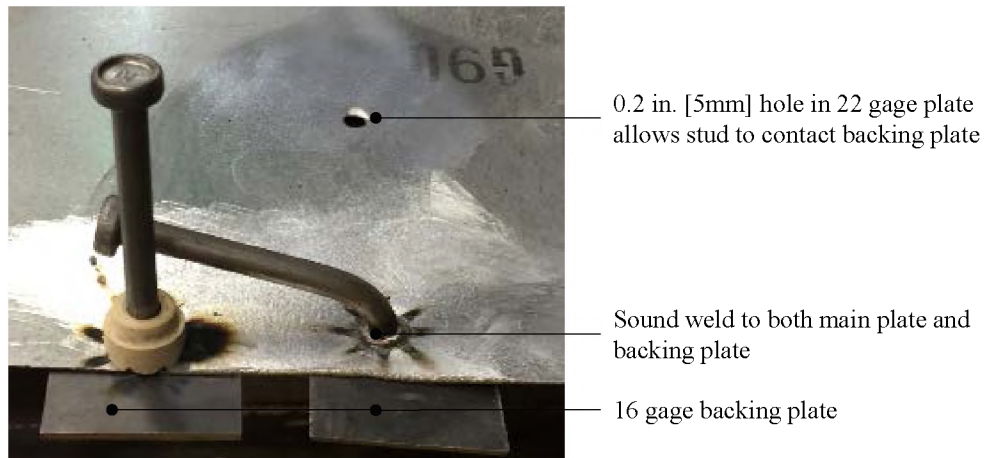
16 gage backing plate

Figure 4-6. Stud connection for 22 gage plate and 30 degree bend test

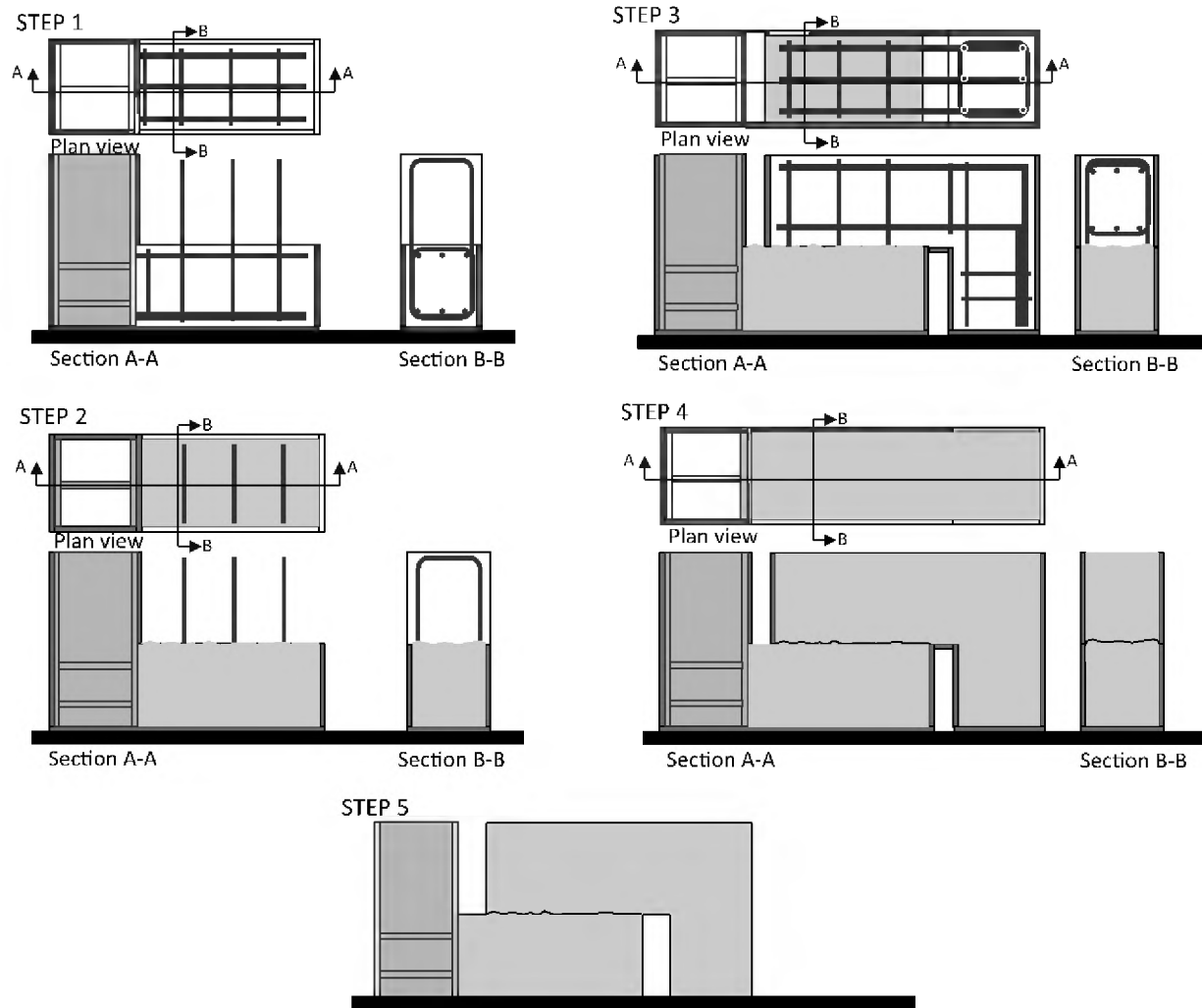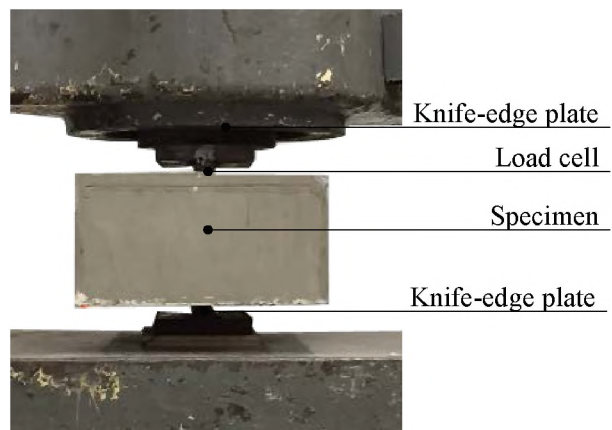*Figure 4-7: Monolithic Specimen Prior to Casting*

Figure 4-8: Steps for the fabrication of the shear friction specimens. The steps will remain the same for both steel reinforcement configurations. Step 1: Bottom mold with surface up. Step 2: Pour concrete in first part (day 1). Step 3: Add additional mold. Step 4: Pour concrete second part (day 2). Step 5: Cure 28 days

Step 1   Step 2

Step 3   Step 4

Step 5

Figure 4-9: Cold-joint Specimen preparation

Knife-edge plate
Load cell
Specimen
Knife-edge plate

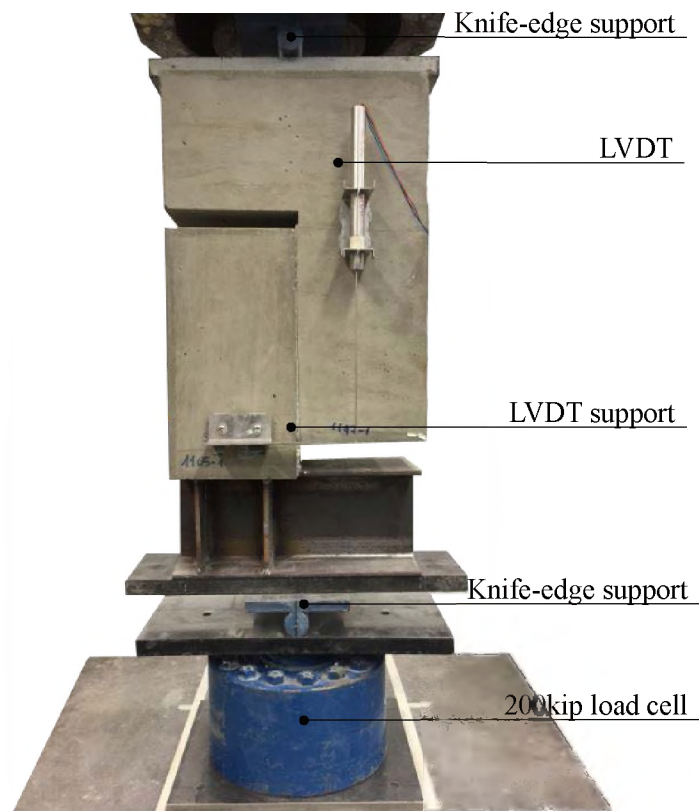*Figure 4-10. Load and position of monolithic specimen during pre-cracking*
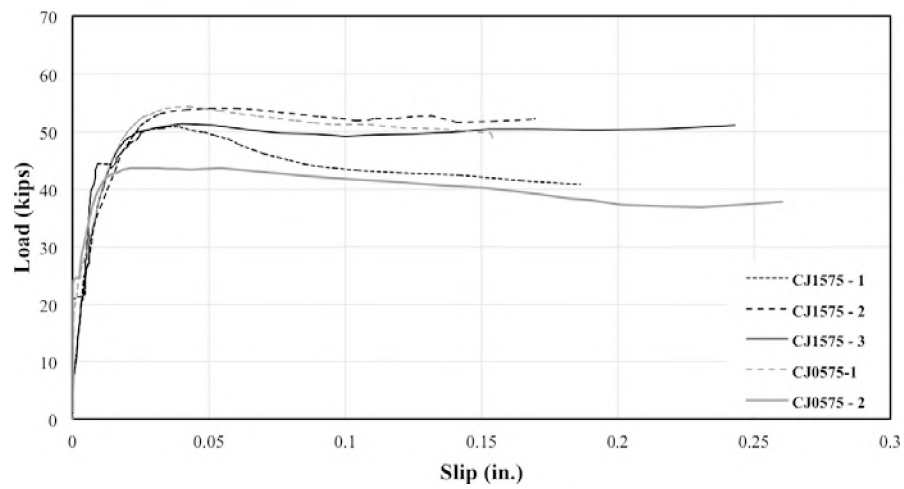
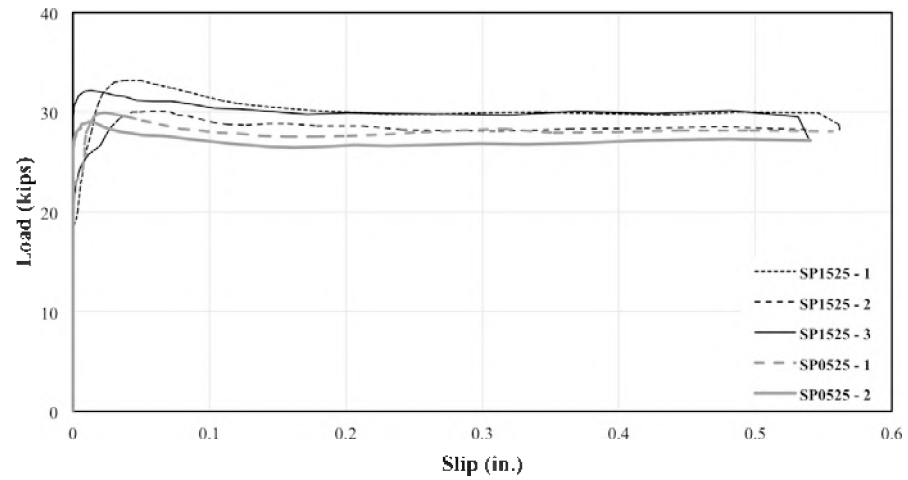*Figure 4-11. Test setup*

Figure 4-12. CJ load-slip curves
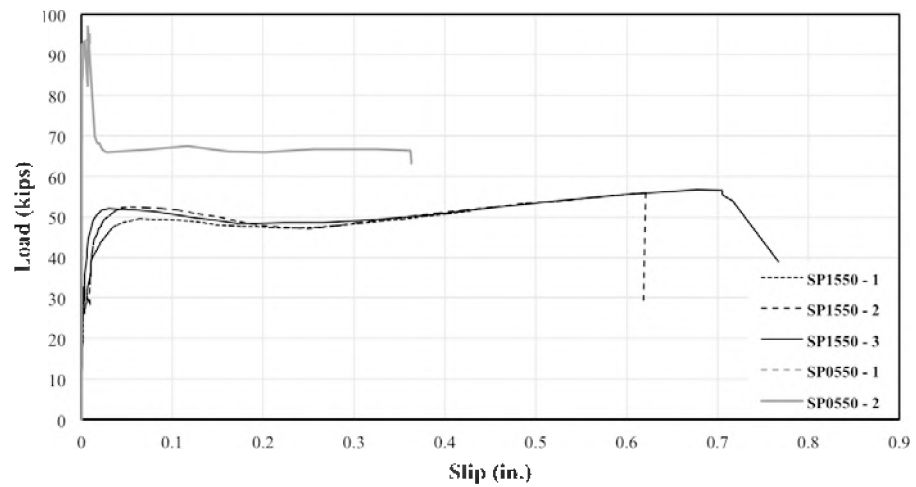
Figure 4-13 SP (r = 25%) load-slip curves

Figure 4-14 SP (r = 50%) load-slip curves

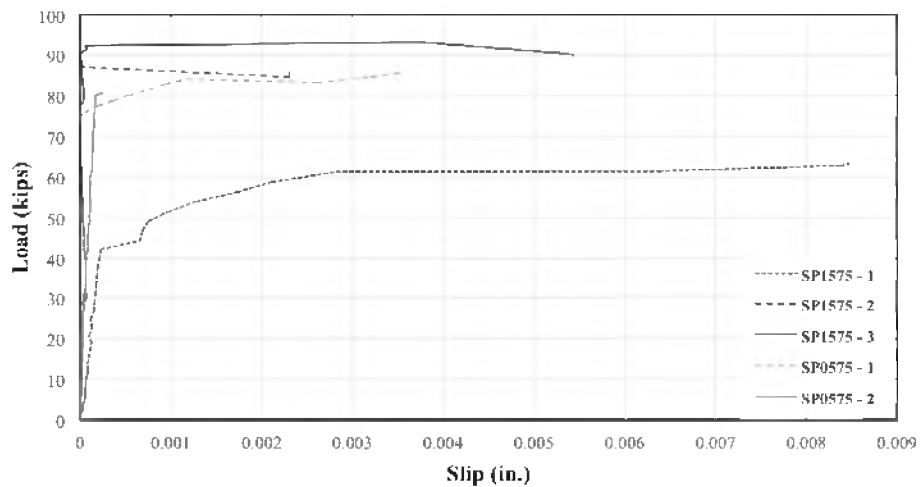*Figure 4-15. SP (ρ = 75%) load-slip curves*
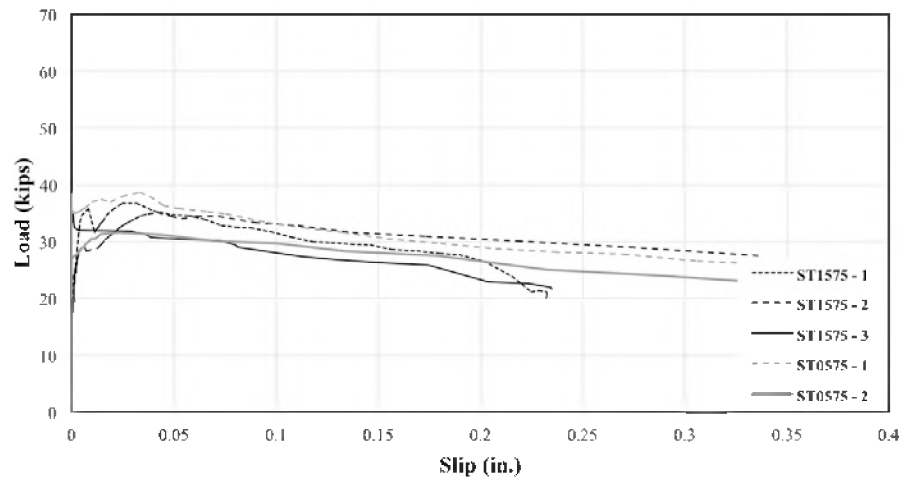
Figure 4-16. ST load-slip curves

| a) | b) | c) | d) | e) |
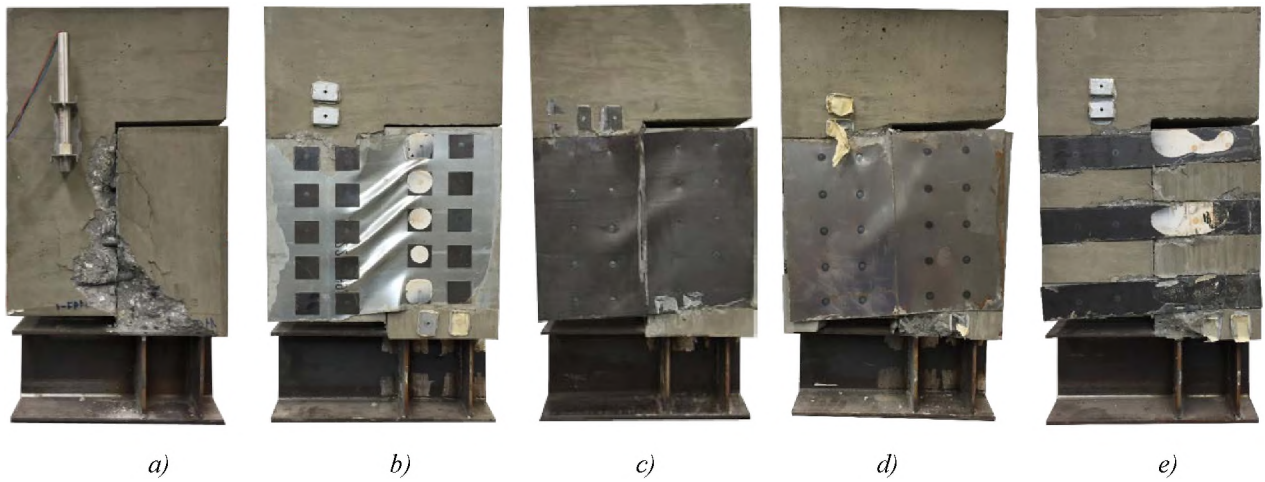
Figure 4-17. Typical failure modes: a) CJ1575-1, b) SP1525-1, c) SP1550-1, d) SP1575-1, e) ST1575-1.
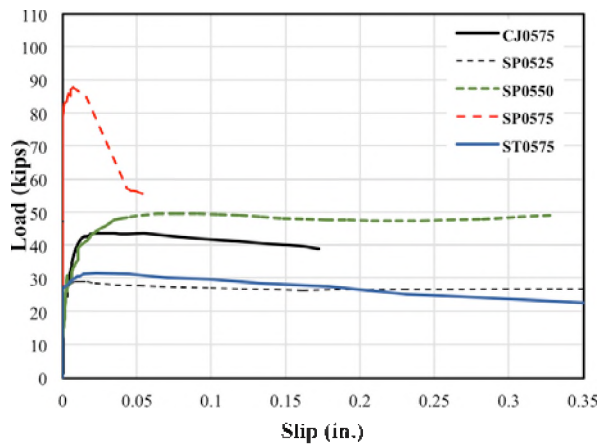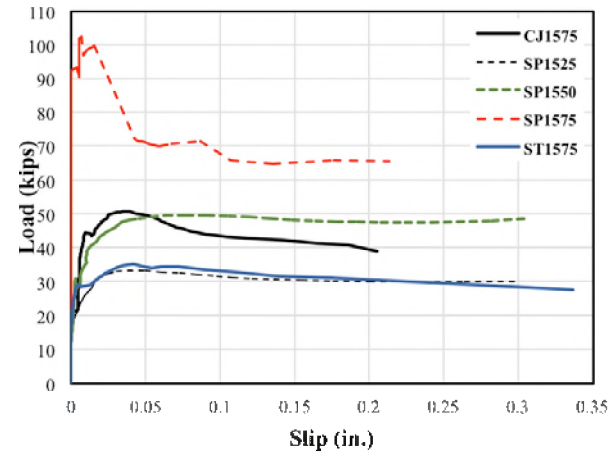
a)   *b)*

Figure 4-18. Load-slip curve comparison: a) 5% LWA, b) 15%LWA
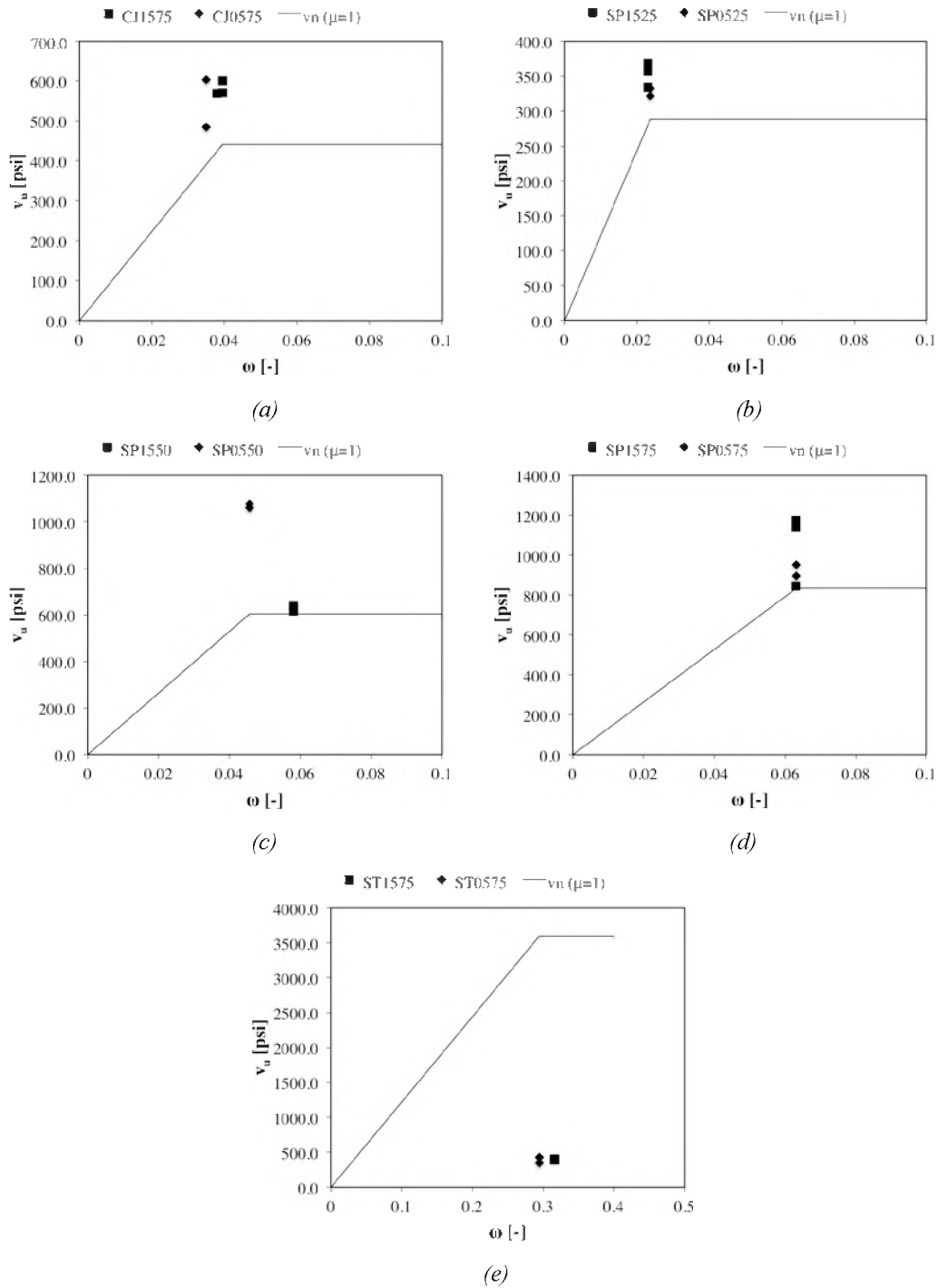
Figure 4-19. Comparison of push-off specimens to ACI shear friction equation, Equation (4-1).

Plate pulls away from concrete

Shear buckling in steel plate

Plate pulls away from concrete
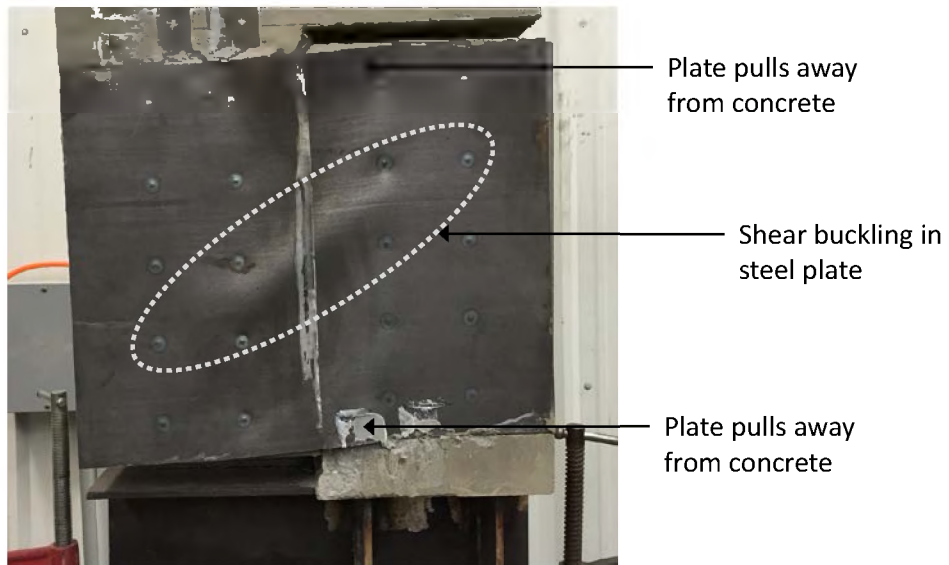
Figure 4-20. Shear buckling of Task 2 Specimen SP 15 50-1.

local bending of steel plate

gap

local crushing of concrete

effective point of fixity
assuming flexural
stiffness of stud without
concrete confinement

theoretical point of stud
fixity in concrete
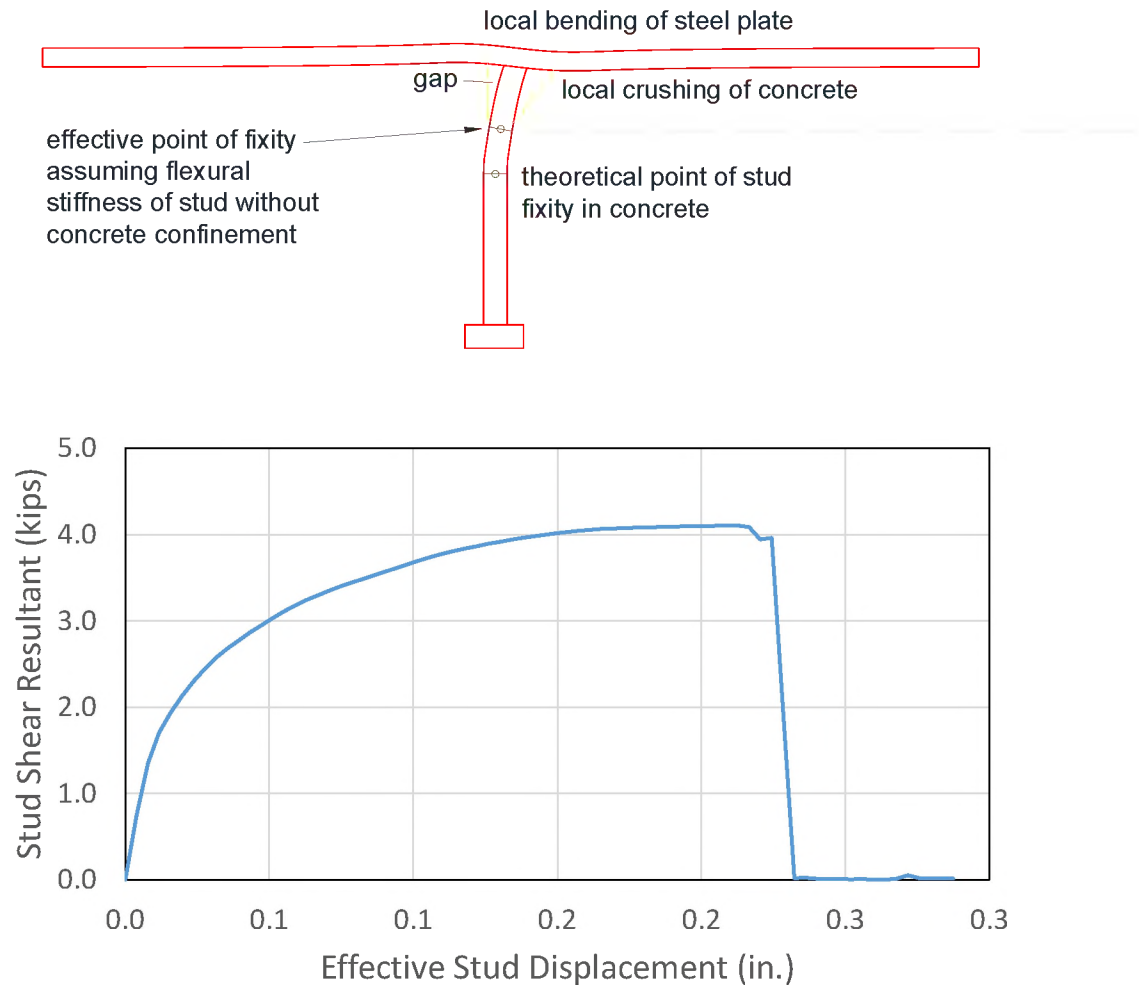
Figure 4-21. Stud in concrete equivalence model and load-displacement behavior.

Figure 4-22: continues over three pages.

(a) Non-linear finite element model in LS-DYNA explicit. This initial model approximate the geometry of specimen SP 15 50-1 but with fewer Nelson studs.

(b) Initital loading. Constant shear in the panel zone. In-plane shear stresses shown (all stresses in Pa).
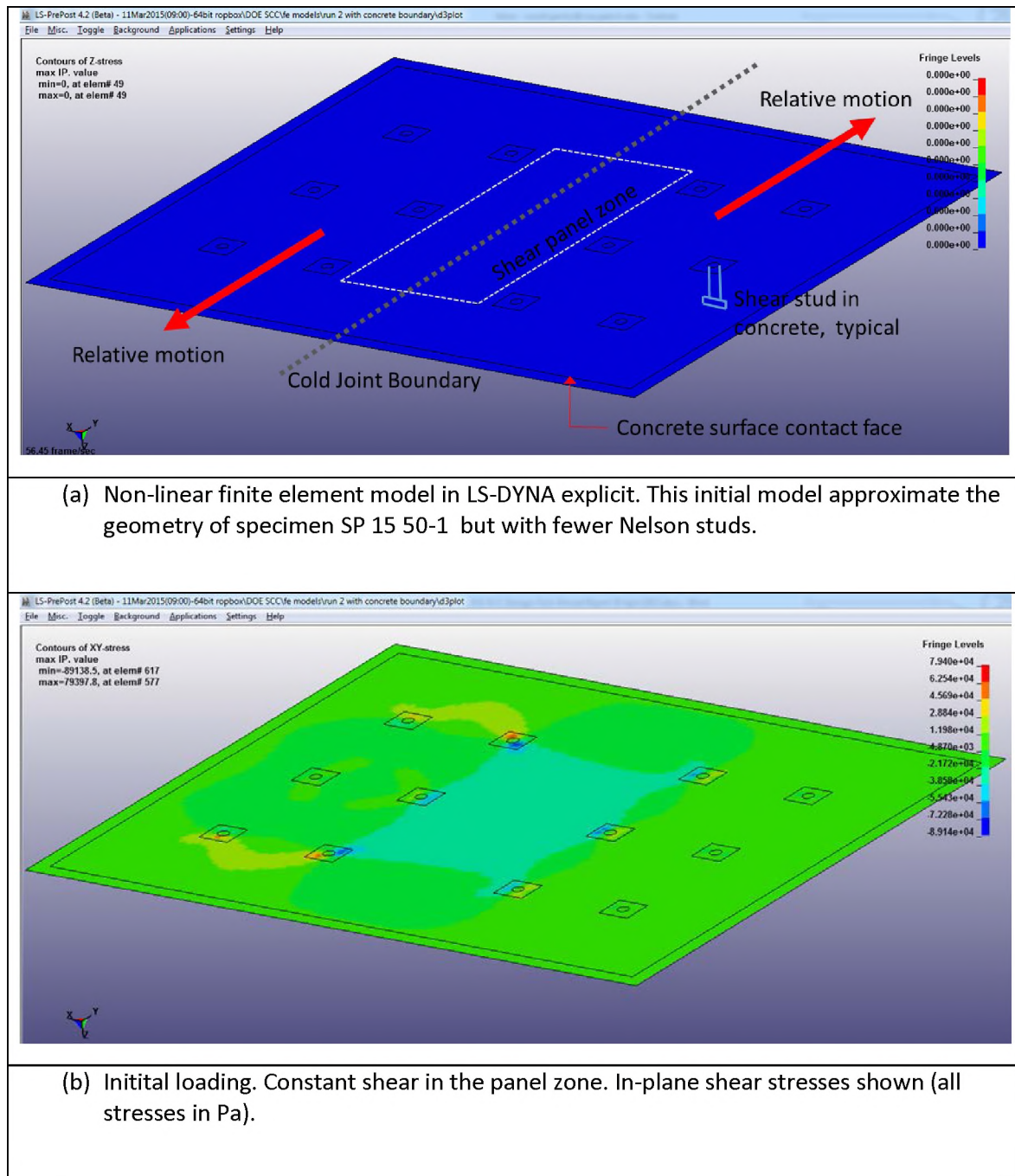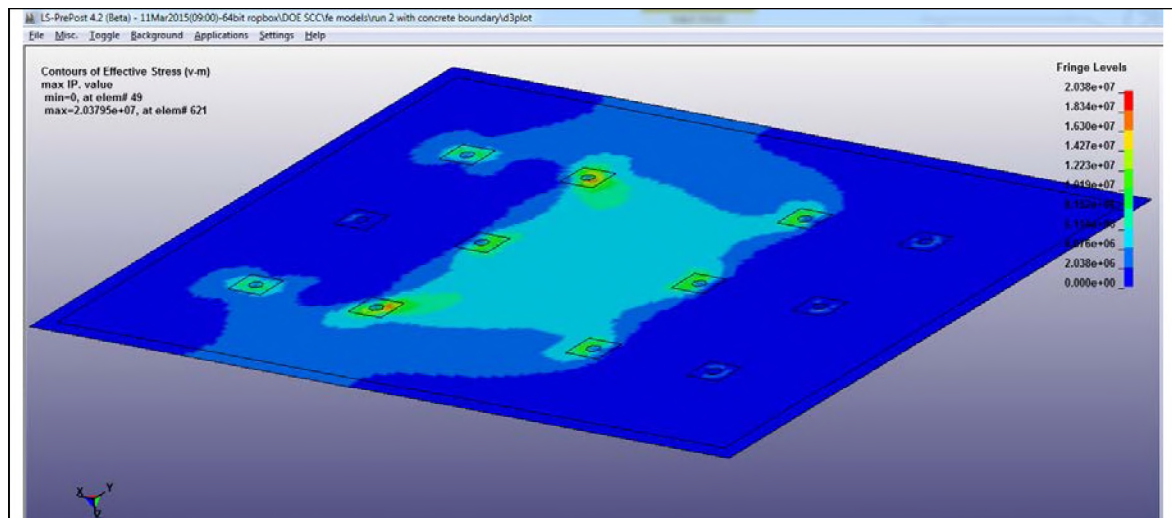
(c) Initial loading. Constant shear in the panel zone. Von Mises stresses shown. Note that outside rows of studs are not participating in the shear transfer.
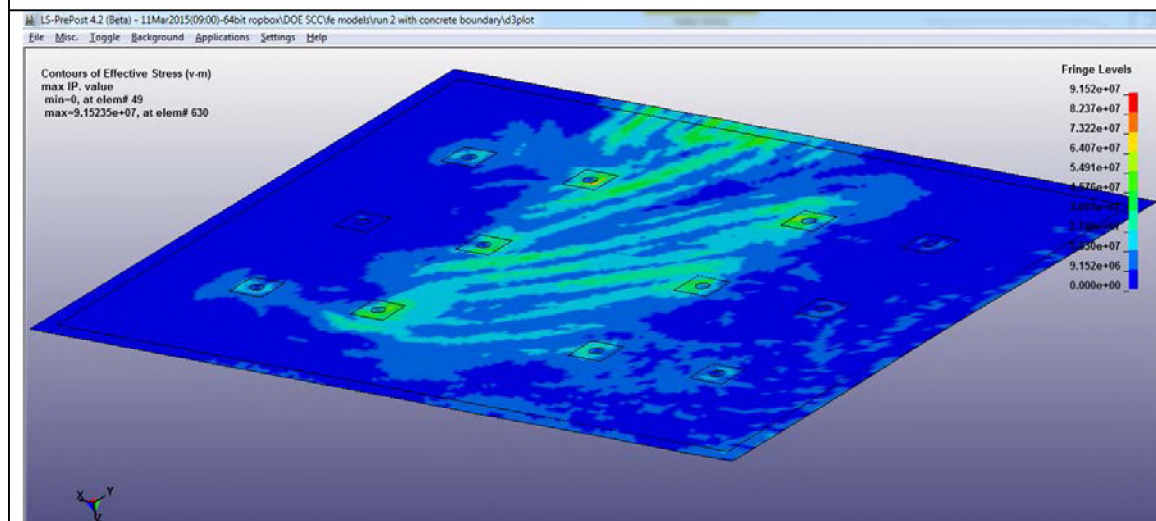
(d) Onset of buckling. Panel zone shear dramatically reduced. Principle tensile stresses align with buckling of plate steel. Buckling is elastic, that is, steel plate does not yield before the bucking initiates. Model also predicts the pulling of the edge of the steel plate.
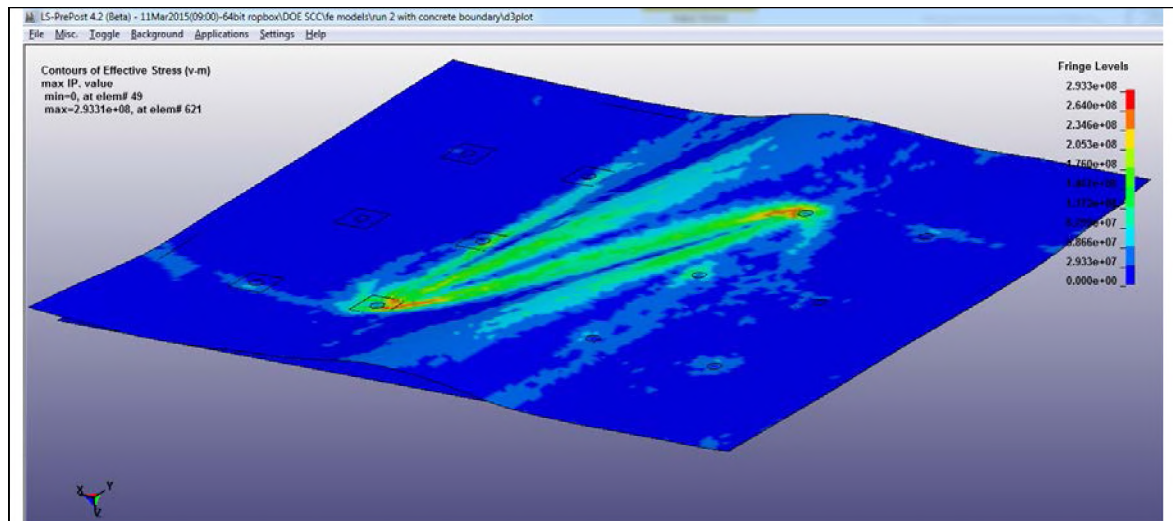
(e) Buckling progresses. Steel plate begins to yield in the vicinity of two studs (see red on stress contour). The buckling distortion as the plate pulls away from the concrete visible along the edges.
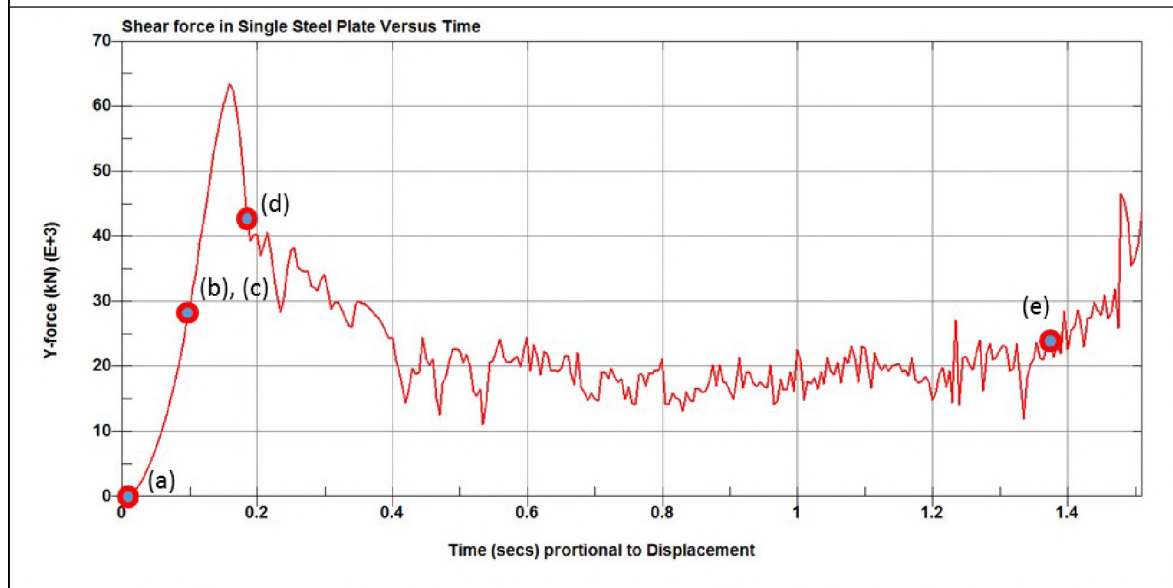
(f) Shear force versus time plot for FE model (note that displacement is proportional to time). Times when stress contour snapshots (a) through (e) are taken are identified on the plot.

Figure 4-22. Results from initial finite element analysis of Task 2 specimens with 0.25% steel plates (steel plate contribution only)

Figure 4-23. Comparison of experimental and FE simulation results for Specimen SPxx25.

5 Task 3 – Assessment of Shear and Flexural Performance

In the project proposal, the discussion focused primarily on using the larger-scale specimens to test steel plate configurations under flexure and shear (where the smaller Task 2 specimens are primarily in shear only). This implied that Task 3 specimens were required to be te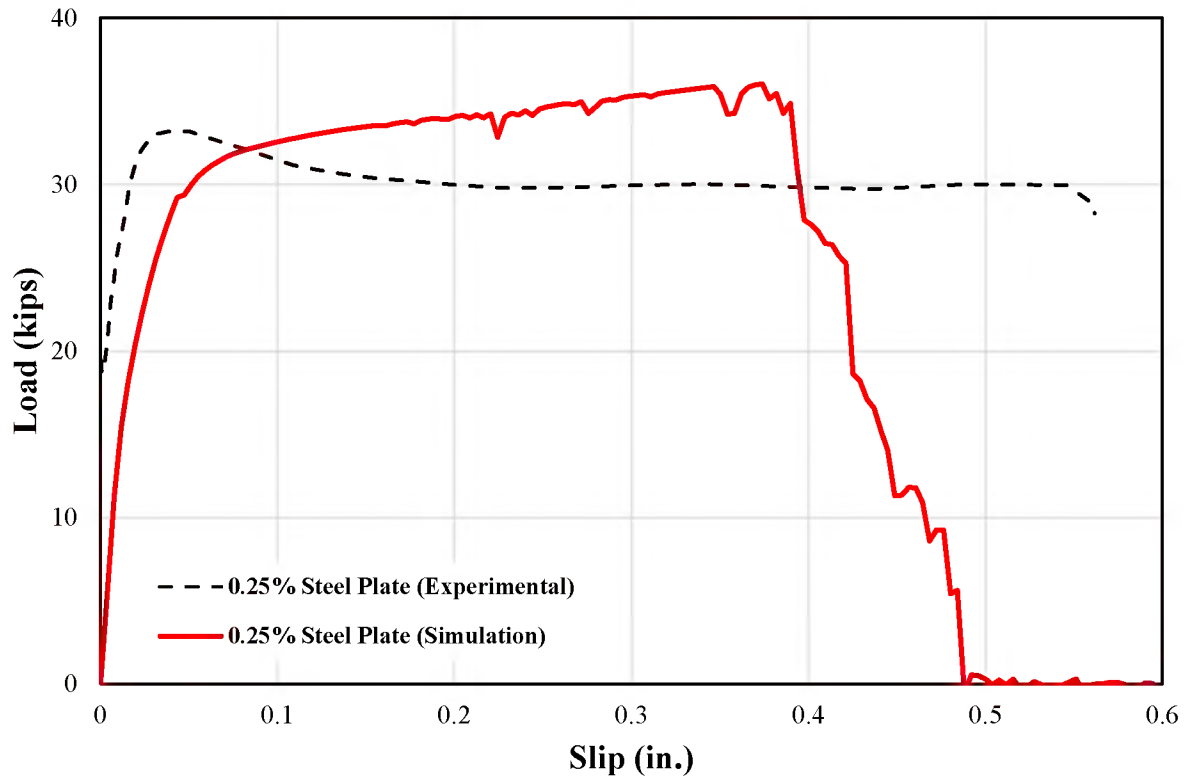sted in order to produce flexure and shear in the steel plates in the plane of the plates. We refer to this condition as in-plane loading. It was also possible to test the specimens to produce out-of-plate loading. In discussions with our industry experts at Westinghouse, it was decided that both in-plane and out-of-plane loadings would be considered for Task 3 specimens, as both types of behavior are important given the wide range of loading conditions applied to modular units (e.g., dead and live loads, seismic loads, blast and containment loading). The effect of in-plane and out-of-plane loading on a modular wall is shown in Figure 5-1. These two loading conditions caused very different behavior in the SC structures that will be addressed in this chapter.

5.1 Test matrix

In Task 3, mid-scale steel plate composite beams, filled with the concrete developed during Task 1 and Task 2, were produced in the Structures Laboratory at Georgia Tech. Tests consisted of six experiments carried out on three beam specimens as shown in Figure 5-2. One of the beams was cast without cold-joints and two beams were cast with cold joints. Each beam specimens was 11 ft. (335 cm) long, with a square cross-section of 18 in. (460 mm) and provided one in-plane and one out-of-plane test article. Two external steel plates installed on opposite sides of the specimens were used as steel reinforcement. The bond between steel plates and concrete was assured by the presents of headed shear studs welded on the steel plates. No internal shear reinforcements was designed for these test as the purpose was to stud the behavior of the cold joint under worst case conditions.

5.2 Materials

The mix design used in Task 3 reflected the developments made during Task 1 and used the same materials. Aggregate properties of the concrete mixture were comparable to the ones reported in Appendix A.

5.2.1 Concrete Mixtures.

The concrete mixture used in specimen construction was the same Task 2 using 15% LWA substitution. SRC mixtures contained Portland cement type 1-2, water, #67 granite coarse aggregates, a blend of 50% manufactural sand and 50% natural sand, and high range water reducers (HRWR). Concrete was produced by a local ready-mix concrete supplier (Thomas Concrete) who adapted our batching and SRC mixing recommendations developed in the Georgia Tech lab (i.e timing of addition of LWA and superplasticizer). At the beginning and end of each batch, concrete flowability and viscosity were determined in accordance with ASTM C1161. Also, five 4x8 in. (100x200 mm) cylinders were cast for every concrete placement. Cylinders were demolded after 24 hours and stored in a fog room where they were kept for 28 days. Compression tests were conducted as per ASTM C39 and the strength values tested consistently around 11 ksi (75 MPa).

5.2.2 Steel plates

Steel plate reinforcement was 0.1875 in. thick with an observed yield stress of 55.6 ksi (380 MPa). Steel plates are bonded to concrete through headed anchors welded to the steel plates using a Nelson Stud Welding system composed of a power supply with a transformer rating of 7600 amps and standard welding gun. The studs were nominal 0.25 in. (6 mm) diameter, 2.75 in. (70 mm) long with a tensile yield stress of 51,000 psi (350 MPa). The number and spacing of studs for each plate was computed in order to meet the AISC N690-12 Appendix N9 requirements. Studs were spaced on a grid of 4.5 in. (115 mm) in the longitudinal and transverse direction (Figure 5-3).

5.3   Specimen preparation

Formworks were designed in order to resist lateral pressure generated by the concrete during casting. In particular, a system of vertical elements (studs) and horizontal elements (wales) was implemented to provide enough confinement along with the use of snap-ties in both directions (Figure 5-4 and Figure 5-5). Concrete was pumped into the specimens in three lifts, with cold-joints formed 20 in. (510 mm) from each end of the beam (Figure 5-6). The cold-joints were placed in a way that allowed the use of each specimen twice. After 28dd, specimens were de-molded and rotated into the horizontal configuration for in-plane and out-of-plane testing.

5.3.1   Observations during casting.

A large part of the "up-scaling" from Task 2 to Task 3 was the transition of the concrete manufacturing from laboratory mixes, made in the Structures Lab at Georgia Tech, to a full-batch mix made at the ready-mix plant. Considerations from the casting are reported below:

-   Concrete needed to leave the plant with a slump spread between 24 to 26 in. (600 and 660 mm) while also passing the "S test".
-   Concrete with slump spread at 26 in. (660 mm) or above leads to uncontrolled separation of the material components.
-   Using a modest dose of retarder the concrete was able to maintain its properties for about one-hour on site.
-   The dosage for HRWR was around 6 ounces per CWT of cement plus fly ash. The dosage was varied slightly for each batch of concrete, to ensure that the SRC left the plant with a slump flow of 25 inches.
-   Once concrete drops to a slump below 22 in. (600 mm) spread it appears to lose its self-roughening properties. These properties can be restored in the truck by adding a small amount of HRWR (around 0.75 ounces per CWT of cementitious materials) directly into the truck and mixing for 5-10 minutes.
-   When concrete poured with the pump above the level of concrete, the last bit of concrete coming from the pump appeared to be heavily mortar rich. This mortar layer could potentially ruin the self-roughening surface by covering the rough surface.
-   Consequentially, the pump hose should be maintained just below the surface of the concrete as it is being placed (like a tremie). This seemed to prevent the separation of the concrete constituents as it comes out of the pump hose and also prevents the formation of the mortar rich layer on the concrete surface.

These observations helped to facilitate the casting during Task 4. Others will be added in Chapter 6 when the manufacture of test specimen of Task 4 is discussed. The development of a SRC was possible only by addressing the construction challenges related to the deployment into a real application.

5.4   Test setup

Figure 5-7 shows the test setup that was used for each specimen. The beam supports were arranged so that end of the specimen that was not under test was protected during the first loading regime. This configuration allowed the possibility to produce two-test articles per specimen.

The Task 4 specimens were placed on roller supports on a 8.5 ft (260 cm) clear span in three-point bending, with the load positioned on a a/d ratio of 2.5, where a represent the distance between the end of the supports and the point of application of the load, and d is the section depth. Thus the point load was located around 45 in. (115 cm) from the cold joint. Instrumentation included a load cell affixed to a hydraulic ram, a displacement device at the point of load application, and an LVDT strain rosette used to measure movement across the cold joint. A set of 3 dial gages were used to assess concrete strain at the point of load application. A set of bonded resistance strain gages were used on the tension side of the specimen to monitor the stress in the steel plate of the module while testing out-of-plane specimens.

Figure 5-8(a) and (b) show the specimens in the load frame in in-plane and out-of-plane configurations, respectively.

5.5 Test results

The in-plane behavior of the Task 3 specimens is depicted in the load-displacement graph shown in Figure 5-9a. The figure shows three experimental results, the expected strength of the specimen as calculated by AISC N690 Appendix N9, and the expected strength from an analytical model. The model calculation accounting for the non-linear behavior of the steel and concrete and shows an essentially tri-linear behavior: high stiffness until cracking of the concrete in tension, an almost imperceptible loss of stiffness that occurs when the concrete first cracks in tension, and a significant loss in stiffness when the steel yields. An example of the modeling procedure is reported in Appendix C.

All of the experiments show higher strengths than either the N690 prediction or the model. This is a significant and positive test result. The monolithic specimen without cold joint, MO-IP, shows the highest strength and ductility. The first in-plane specimen with a cold joint, CJ-IP-1, shows good behavior with a high strength and good ductility. The second in-plane specimen, CJ-IP-2, slightly reduced ductility but with good overall performance.

The out-of-plane behavior of the Task 3 specimens is shown in Figure 5-9b. Once again the figure shows three experiments along with the capacity calculated from AISC N690 Appendix N9 and from non-linear beam theory. In this case, the monolithic out-of-plane specimen (MO-OOP) failed prematurely, reaching a capacity of only 58 kips. This is an artifact of retesting the monolithic specimen earlier in in-plane loading as the beam actually continued to fail at the prior point of in-plane distress, even though this was distant from the loading point. We fully believe that the monolithic specimen would demonstrate good behavior if it were not pre-cracked. The first cold-joint specimen, CJ-OOP-1, demonstrated excellent behavior, with a capacity greater than predicted by AISC N690 N9 and by the analytical model along with good ductility.

The second cold-joint specimen, CJ-OOP-2 did not perform as well. Though the specimen did reach the predicted flexural strength, once it did it failed dramatically and the ultimate failure mode (shown in Figure 5-10 (a) and (b) comes from the failure of the Nelson stud welds as depicted in Figure 5-10 (c). Figure 5-11 (a) and (b) shows a comparison between out-of-plane monolithic and cold joint specimen behavior. In the case of no cold joint, the force travel from the point of application of the load to the support following a straight path. In the case of a cold-joint, at the beginning the stress propagate similarly to the monolithic (same crack angle) up to the cold join. Once there, the crack propagates down thought the joint and from there travels down into the steel plates causing the shearing of the studs. The full flexural capacity of the section is achieved in this specimen, but the post-yield behavior could be improved.

Upon examination of the surface of the joint on this specimen, a rather slick and non-roughened cold joint was observed. We determined that this slick cold joint resulted from a lens of concrete with little coarse aggregate that resulted from the end of a concrete pour using a concrete pump. As the concrete pumping operation ceased, the pump is throttled back and the large aggregate comes through the pump quickly, leaving a mass of mortar (sand, cement and water) left in the pipe to discharge into the mold. This has the potential to cause a weakness adjacent to the cold-joint, which is a highly undesirable outcome.
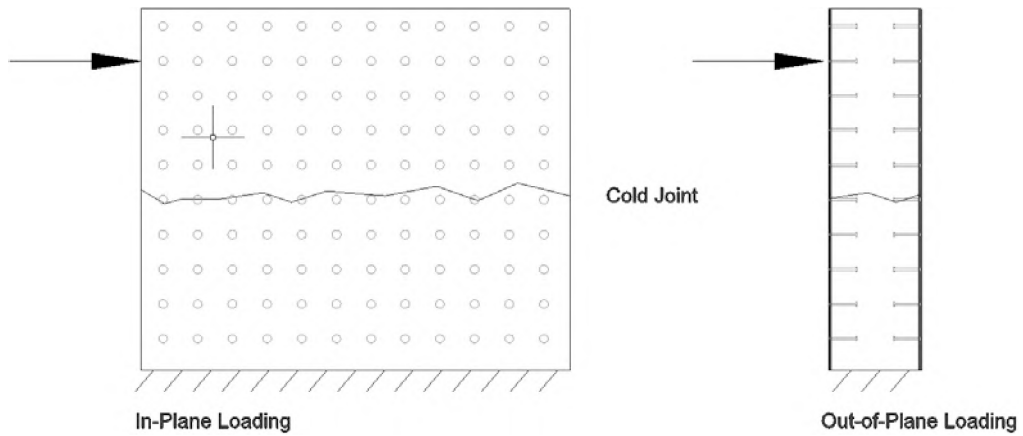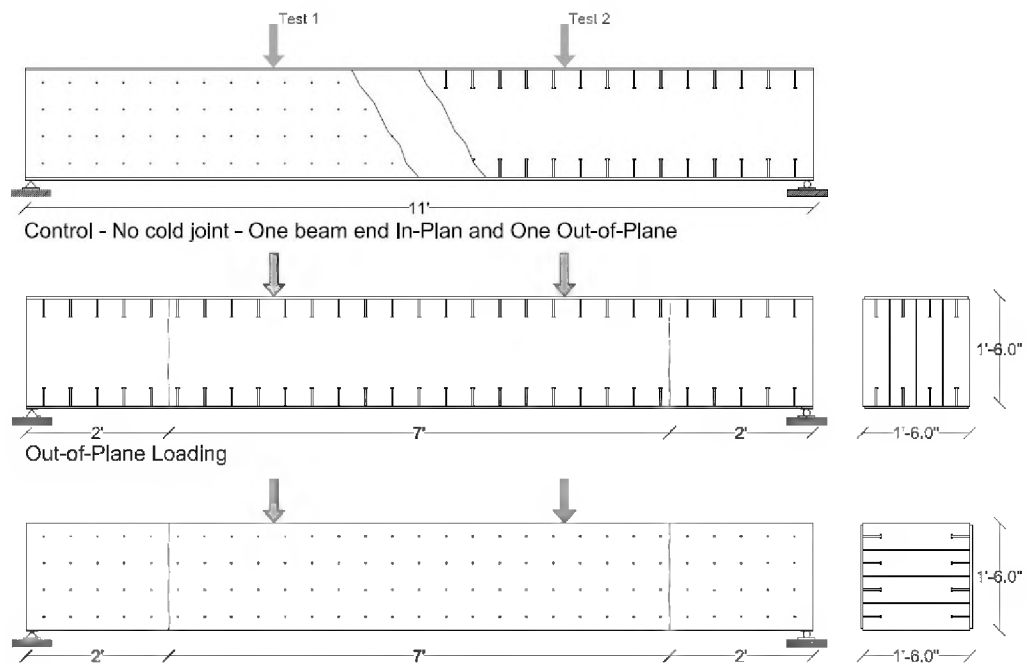
Figure 5-1. In-Plane and Out-of-Plane loading

Figure 5-2. Task 3 Specimens

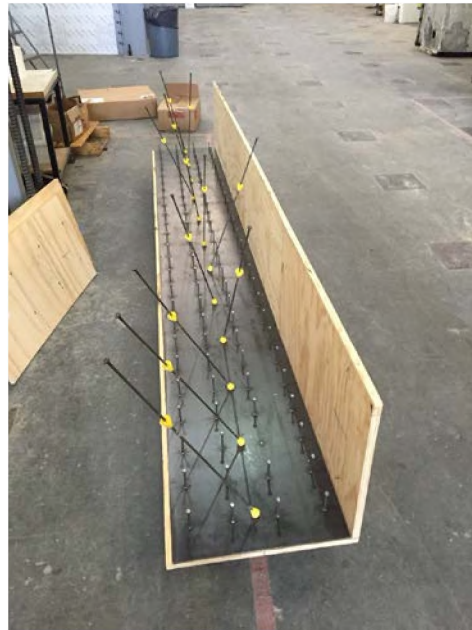<div align="center">a)   b)</div>

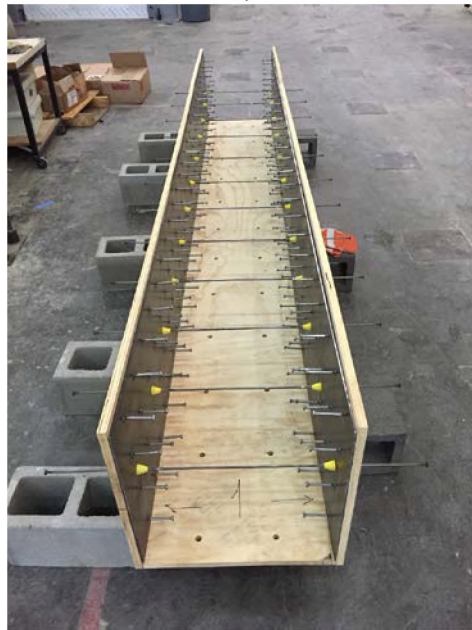*Figure 5-3. Steel plate preparation a) and studs configuration b)*

a)

b)

c)

d)

e)

Figure 5-4. Formwork preparation.

a)

b)

Figure 5-5. Formwork preparation 2: a) snapties, b) wales

Concrete placement 3

Concrete placement 2

Concrete placement 1

Figure 5-6. Concrete placement for Task 3 specimens.

a)

b)

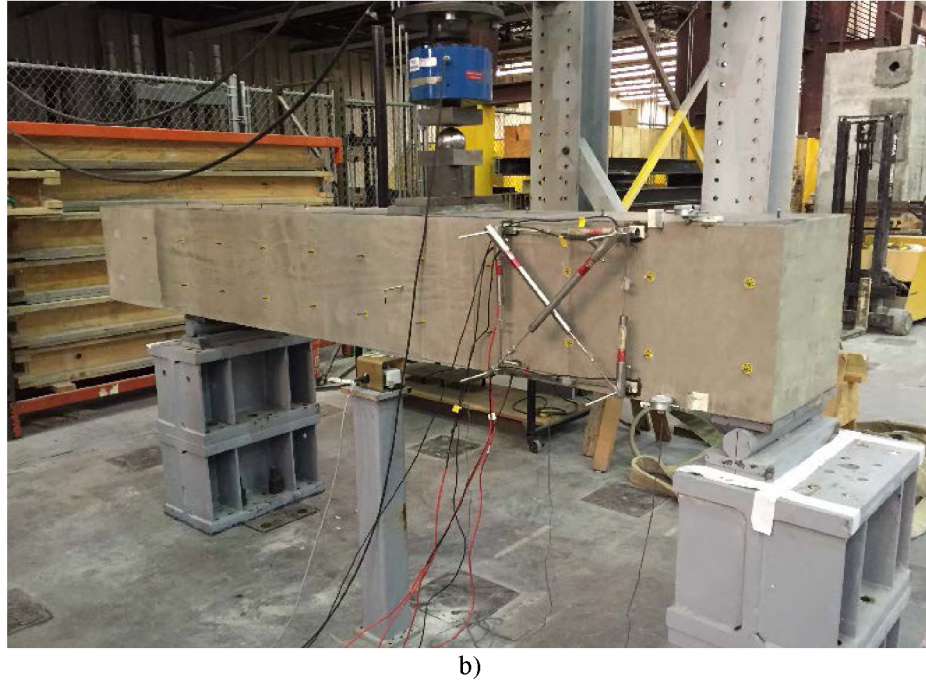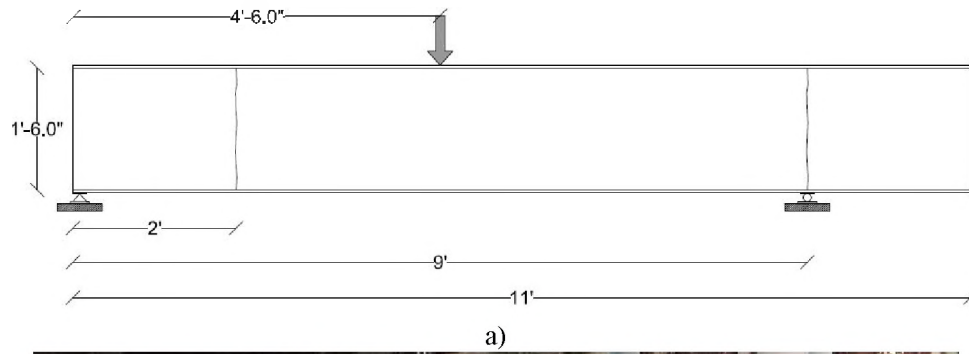*Figure 5-7. Task 3 test setup.*

a)   b)
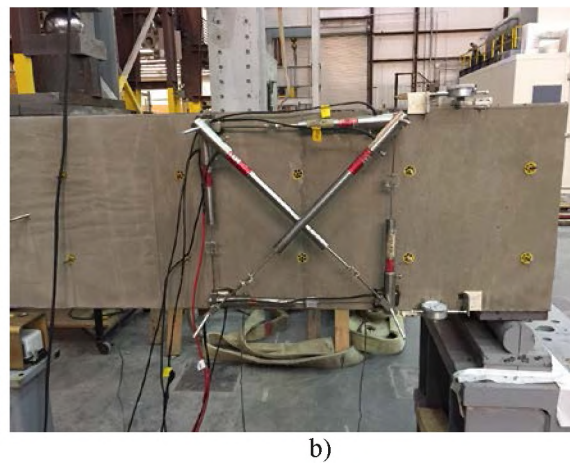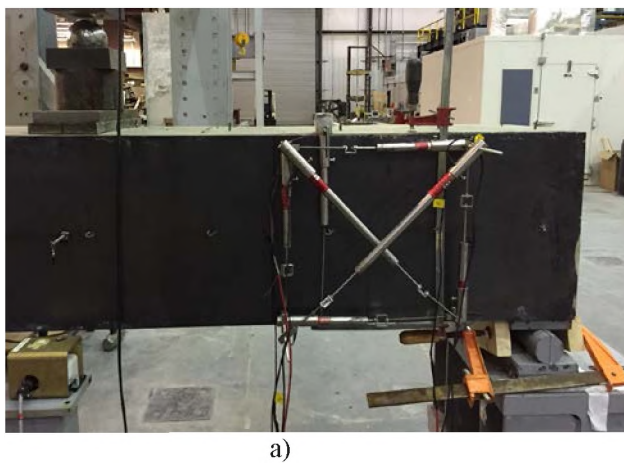
Figure 5-8. Test setup: a) In-Plane, b) Out-of-Plane
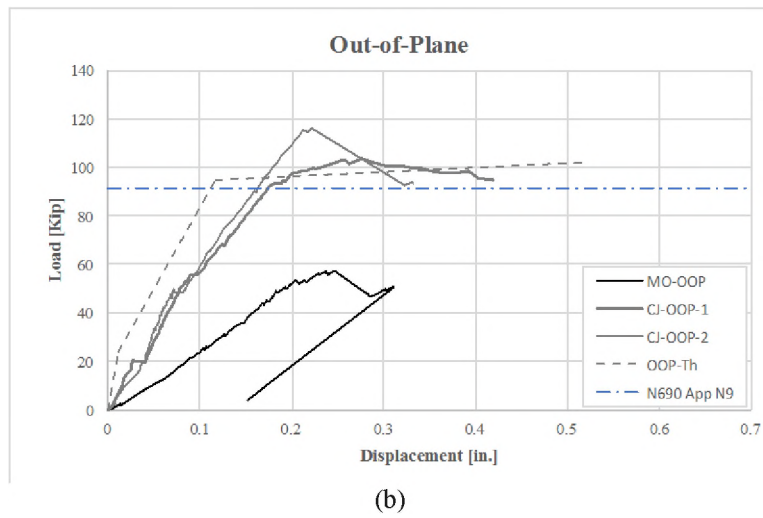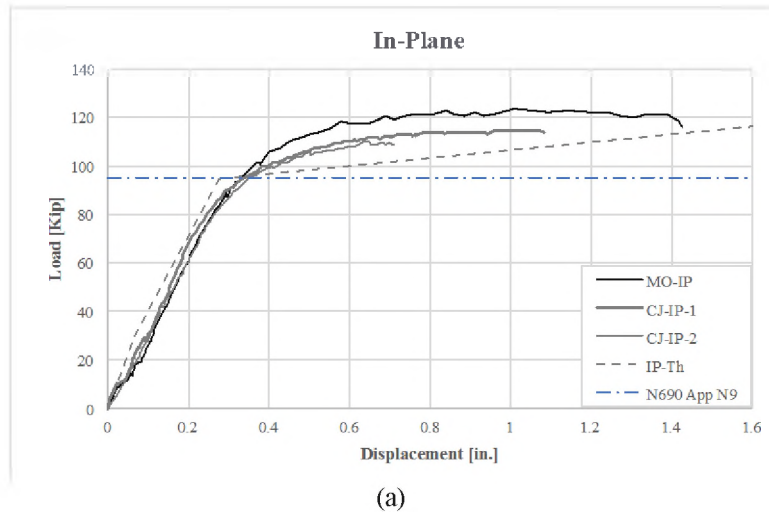
(a)

(b)

Figure 5-9. Test results: (a) In-Plane, (b) Out-of-Plane

(a)

(b)

(c)

Figure 5-10. Failure mode: a) In-Plane, b) Out-of-Plane, c) detail of stud shearing off

(a)

(b)

Figure 5-11. Force transfer: (a) monolithic, (b) with cold joint

6 Task 4 – Validation through Full-Scale Testing and Modeling

In Task 3 we explored the failure of concrete and steel modular units at cold joints. The mid-size specimens used in Task 3 were approximately one-half the scale of the modular units currently used in the AP 1000 reactor buildings. The full-scale Task 4 specimen was received directly from Westinghouse was cut from a C20-06 module constructed for validation of the modules currently being installed in the Vogtle and V.C. Summer plants.

6.1 Description of the Task 4 Test Article

The Task 4 specimen was received from Westinghouse on March 7, 2016. This C20-06 module was fabricated at Oregon Iron Works and a section of the module (Figure 4-1) was cut and shipped to Georgia Tech. The test article was 26 ft. 6 in. (810 cm) long, and had a cross-section of 3 ft. (90 cm) wide by 2 ft. 6 in. (75 cm) deep (Figure 4-2). The module had the typical steel angle longitudinal members and steel channel members used to retain the two faces of the module. Steel studs, 3/4 in. x 6 in. (19 mm x 150 mm) on a nominal 6 in. (150 mm) square grid spacing pattern, were welded to both interior faces of the module (Figure 4-3).

6.2 Construction of the Task 4 Test Article

Georgia Tech constructed formwork for the test article to enclose the two open sides of the module. The module was then affixed vertically to the strong wall of the structures lab, in preparation for concrete placement (Figure 4-5). The self-roughening self-consolidating concrete developed in Task 1 of the project was placed into the beam in three lifts, with cold-joints formed 6 ft. (180 cm) from each end of the beam (Figure 4-6). The cold-joints were placed so as to be mid-way between the steel channels separating the two faces of the module plates. We considered this to be the worst-case scenario, so that any potential slip across the cold-joint boundary, as was seen in the Task 3 specimens, would be carried only by the concrete, and not bridged by the steel channel. When the concrete had cured 10 days, the specimen was removed from the wall and rotated into the horizontal configuration for flexural testing (Figure 4-4).

6.3 Concrete Materials and Placement

As in Task 3, the self-roughening SCC was supplied by a ready-mix supplier, Thomas Concrete. Georgia Tech worked with Thomas Concrete to tailor the concrete mix for production in a ready-mix environment – as opposed to the laboratory mixes that were used in Task 1 and Task 2. This were significant changes and findings associated with making the mix at the plant – and additional lessons learned with the three concrete pours made during Task 4. These are as follows:

1. It was necessary to add a set retarder to the concrete mix to ensure working time for concrete transport. Sika Plastiment retarder at a dose of 1.5 ounces per hundred pounds of cementitious materials (cement plus fly ash) was added to the mix.
2. It may be necessary to add an additional dose of superplasticizer and a small amount of water at the site.
3. Some segregation can be anticipated if the slump exceeds 27 inches. This occurred in the last concrete placement for the Task 4 specimen (Figure 4-7). Note that the segregation did not impact the structural test as the first cold joint, which did not show this segregation, was tested.
4. Concrete placement for most modular reactors will be by concrete pump. We used a professional concrete pump service for Task 3 and Task 4. We observed that the SCC placed by pump is subject to creating a mortar rich slurry near the end of a given lift of concrete. As the pump ceases operation, the large aggregate exits the pipe first, and a quantity of mortar follows. This mortar may cover the large aggregate, including the lightweight aggregate, which should form the surface of the cold joint. It is therefore suggested that the pipe leading into the modular unit be at all times just below the surface of the concrete, and any mortar placed inadvertently goes beneath the surface of the placement.

6.4   Testing of the Task 4 Specimen

The Task 4 specimen was placed on roller supports in the 1 million pound test frame (4500 kN) in the structures lab. The specimen was tested in out-of-plane flexure/shear as the Task 3 specimens showed that these were the most critical configurations for cold-joint performance. The specimen was tested on a 20 ft. (610 cm) clear span in three-point bending, with the load positioned 8 ft. (240 cm) from the end of the beam (Figure 4-9). Thus the point load was 2 ft. (60 cm) from the cold joint. Figure 4-10 shows the specimen in the million pound load frame.

Instrumentation included a load cell affixed to the hydraulic ram, a displacement device at the point of load application, and an LVDT strain rosette used to measure movement across the cold joint. A set of 3 dial gages were used to assess concrete strain at the point of load application. A set of bonded resistance strain gages were used on the tension side of the specimen to monitor the stress in the steel plate of the module.

6.5   Initial Test Data and Interpretation

The structural test described above has just been completed as of this writing. The interpretation of the test results is therefore preliminary, and will be expanded upon in the final project reports.

Figure 6-10 depicts two key sets of data from the experiment. In the upper graph, the load-displacement data is shown. As shown in this graph, the specimen behaves linearly up to a load of between 200 kips and 250 kips (890 kN and 1110 kN). A simple calculation shows that the net shear stress in the beam at this time is around $2(f'_c)^{1/2}$, which is generally taken as the contribution of the concrete to the shear strength of a reinforced concrete beam. At this point the specimen begins to lose stiffness, but continues to carry an increasing load. A secondary stiffness is noted on graph of the load-displacement relationship. At a load of around 650 kips (2890 kN) an additional and more significant loss of stiffness occurs, and the behavior of the beam becomes essentially plastic. Significant ductility is noted in the specimen, and the specimen continues to carry load on a slightly increasing slope as the displacement continues to increase.

The lower graph in Figure 6-10 depicts the load versus strain behavior. The location of the two strain gages is shown in Figure 4-9. Interpretation of the strain data is somewhat difficult, as the steel plates at the bottom of the beam are in global tension due to flexure of the specimen, as well as local bending as the concrete in the vicinity of the gages cracks. The most useful gage is the load point gage (blue line) on the graph. The simplest interpretation of this gage is that it indicates the onset of flexural yielding of the specimen (650 kips - 2890 kN). This is confirmed by the modeling of the specimen, discussed below.

The second strain gage in the lower graph (orange line), depicts the strain gage on the tension plate just under the cold joint. This strain gage shows a significant event at a load level of around 400 kips (1780 kN). As this point a diagonal shear crack propagated down from the load point and intersected the cold joint. The crack then ran vertically down the cold joint. We conclude that the increase in strain in the plate at this load level comes from the local debonding of the steel plate in the vicinity of the cold joint, which leads to the spread of the tension in the plate from the point of maximum moment (at the load point) to the point of debonding (at the cold joint).

Figure 6-11 depicts the readings from the two vertical and two horizontal LVDTs that cross the cold joint (see Figure 4-9 for LVDT numbering). The readings from LVDTs 2 and 4 capture the formation and opening of shear cracks that pass through the cold-joint zone. LVDT 2 also captures the closing of shear cracks that occurred late in the loading regime, at a point when other flexural cracks opened at other locations in the beam. The readings from LVDT 1 are quite small, and indicate the compressive strain in the concrete at the top of the beam. These readings are quite noisy and the large offset in LVDT 1, at the 400 kip load level, represents a slip in the transducer on the support, and not a tensile strain in the concrete. LVDT 3 captures the opening of the cold joint on the tension side of the beam.

Crack patterns in the beam are shown in Figure 4-11. The initial cracks in the beam were flexural cracks, primarily vertical, that formed at a spacing of about 10 inches along the bottom of the beam. The first shear crack occurred with a significant release of energy and spread from the load point down diagonally to the mid-height of the cold joint. At that point the crack ran vertically down to the bottom steel plate. As the plate was loaded further, the shear crack began to spread down past the and across the cold joint, maintaining its original angle of about 30 degrees with the horizontal (see green dashed line in the figure). At a later point a second major shear crack occurred, largely parallel with the first.

The cracks indicate the formation of a compression strut between the application of the load point and the steel channel in the module (shown in blue in the figure). This strut would be described as a CTT (compression-tension-tension) strut and is held in equilibrium by tension in the steel plate at the bottom of the beam and tension in the vertical steel channel. Note that this is an important finding, because it recognizes the contribution of the steel channel, which is designed to cross the module faces to carry the hydrostatic loading due to construction, but is not usually considered for structural loading capacity.

6.6   Modeling of the Task 4 Specimen

It is beyond the scope of the project to assess or develop new methods of calculating the flexural and shear strengths of SC modules. The focus is on developing simple calculations, in keeping with AISC N690 Appendix N9, that will aid in the placement and assessment of cold-joints in the modules. To model the results of the Task 4 specimen, a series of three flexural capacity calculations were made. The model with the largest flexural capacity is then used to assess with the shear capacity of the module, calculated at the cold-joint and considering the possibility of cold-joint failure, is sufficient to develop the flexural capacity of the module.

These calculations were based on idealized cross-sections as shown in Figure 4-16. In Figure 4-16(a), only the two steel plates are considered. The flexural capacity of the section is calculated as 2,655 kip-feet (3600 kN-m) assuming a steel yield stress of 60 ksi (415 MPa) (from data supplied by Westinghouse). In Figure 4-16(b), the two steel plates and the continuous steel angles are considered. The flexural capacity of the section is calculated as 3,229 kip-feet (4377 kN-m) assuming that the steel plate and the four angles are fully yielded.

Finally, in Figure 4-16(c), the two steel plates and the transformed area of the concrete in compression is considered. In this instance the flexural capacity of the section is calculated to be 3,854 kip-feet (5225 kN-m). The neutral axis location and moment-curvature relationship for the section shown in Figure 4-16(c) is depicted in Figure 6-14. The predicted capacity of the beam in three-point bending, taken from the calculated moment-curvature relationship (803 kips or 3571 kN), is close to the observed peak load from the test (738 kips or 3282 kN, see Figure 6-10). We anticipate that the 10% observed over-prediction in strength is due to the fact that the beam is failing in shear at the end of the test, and that the theoretical plastic moment, that is the complete yielding of the steel plates and the angles, is not achieved during the test.

Using the flexural strength from the calculation, the shear demand on the joint can be calculated. It is proposed that a modified strut and tie model (STM) as is used in the ACI 318 Building Code Requirements for Structural Concrete (Figure 6-15). The compressive capacity of the strut will be a function of the compressive strength and roughness characteristics of the concrete across the cold-joint boundary.

6.7   Task 4 Conclusions

The Task 4 specimen test was successful and necessary to validate the overall findings of the research project. Completion of this task delayed the project by 3 months, due to the need to procure the full-scale module from Westinghouse and complete the preparations for this major test in our laboratory.

It is clear that full-scale testing is necessary for validation, even though mid-scale testing such as that completed in Task 3 was critical in highlighting the behavior of in-plane versus out-of-plane bending and the potential problems that can occur when poorly roughen cold joints are used.
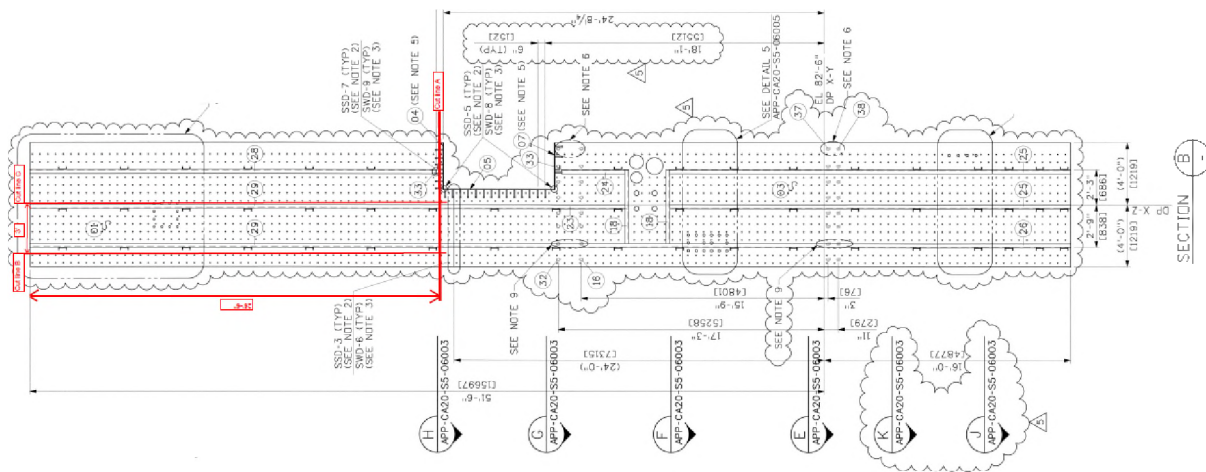
Figure 6-1: CA20-06 module supplied by Westinghouse and portion cut and shipped to Georgia Tech.

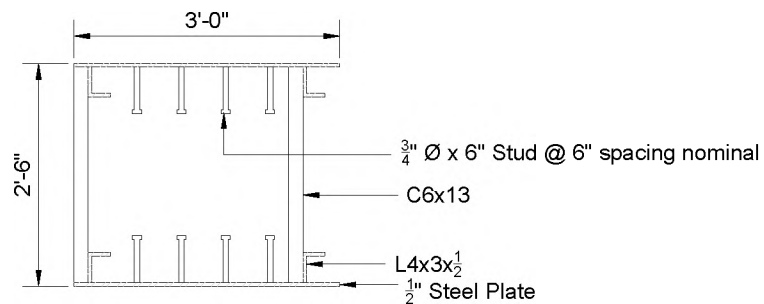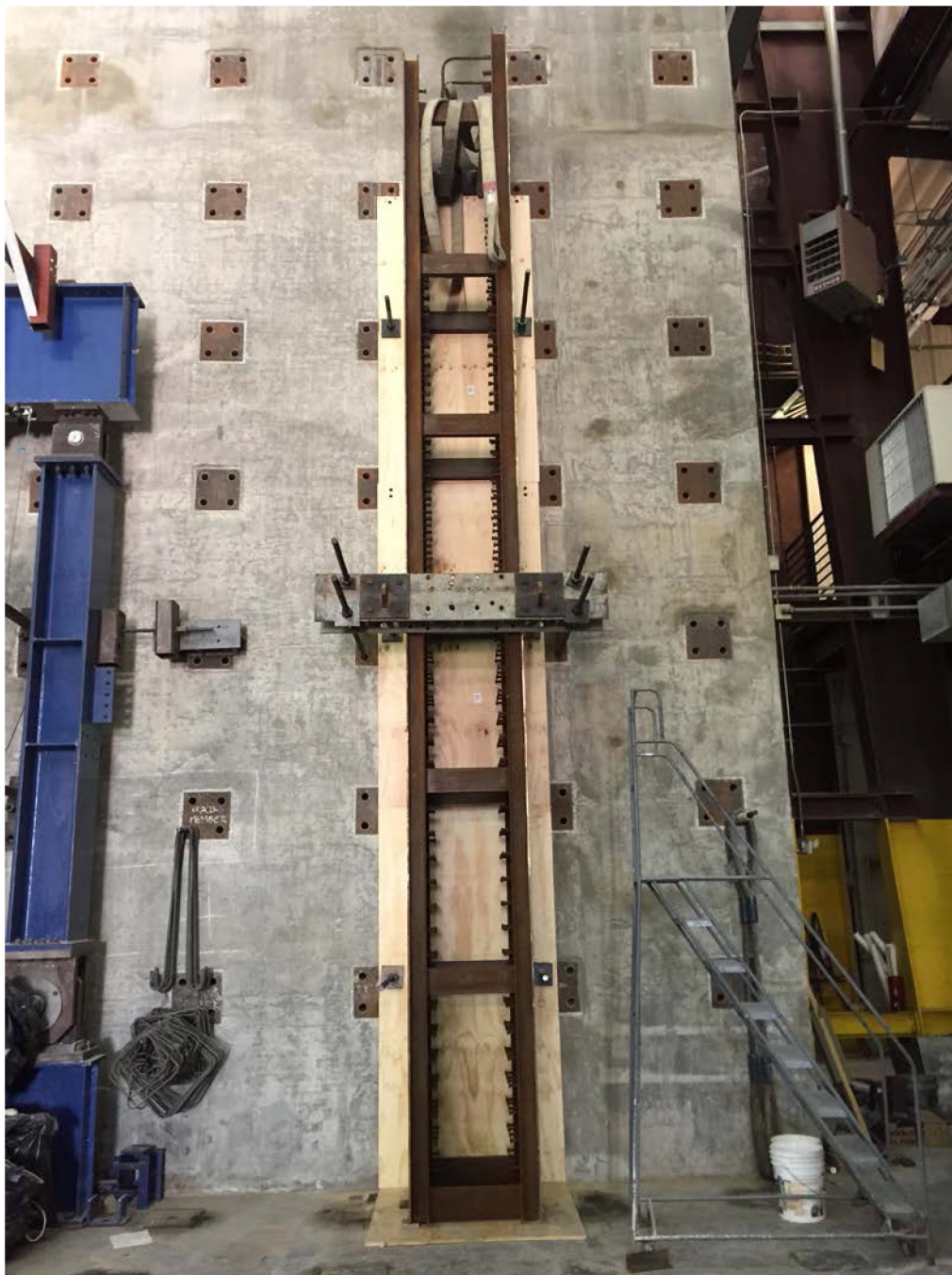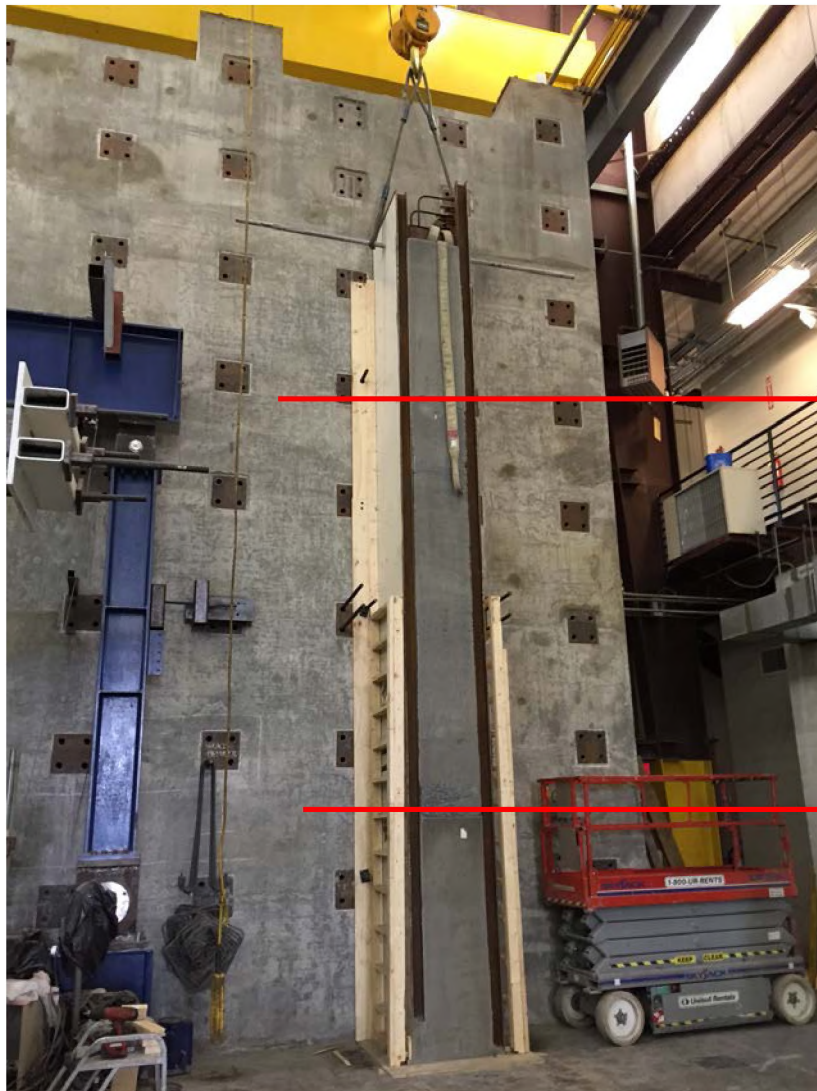*Figure 6-2: CA20 module section as received from Westinghouse.*

Figure 6-3. Cross-section of the section cut from the CA20 module.

Figure 6-4. CA20 module affixed to strong wall.

Figure 6-5. CA20 module filled with concrete placed in three lifts, forming two cold-joints.

Figure 6-6. CA-20 module rotated into the horizontal position.

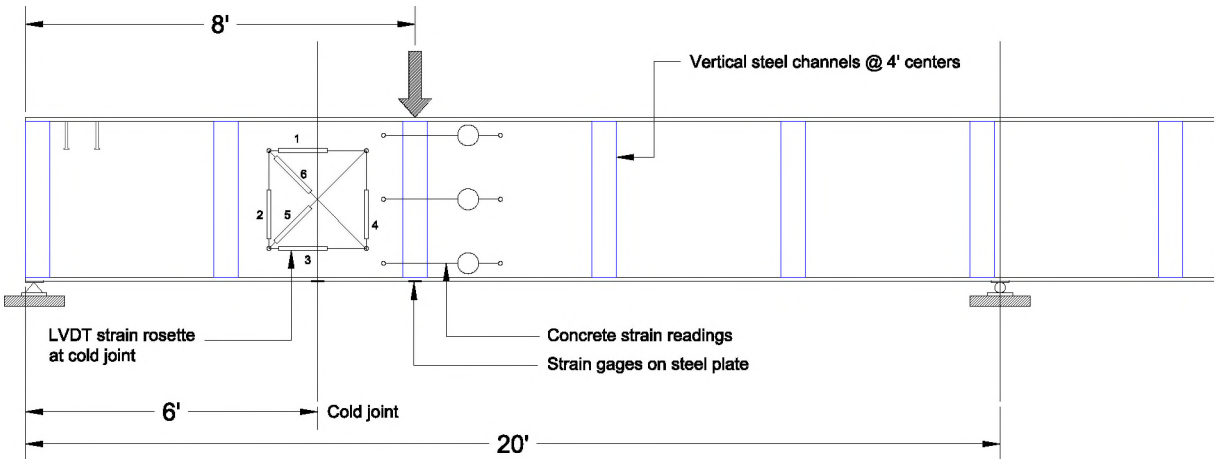*Figure 6-7. Segregation in SCC due to excessive slump.*

Figure 6-8. Task 4 specimen, test configuration and instrumentation.

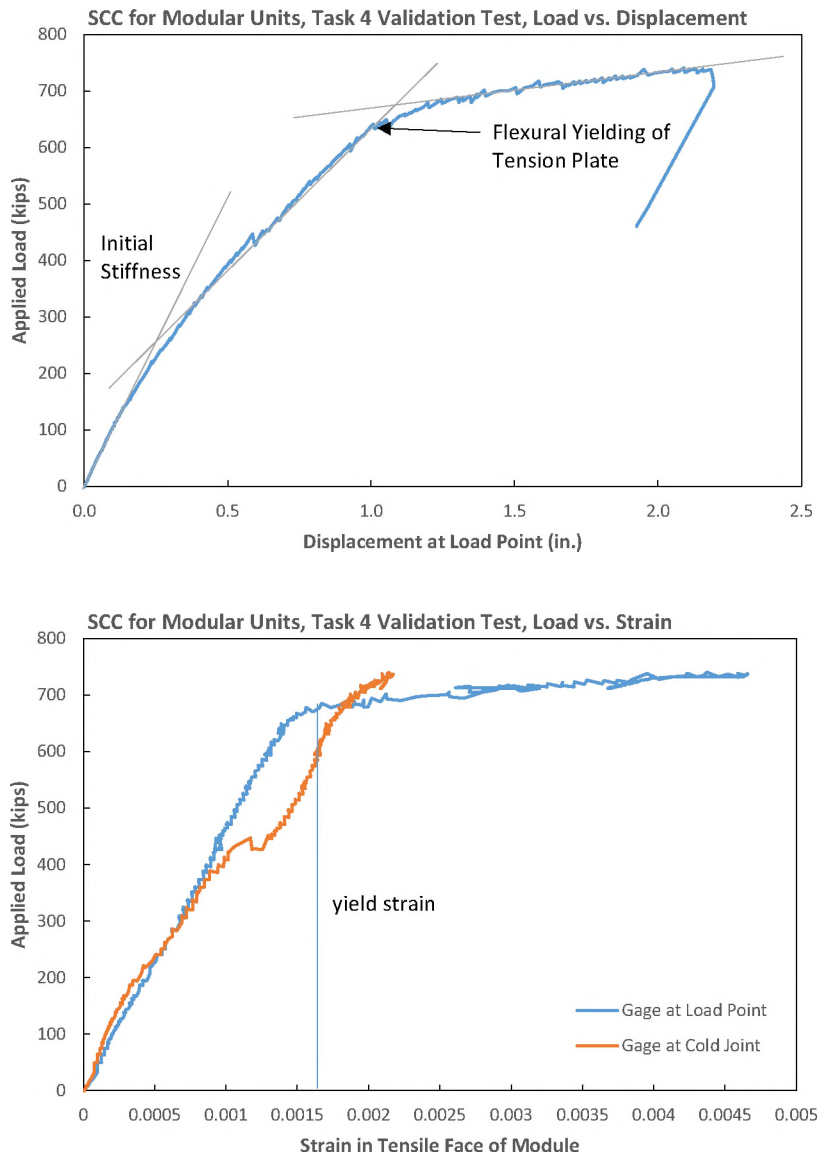*Figure 6-9. Task 4 specimen in test frame.*

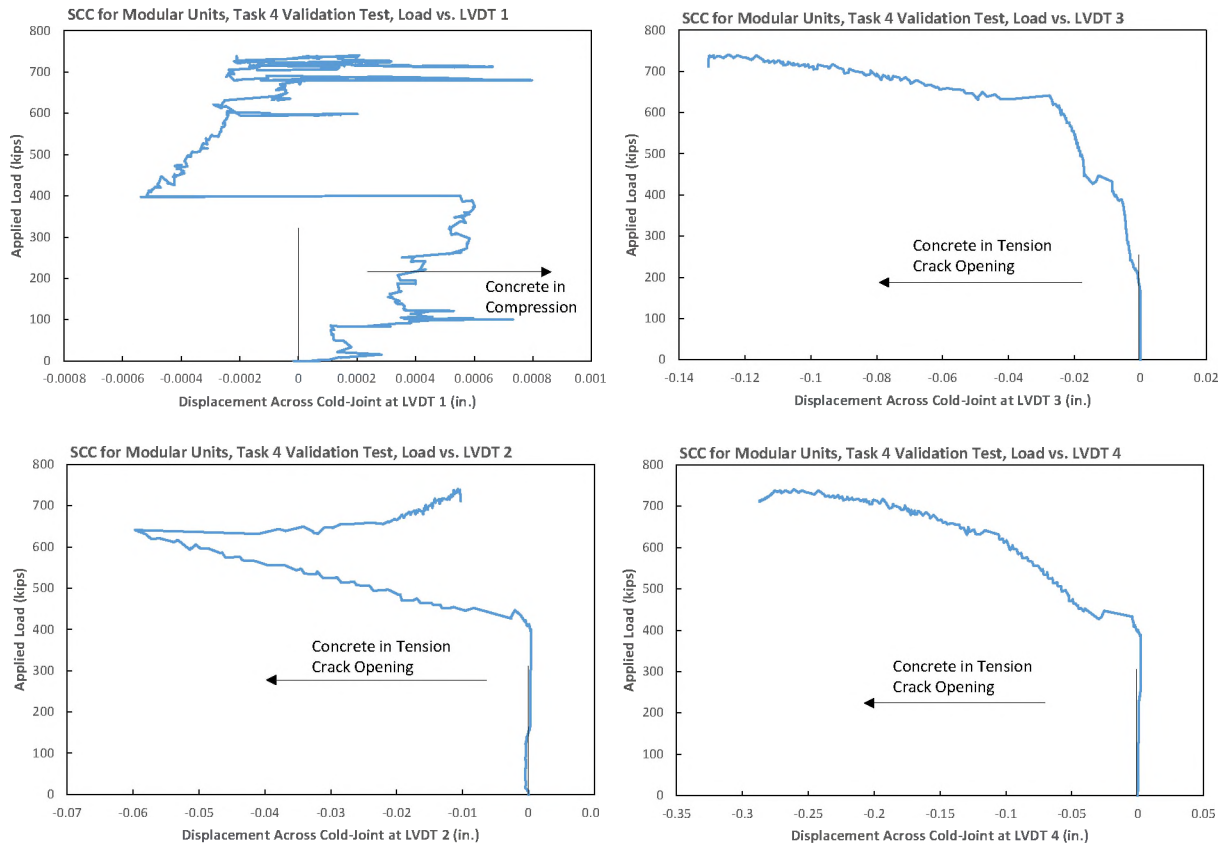*Figure 6-10. Task 4 load-displacement and load-strain test results.*
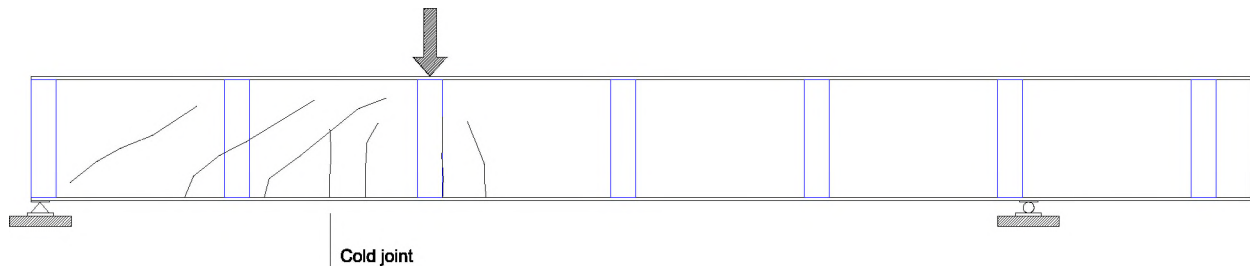
Figure 6-11. LVDT measurements at the cold joint.

Figure 6-12. Crack patterns in the failed specimen.
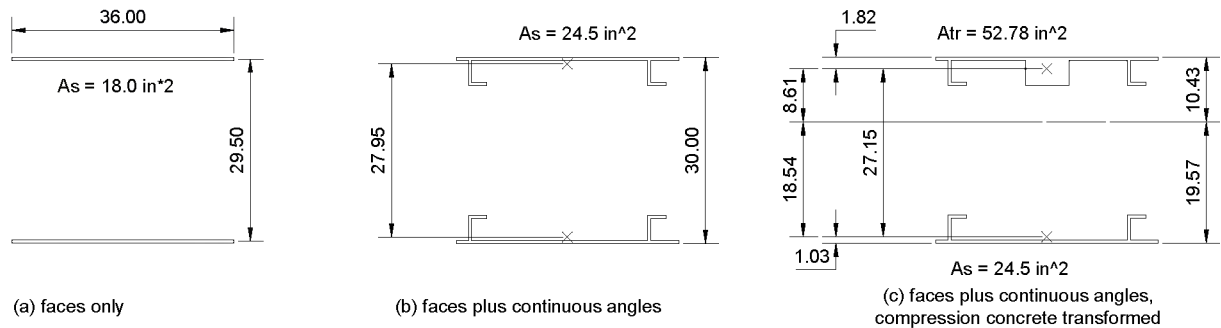

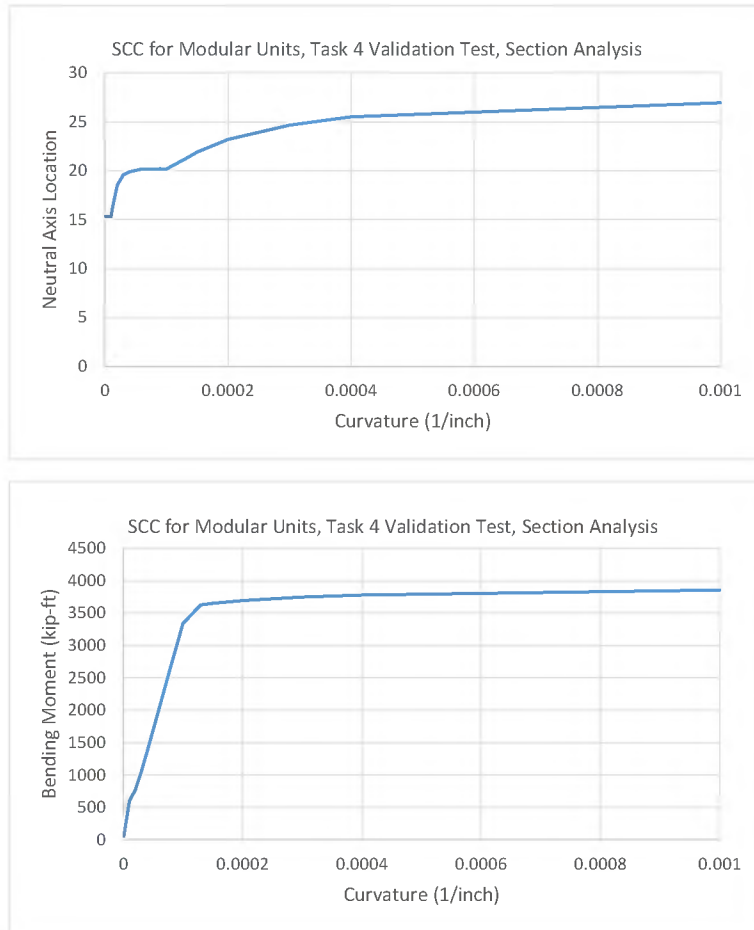*Figure 6-13. Simplified flexural modeling of the Task 4 specimen.*

Figure 6-14. Calculated neutral axis and moment-curvature relationship for Task 4 specimen.
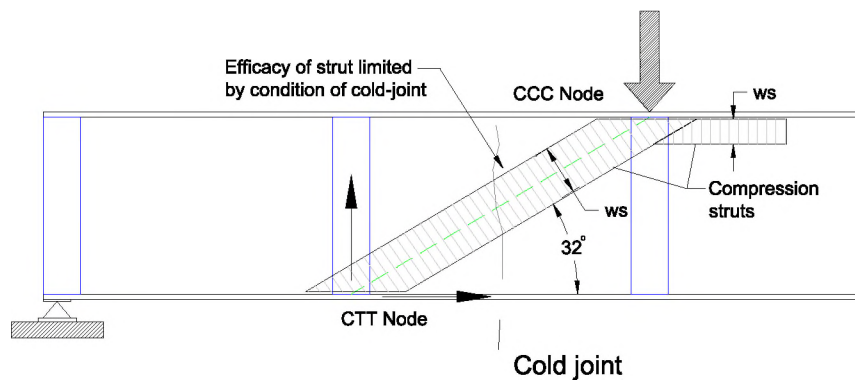

Figure 6-15. Proposed strut and tie model (STM) for modular unit.

7 Task 5 – Draft Code Requirement for Shear Friction Design of Cold Joints

In comparison to the four major experimental tasks, Task 5 is relatively minor but of critical importance. Task 5 intends to provide guidance to AISC 690 Appendix N9, Specification for Safety-Related Steel Structures for Nuclear Facilities (Including Supplement No. 1), the design standard for steel plate composite structures used in nuclear reactor structures.

First, it is important to note that some of these recommendations go beyond the scope of AISC 690 N9, which is a design standard. Many of the observations and conclusions that we have made during the project focus on concrete mix design, the staging of construction, and the specifics of concrete placement inside of SC modules. These recommendations have relevance to SC construction, but should be consider as edits to material specifications, construction specifications, and not to AISC 690 N9 itself.

7.1 Recommendations specific to AISC 690 N9:

1. We see no need to limit the compressive strength of the concrete to 8 ksi (55 MPa) as given in Section N9.1 1(e). We note that self-consolidation concrete used in this research is often stronger than 8 ksi due to the high fraction of Portland cement and supplementary cementitious material used in the mix design. If the code committee is trying to control a balance between concrete and steel ratios, higher strength concrete can easily be accommodated. A limit of 12 ksi might be more reasonable.

2. Section N9.4 describes the design of connections but it is not made clear whether the acknowledgement of a cold-joint in the concrete structure is to be considered a connection. If the designer concludes that the cold-joint met the requirement for a connection, then the strength requirements of Section N9.4.1 come into play and the SC structure must be strengthened in the vicinity of the cold joint. We do believe that such strengthening is necessary, but rather that a calculation of shear demand and capacity at the cold-joint needs to be made. In many cases such a calculation will demonstrate that no capacity increase is necessary.

3. Two methods of force transfer across the cold-joint boundary are possible. One is the traditional shear friction concept that was the basis for our proposal to DOE and is found in Chapter 22 of ACI 318-14. The second and perhaps more promising proposal is to develop a strut and tie model approach to assess the force transfer (in flexure and shear) across a cold-joint boundary. This concept was identified in our Task 4 report dated 11 May 2016. This is something that we feel should be developed, but the full development of strut and tie models for SC structure is beyond the scope of our project.

4. Currently, the AISC N690-12 Appendix N9 code used for the design of SC modular currently has no shear-friction provisions. Shear-friction provisions are given in ACI 349-06, "Code Requirements for Nuclear Safety-related Concrete Structures". Figure 4-19 clearly shows that ACI shear friction provisions are able to establish the capacity of push-off specimens with cold-joint.

   A linear regression analysis was performed on a subset of the Task 3 data sets (specimens in the SP15 and SP05 series, see Table 4-5), in order to calculate values of μ for these cases.

   Figure 7-1 shows the linear regression for the cold joint specimens (SP) in terms of ω and ρ. The equations of the regression line are found to be:

$$v_u = 13.5\,\omega + 0.10 \qquad (ksi) \qquad\qquad (7.1)$$
$$v_u = 80.7\,\rho + 0.10 \qquad (ksi) \qquad\qquad (7.2)$$

The intercepts of the equations are quite close to zero, as expected, meaning that with no reinforcing crossing the cold-joint boundary we expect the capacity of the cold joint to be essentially zero.

The conversion of ω to ρ is made taking the steel yield stress to be 60 ksi and the concrete strength to be 10 ksi, both typical of the Task 3 specimens. Again, given a steel yield stress of 60 ksi for the steel plate, the effective coefficient of friction is calculated to be 80.7 / 60 or 1.35. This is well above the ACI recommendations for 1.0 for intentionally roughened surfaces in internally-reinforced concrete. We therefore conclude that externally-reinforced steel composite plate construction, having cold-joints intentionally roughened using SCC, can use a coefficient of friction of 1.35 for the strength calculations of cold joints.
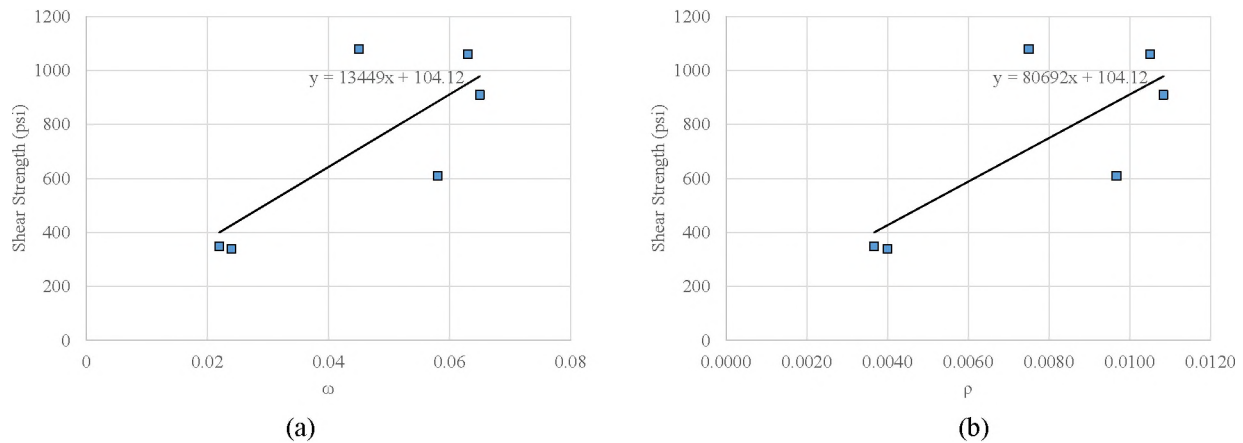

(a)   (b)

Figure 7-1. Relationship between external reinforcement ratio and shear strength,
used to establish effective coefficient of friction (psi units).

7.2   Other Recommendations

The recommendations are most appropriately applied to the material and construction specifications for SC structures. For SC structures used in nuclear reactors, which is the focus of this research, these documents are likely proprietary, and the Georgia Tech team is making these recommendations generically, without access to the underlying specifications.

1. Self-consolidating concrete should be allowed in the construction of SC modules. Limits should be placed on the lower and upper bounds of slump as determined by ASTM C1611. At this point we recommend a slump range of 20 to 25 inches.

2. Self-roughening self-consolidating concrete is advantageous at cold joint. But, for self-roughening to be successful, a rather high slump flow of the concrete mix must be maintained. In this case a slump range in the range of 22 to 25 in. is recommended. It is also recommended that the slump be monitored periodically during concrete placements.

3. Upon examination of the surface of the joint on one of the Task 3 specimens, a rather slick and non-roughened cold joint was observed. We determined that this slick cold joint resulted from a lens of concrete with little coarse aggregate that resulted from the end of a concrete placement using a concrete pump. As the concrete pumping operation ceased, the pump is throttled back and the large aggregate comes through the pump quickly, leaving a mass of mortar (sand, cement and

water) left in the pipe to discharge into the mold. This has the potential to cause a weakness adjacent to the cold-joint, which is a highly undesirable outcome.

To limit this possibility, we recommend that the pipe from the concrete pump be kept at a few inches below the surface of the fresh concrete as the concrete is being placed. This promotes continuous mixing of the concrete and will prevent the smooth cold joint encountered in Task 3. Note that we applied this procedure during the production of the Task 4 specimen, and did not have a problem.

Appendix A – Self-Roughening Concrete Constituent Material Data

#67

Gradation curve for Coarse aggregates
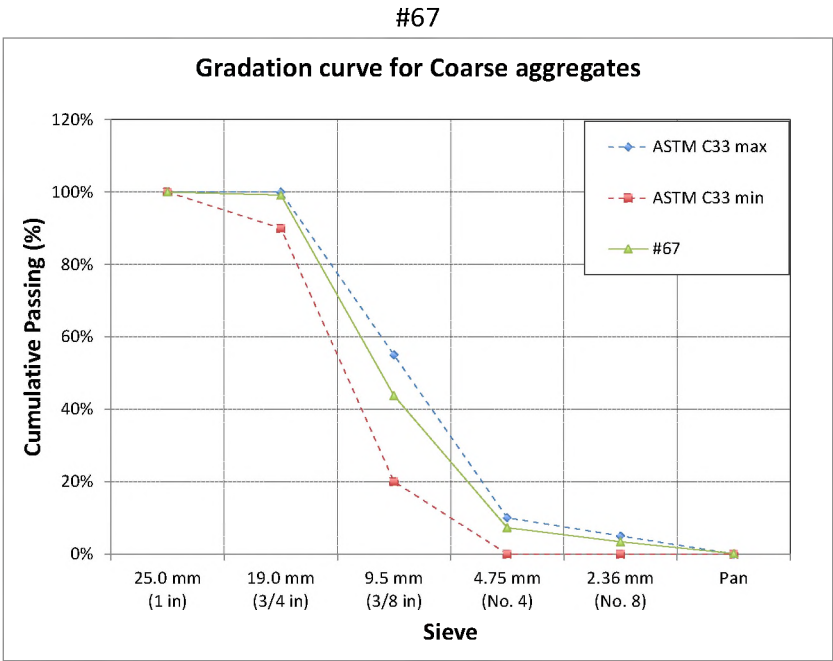
Finesses Modulus: 6.46

No. 100	No. 50	No. 30	No. 16	No. 8	No. 4	⅜"	¾ "	1 ½"
150 μm	300 μm	600 μm	1.18 mm	2.36 mm	4.75 mm	9.5 mm	19 mm	37.5
1	2	3	4	5	6	7	8	9

⋀

PHYSICAL CHARACTERISTICS OF #67 VULCAN AGGREGATE

Density
• Dry Loose (ASTM C29)   96 lb/ft³ (1538 kg/m³)
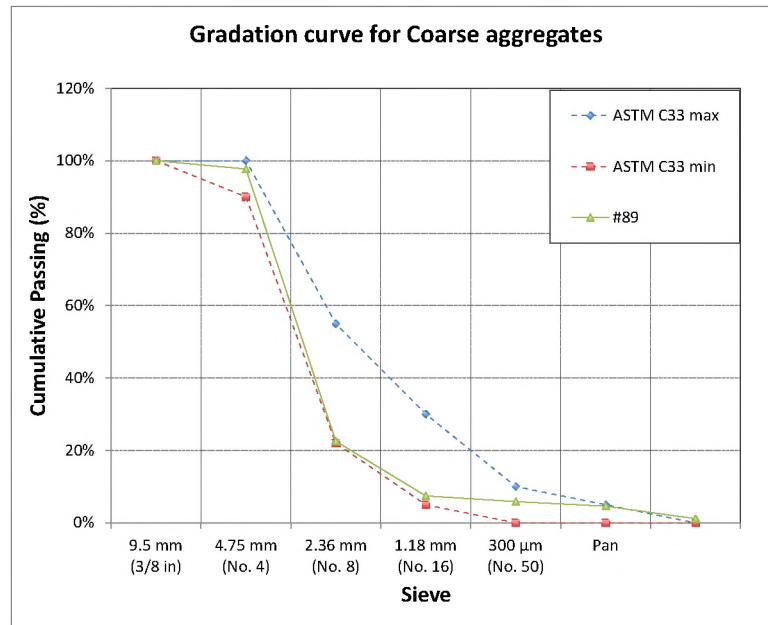• Saturated Surface Dry Loose (ASTM C29)   102 lb/ft³ (1633 kg/m³)

Specific Gravity
• Dry (ASTM C127)   2.75
• Saturated Surface Dry (ASTM C127)   2.80

Absorption
• Saturated Surface Dry (ASTM C127)   0.51%

#89

Gradation curve for Coarse aggregates

Finesses Modulus: 5.62

No. 100	No. 50	No. 30	No. 16	No. 8	No. 4	⅜"	¾ "	1 ½"
150 µm	300 µm	600 µm	1.18 mm	2.36 mm	4.75 mm	9.5 mm	19 mm	37.5
1	2	3	4	5	6	7	8	9

∧

PHYSICAL CHARACTERISTICS OF #89 VULCAN AGGREGATE

Density
• Dry Loose (ASTM C29)   92.3 lb/ft³ (1479 kg/m³)
• Saturated Surface Dry Loose (ASTM C29)   98.0 lb/ft³ (1570 kg/m³)
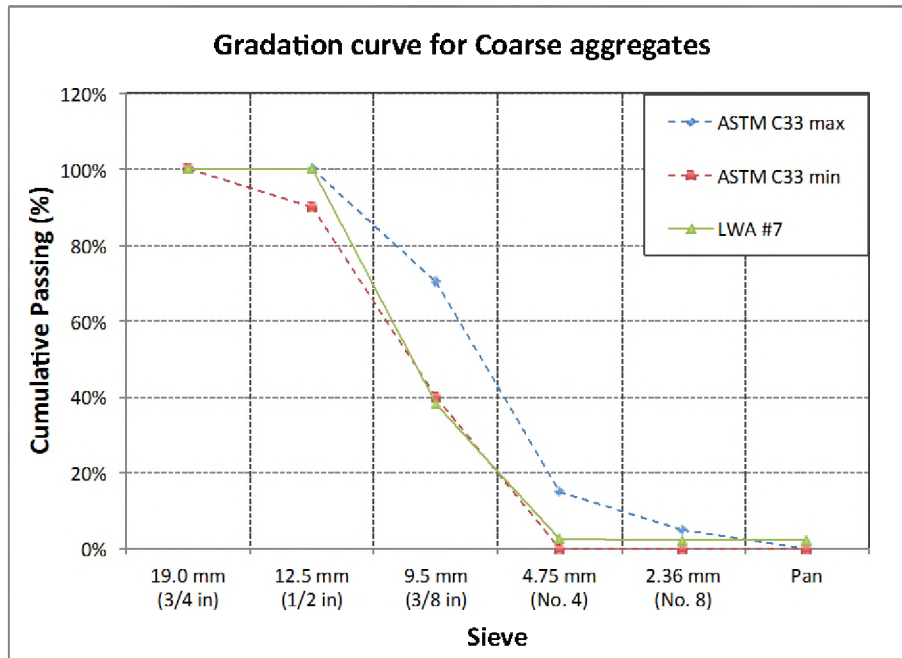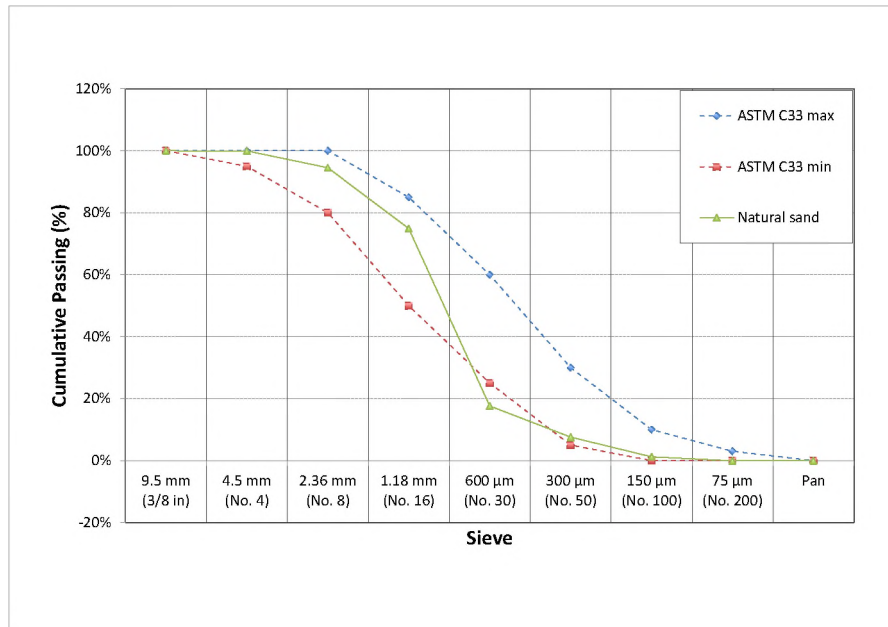
Specific Gravity
• Dry (ASTM C127)   2.65
• Saturated Surface Dry (ASTM C127)   2.71

Absorption
• Saturated Surface Dry (ASTM C127)   0.64%

LWA

Gradation curve for Coarse aggregates

Finesses Modulus: 7.55

No. 100	No. 50	No. 30	No. 16	No. 8	No. 4	⅜"	¾ "	1 ½"
150 μm	300 μm	600 μm	1.18 mm	2.36 mm	4.75 mm	9.5 mm	19 mm	37.5
1	2	3	4	5	6	7	8	9

Λ

PHYSICAL CHARACTERISTICS OF EXPANDED STALITE AGGREGATE 1/2" (12.5mm)

Density
• Dry Loose (ASTM C29)   50 lb/ft³ (805 kg/m³)
• Saturated Surface Dry Loose (ASTM C29)   52 lb/ft³ (833 kg/m³)

 Specific Gravity
• Dry (ASTM C127)   1.45
• Saturated Surface Dry (ASTM C127)   1.52

Absorption
• Saturated Surface Dry (ASTM C127)   6%
• Under High Pumping Pressure of 150 psi (1033 kPa) 9.4%

Natural Sand

Finesses Modulus: 3.04

No. 100	No. 50	No. 30	No. 16	No. 8	No. 4	⅜"	¾ "	1 ½"
150 µm	300 µm	600 µm	1.18 mm	2.36 mm	4.75 mm	9.5 mm	19 mm	37.5
1	2	3	4	5	6	7	8	9

∧

Density
• Dry Loose (ASTM C29)   2627 kg/m^3) 164 lb/ft^3 (2627 kg/m^3)

Specific Gravity
• Dry (ASTM C127)   2.639

Absorption
• Saturated Surface Dry (ASTM C127)   0.401%

Manufactured Sand
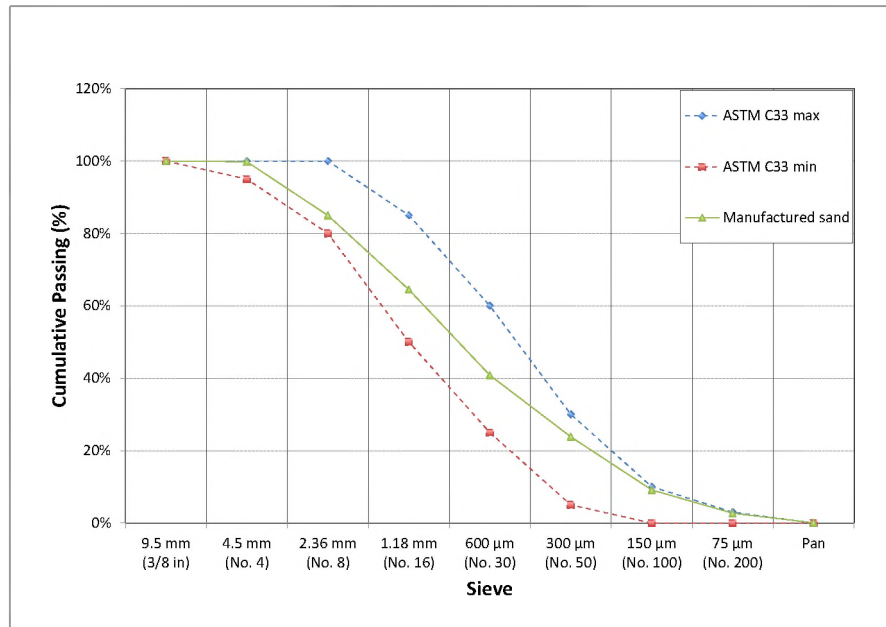
Finesses Modulus: 2.77

No. 100	No. 50	No. 30	No. 16	No. 8	No. 4	⅜"	¾ "	1 ½"
150 µm	300 µm	600 µm	1.18 mm	2.36 mm	4.75 mm	9.5 mm	19 mm	37.5
1	2	3	4	5	6	7	8	9

Λ

Density
• Dry Loose (ASTM C29)   166 lb/ft^3 (2659 kg/m^3)

Specific Gravity
• Dry (ASTM C127)   2.653

Absorption
• Saturated Surface Dry (ASTM C127)   0.422%

Appendix B – Steel plate Design

#3 Properties

$$A_3 := \left(\frac{3}{8}\text{in}\right)^2 \cdot \frac{\pi}{4} = 0.11 \cdot \text{in}^2$$

$$f_y := 92\text{ksi}$$

Shear friction Concrete area (Ac):

$$t_c := 7.5\text{in}$$

$$h_c := 12\text{in}$$

$$A_c := t_c \cdot h_c = 90 \cdot \text{in}^2$$

Steel reinforcement ratios:

0.25% - 1 two-leg stirrups No 3 $\rho_{25} := \dfrac{2A_3}{A_c} = 0.25 \cdot \%$

0.50% - 2 two-leg stirrups No 3 $\rho_{50} := \dfrac{4A_3}{A_c} = 0.49\%$

0.75% - 3 two-leg stirrups No 3 $\rho_{75} := \dfrac{6A_3}{A_c} = 0.74\%$

Steel plate design based on yield

Plate height $d_p := h_c$ and using a f_y of the plate equal to 36ksi $\quad f_{yplate} := 36\text{ksi}$

$$t_{25} := \frac{A_3 \cdot f_y}{f_{yplate} \cdot h_c} = 0.024\text{in} \qquad t_{50} := \frac{2A_3 \cdot f_y}{f_{yplate} \cdot h_c} = 0.047\text{in} \qquad t_{75} := \frac{3A_3 \cdot f_y}{f_{yplate} \cdot h_c} = 0.071\text{in}$$

Using the real f_y of the steel plates:

$$f_{y22} := 48\text{ksi} \qquad\qquad f_{y16} := 45\text{ksi} \qquad\qquad f_{y13} := 3\text{Jksi}$$

$$t_{25r} := \frac{A_3 \cdot f_y}{f_{y22} \cdot h_c} = 0.018\text{in} \qquad t_{50r} := \frac{2A_3 \cdot f_y}{f_{y16} \cdot h_c} = 0.038\text{in} \qquad t_{75r} := \frac{3A_3 \cdot f_y}{f_{y13} \cdot h_c} = 0.082\text{in}$$

$$t_{0.25} := \frac{2A_3}{d_p} \cdot \frac{f_y}{f_{yplate}} = 0.047 \cdot \text{in} \qquad \text{22 Gauge (0.03125 in.)}$$

$$t_{0.50} := \frac{4A_3}{d_p} \cdot \frac{f_y}{f_{yplate}} = 0.094 \text{-} \text{in} \qquad \text{16 Gauge (0.0625 in.)}$$

$$t_{0.75} := \frac{6A_3}{d_p} \cdot \frac{f_y}{f_{yplate}} = 0.141 \text{-} \text{in} \qquad \text{13 Gauge (0.09375 in.)}$$

$$t := \frac{2A_3}{1\text{in}} \cdot \frac{f_y}{f_{yplate}} = 0.565 \cdot \text{in} \qquad \text{00 Gauge (0.0375)}$$

Appendix C – Analytical model for Task 3 specimens
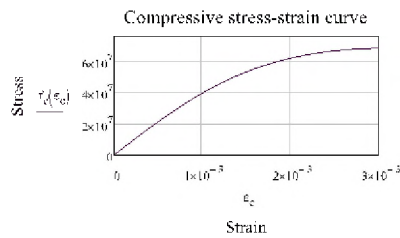
TASK 3 - SPECIMEN DESIGN IN-PLANE

Beam geometry

$b := 18in$	Cross-setion widht
$h := 18in$	Cross-section height
$l_0 := 8.5ft$	Clear span
$a := 2.5 \cdot h = 45 \cdot in$	Point of load application

Concrete properties

$f_c := 11000psi$	Compressive strength ;
$\varepsilon_{cu} := 0.003$	Ultimate compressive strain
$E_c := 57000\sqrt{f_c \cdot psi} = 5.978 \times 10^6 \cdot psi$	Compressive modulus of elasticity
$f_{ct} := 7.5\sqrt{f_c \cdot psi} = 786.607psi$	Tensile strength

Analytical approximations to the compressive stress-strain curve - Todeschini's model

$$\varepsilon_{c0} := \frac{1.71 \cdot f_c}{E_c} = 3.146 \times 10^{-3}$$

Compressive strain at peak

$$f''_c := 0.9 \cdot f_c = 9.9 \times 10^3 \cdot psi$$

Compressive stress at peak

$$f_c(\varepsilon_c) := \frac{2 \cdot f''_c \left(\frac{\varepsilon_c}{\varepsilon_{c0}}\right)}{1 + \left(\frac{\varepsilon_c}{\varepsilon_{c0}}\right)^2}$$

Stress-strain curve equation

Compressive stress-strain curve

COMMENTS

(This procedure is valid for in-plane configuration. which means in the case of Task 3 specimens that the steel faceplate are located on the two sides of the specimen)

Steel plate properties

$t_s := \dfrac{3}{16} \cdot in$ Steel plate thickness

$A_s := t_s \cdot b = 3.375 \cdot in^2$ Area of reinforcement

$d := h = 18 \cdot in$ Effective depth

$\rho := \dfrac{2 A_s}{b \cdot (h - 2 t_s)} = 0.0213$ Reinforcement ratio

$f_y := 55 ksi = 379 \cdot MPa$ Yield strength

$E_s := 29000 ksi = 199948 \cdot MPa$ Tensile modulus of elasticity

$\varepsilon_{sy} := \dfrac{f_y}{E_s} = 0.0019$ Yield strain

Analytical approximations to the tensile stress-strain curve

$f_s(\varepsilon_s) := \begin{vmatrix} (E_s \cdot \varepsilon_s) & \text{if } \varepsilon_s \le \varepsilon_{sy} \\ f_y & \text{otherwise} \end{vmatrix}$ Stress-strain curve equation

Tensile stress-strain curve
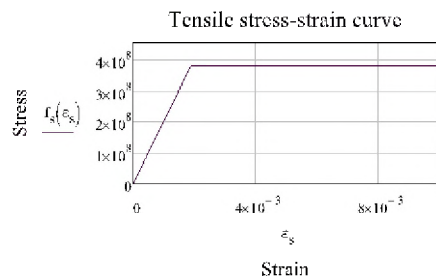
<u>Cracking</u>

$$I_g := \frac{b \cdot h^3}{12} = 8.748 \times 10^3 \cdot in^4$$ Gross moment of inertia

$$M_{cr} := f_{ct} \cdot \frac{I_g}{\frac{h}{2}} \quad 63.715 \cdot ft \cdot kip$$ Cracking moment

<u>Yielding</u>

(Computed imposing yielding of the bottom steel plate - ε_{sy})

<u>Compatibility</u>

$$\varepsilon_{cY}(x) := \frac{\varepsilon_{sy}}{d - x} \cdot x$$ Concrete compressive strain

$$\varepsilon_{sY}(x) := \varepsilon_{sy}$$

$$\varepsilon_{scY}(x) := \frac{\varepsilon_{sy}}{d - x} \cdot x$$ Tensile strain in the top steel plate

$$C_{cY}(x) := b \cdot \int_0^x \frac{2 \cdot f''_c \left(\frac{\frac{\varepsilon_{sy}}{d-x} \cdot y}{\varepsilon_{c0}} \right)}{1 + \left(\frac{\frac{\varepsilon_{sy}}{d-x} \cdot y}{\varepsilon_{c0}} \right)^2} \, dy$$ Compressive force in the concrete

$$T_{sY}(x) := t_s \cdot f_s(\varepsilon_{sy}) \cdot (h - x)$$ Tensile force in the lateral steel plates

$$C_{scY}(x) := t_s \cdot f_s \left(\frac{\varepsilon_{sy}}{d - x} \cdot x \right) \cdot x$$ Compressive force in the lateral steel plates

<u>Check equilibrium and compatibility</u>

The neutral axis depth at yielding is: $c_{y\_g} := 1 in$ (The guess value c_{y_g} is completly arbitrary and it is required by Mathcad to solve the equation)

$$c_y := root\left(C_{cY}(c_{y\_g}) + C_{scY}(c_{y\_g}) - T_{sY}(c_{y\_g}), c_{y\_g}\right) = 4.13387454 \cdot in$$

$C_{cY}(c_y) \quad 130.285 \cdot kip \qquad T_{sY}(c_y) \quad 142.994 \cdot kip \qquad C_{scY}(c_y) \quad 12.709 \ kip$

The yielding moment is:

$$M_y := C_{cY}(c_y) \cdot y_{cb} + T_{sY}(c_y) \cdot (d - c_y) + C_{scY}(c_y) \cdot (c_y) = 197.697 \cdot ft \cdot kip$$ (Computed considering a linear stress distribution of the two steel plates. The distance between th and the centroids is 2/3 of the triangonal area)

Ultimate (no φ factors applied)

Compatibility

$\varepsilon_{cu} := 0.003$

$\varepsilon_{tc}(y) := \dfrac{\varepsilon_{cu}}{y} \cdot y$ Compressive strain in the top steel plate

$\varepsilon_t(y) := \dfrac{\varepsilon_{cu}}{y} \cdot (d - y)$ Tensile strain in the bottom steel plate

Equilibrium

$C_{cU}(y) := b \cdot \displaystyle\int_0^y \dfrac{2 \cdot f'_c \cdot \left(\dfrac{\varepsilon_{cu}}{\varepsilon_{c0}}\right)}{1 + \left(\dfrac{\varepsilon_{cu}}{\varepsilon_{c0}}\right)^2} \, dy$ Compressive force in the concrete

$C_{scU}(y) := t_s \cdot f_s\big(\varepsilon_{tc}(y)\big) y$ Compressive force in the top steel plate

$T_{sU}(y) := t_s \cdot f_s\big(\varepsilon_t(y)\big)(h - y)$ Tensile force in the bottom steel plate

Check equilibrium and compatibility

The neutral axis depth at yielding is: $\ c_{u\_g} := 1\,in$

$c_u := root\Big(C_{cU}(c_{u\_g}) - T_{sU}(c_{u\_g}) + C_{scU}(c_{u\_g}), c_{u\_g}\Big) = 0.935 \cdot in$

$C_{cU}(c_u) = 166.35 \cdot kip$ $C_{scU}(c_u) = 9.638 \cdot kip$ $T_{sU}(c_u) = 175.987 \cdot kip$

The ultimate moment is:

$M_u := C_{cU}(c_u) \cdot y_{cu} - T_{sU}(c_u)(d - c_u) + C_{scU}(c_u)(c_u) = 259.663 \cdot ft \cdot kip$

Check concrete strain

$CheckConcreteStrainU := \begin{vmatrix} \text{"OK"} & \text{if } \varepsilon_{cu} < \varepsilon_{cu} \\ \text{"Not good"} & \text{otherwise} \end{vmatrix}$

$CheckConcreteStrainU = \text{"OK"}$

Check reinforcement strain

$\varepsilon_t(c_u) = 0.05478$

$\varepsilon_{tc}(c_u) = 0.003$

Moment curvature data

$\chi_{crck} := \dfrac{M_{cr}}{E_c \cdot I_g} = 0.0000146 \cdot \dfrac{1}{in}$ $\chi_Y := \dfrac{\varepsilon_{sY}(c_Y)}{d - c_y} = 0.0001368 \cdot \dfrac{1}{in}$ $\chi_U := \dfrac{\varepsilon_t(c_u)}{d - c_u} = 0.0032101 \cdot \dfrac{1}{in}$ (Curvatures at cracking, yielding and ultimate)

$P_{crck} := \dfrac{M_{cr} \cdot L_0}{a \cdot (L_0 - a)} = 30.404 \cdot kip$ $P_y := \dfrac{M_y \cdot L_0}{a \cdot (L_0 - a)} = 94.339 \cdot kip$ $P_u := \dfrac{M_u \cdot L_0}{a \cdot (L_0 - a)} = 123.909 \cdot kip$ (Loads at cracking, yielding and ultimate)

$\Delta_{cr} := \dfrac{\chi_{crck} \cdot a \cdot (L_0 - a)}{3} = 0.0125 \cdot in$ $\Delta_y := \dfrac{\chi_Y \cdot a \cdot (L_0 - a)}{3} = 0.1169 \cdot in$ $\Delta_u := \dfrac{\chi_U \cdot a \cdot (L_0 - a)}{3} = 2.745 \cdot in$ (Mid-span displacements at cracking, yielding and ultimate)

In-Plane Shear Strength [Appendix N9 AISC 690-15]

$\rho_0 := \dfrac{2 t_s \cdot h \cdot f_y}{65.6 \cdot b \cdot h \cdot \sqrt{psi \cdot f_c}} = 0.167$ $\kappa := 1.11 - 5.16 \cdot \rho_0 = 0.251$

$V_{ni} := \kappa \cdot f_y \cdot 2 \cdot A_s = 93.053 \cdot kip$

At ultimate the steel faceplate located at the bottom of the is already yield. However, the strain in the compression is governed by the concrete in respect of the compatibility and equilibrium. The maximum allowed concrete strain has been selected by manually changing the value εcuu up to the point in which the equation converge in a real and positive solution. After than some mechanism of failure might occur.

Appendix D – Papers and Presentations Resulting from the Project

The following papers that were published during the FY 2013 are included in this Appendix together with two presentations. It is indicated if they were already provided with a previous report; but for completeness all are included here.

a) 2 summaries published/presented at the Annual Meetings (Report 2014 October 21st 2014 Charlotte, NC Report 2015 September 29th 2015 Arlington, VA).
b) 1 presentation on the annual nuclear power conference (May 19th 2015 Pocatello, ID).
c) 1 presentation on the project at the spring ACI convention (April 18th 2016 Milwaukee, WI).
d) 1 conference paper published/presented at the RILEM Symposium on Self-Compacting Concrete (May 15-18 2016 Washington, DC).

(This page intentionally left black)

Georgia Institute of **Tech**nology

Self-Consolidating Concrete Construction for Modular Units

Russell Gentry (PI)
Kimberly Kurtis (Co-PI)
Larry Kahn (Co-PI)
Giovanni Loreto (Researcher)
School of Civil and Environmental Engineering (CEE) – Georgia Institute of Technology

Bojan Petrovic (Co-PI)
Nuclear and Radiological Engineering) – Georgia Institute of Technology

Industry partner:
Jurie van Wyk (Westinghouse)
Carlos Cantarero-Leal (Westinghouse)

Tuesday, OCTOBER 21, 2014 – Charlotte, NC

---

1. Intro

2. Task 1 – Development of Self-Roughening Concrete (SRC) Mix Design

3. Task 2 – Assessment of Cold Joint Shear Friction Capacity

4. Preliminary Conclusions

Tuesday, OCTOBER 21, 2014 – Charlotte, NC
Self-Consolidating Concrete Construction for Modular Units

1. Intro

2. Task 1 – Development of Self-Roughening Concrete (SRC) Mix
   Design

3. Task 2 – Assessment of Cold Joint Shear Friction Capacity

4. Preliminary Conclusions

Tuesday, OCTOBER 21, 2014 – Charlotte, NC
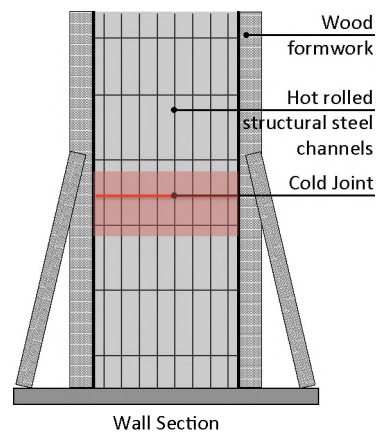Self-Consolidating Concrete Construction for Modular Units

---

1. Intro
Concrete Material
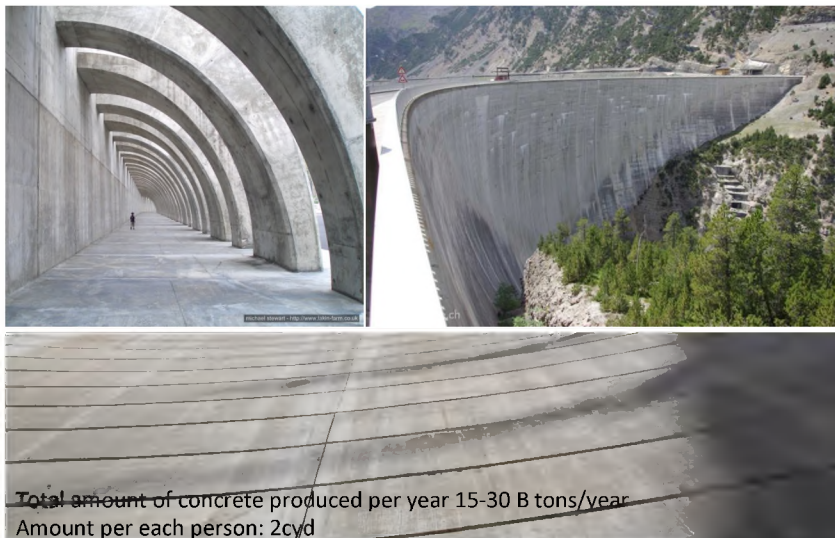
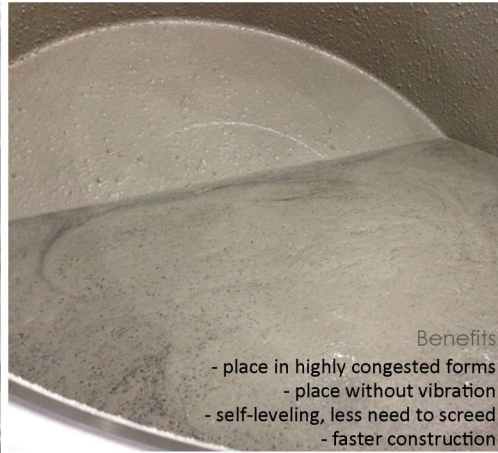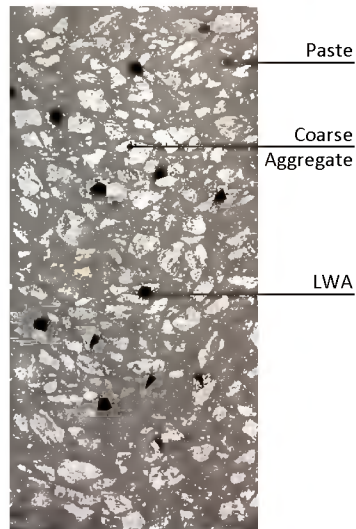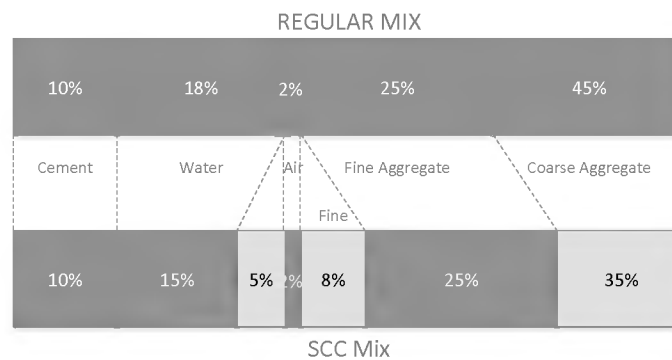Total amount of concrete produced per year 15-30 B tons/year
Amount per each person: 2cyd

Tuesday, OCTOBER 21, 2014 – Charlotte, NC
Self-Consolidating Concrete Construction for Modular Units

1. Intro
Concrete Wall

1. Intro
Objectives and outcomes

- Development of a self-consolidating concrete mixtures so that concrete placement can be made into steel plate composite (SC) modular structures without the need for continuous concrete placement.
Task 1: Development of SCC with Shear-Friction Capacity for Mass Placement

- SCC mixtures to ensure sufficient shear capacity across cold- joints (self-roughening), while minimizing shrinkage and temperature increase during curing to enhance concrete bonding with the steel plates.
Task 1: Development of SCC with Shear-Friction Capacity for Mass Placement
Task 2: Assessment of Cold Joint Shear-Friction Capacity

- SCC mixtures featuring a self-roughening capability to produce adequate shear friction between cold joints and to produce draft provisions addressing shear-friction, for consideration in the AISC N690-12 Appendix N9 code used for the design of SC modular structures.
Task 3: Assessment of Shear and Flexural Performance
Task 4: Validation through Full-Scale Testing and Modeling
Task 5: Draft Code Requirement for Shear Friction Design of Cold Joints

1. SCC – Definition and background
Why self-roughening
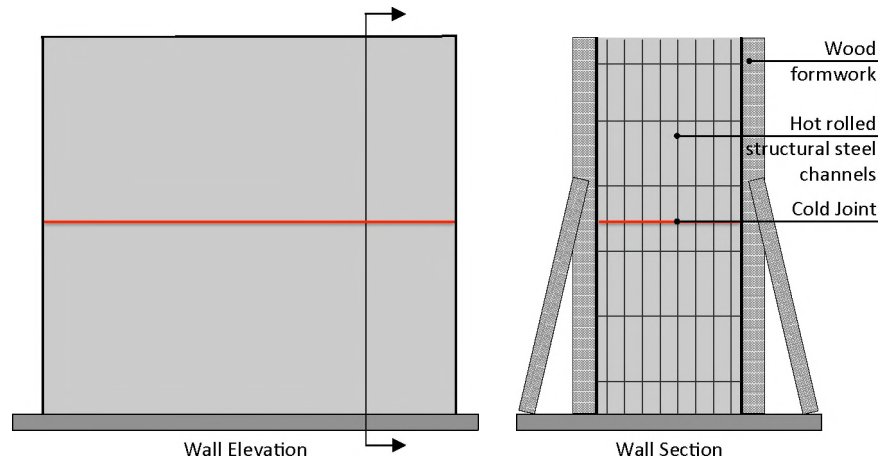
Wall Elevation

Wall Section

Wood formwork

Hot rolled structural steel channels

Cold Joint

Tuesday, OCTOBER 21, 2014 – Charlotte, NC
Self-Consolidating Concrete Construction for Modular Units

1. SCC – Definition and background
Joints in Concrete Construction

Wall Section

Wood formwork

Hot rolled structural steel channels

Cold Joint

Cold Joint
When wet concrete is cast up to dry concrete.

Tuesday, OCTOBER 21, 2014 – Charlotte, NC
Self-Consolidating Concrete Construction for Modular Units

1. SCC – Definition and background
Regular vs. SCC

Benefits
- place in highly congested forms
- place without vibration
- self-leveling, less need to screed
- faster construction

REGULAR   SCC

Tuesday, OCTOBER 21, 2014 – Charlotte, NC
Self-Consolidating Concrete Construction for Modular Units

---

1. Intro

2. Task 1 – Development of Self-Roughening Concrete (SRC) Mix Design

3. Task 2 – Assessment of Cold Joint Shear Friction Capacity

4. Conclusions

Tuesday, OCTOBER 21, 2014 – Charlotte, NC
Self-Consolidating Concrete Construction for Modular Units

2. Development of SRC Mix Design
Strategies

Paste

Coarse
Aggregate

LWA

Tuesday, OCTOBER 21, 2014 – Charlotte, NC
Self-Consolidating Concrete Construction for Modular Units

---

2. Development of SRC Mix Design
How is SCC made?

REGULAR MIX

10%	18%	2%	25%	45%

Cement	Water	Air	Fine Aggregate	Coarse Aggregate

Fine

10%	15%	5%	2%	8%	25%	35%

SCC Mix

Definition [ACI 237R – 07]
 Self-consolidating concrete (SCC) is an highly flowable, nonsegregating concrete that
 can spread into place, fill the formwork, and encapsulate the reinforcement without
 any mechanical consolidation.

Tuesday, OCTOBER 21, 2014 – Charlotte, NC
Self-Consolidating Concrete Construction for Modular Units

2. Development of SRC Mix Design
Strategies

Mix Component	67M
Cementitious (lb/yd^3)	
Cement Type II	617
Fly Ash, Class F	459
Total Powder	*1076*
Water (lb/yd^3)	343
w/cm	*0.319*
Coarse Aggregates (lb/yd^3)	
# 67	981
# 89	305
Total Coarse	*1286*
Fine Aggregates (lb/yd^3)	
Natural sand	679
Manufactured sand	679
Total Fine	*1357*
Total Aggregates	*2796*
Admixures (fl oz./cwt)	
HRWR	0.18
TOT	4063

Tuesday, OCTOBER 21, 2014 – Charlotte, NC
Self-Consolidating Concrete Construction for Modular Units

2. Development of SRC Mix Design
Strategies

Mix Component	67M
Cementitious (lb/yd^3)	
Cement Type II	617
Fly Ash, Class F	459
Total Powder	*1076*
Water (lb/yd^3)	343
w/cm	*0.319*
Coarse Aggregates (lb/yd^3)	
# 67	981
# 89	305
Total Coarse	*1286*
Fine Aggregates (lb/yd^3)	
Natural sand	679
Manufactured sand	679
Total Fine	*1357*
Total Aggregates	*2796*
Admixures (fl oz./cwt)	
HRWR	0.18
TOT	4063

- Cement and Fly Ash quantity
- High paste content
- Fresh properties [flowability, segregation resistant]
- Reduced heat generation
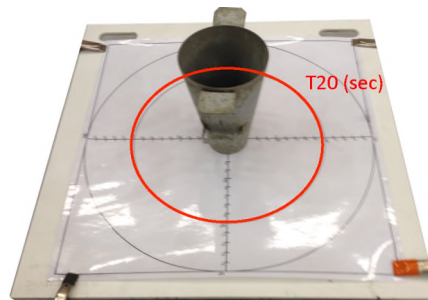
Tuesday, OCTOBER 21, 2014 – Charlotte, NC
Self-Consolidating Concrete Construction for Modular Units

2. Development of SRC Mix Design
Strategies

Mix Component	67M
Cementitious (lb/yd³)	
Cement Type II	617
Fly Ash, Class F	459
Total Powder	*1076*
Water (lb/yd³)	343
w/cm	*0.319*
Coarse Aggregates (lb/yd³)	
# 67	981
# 89	305
Total Coarse	*1286*
Fine Aggregates (lb/yd³)	
Natural sand	679
Manufactured sand	679
Total Fine	*1357*
Total Aggregates	*2796*
Admixures (fl oz./cwt)	
HRWR	0.18
TOT	4063

- Smaller aggregates and controlled gradation curve
- Use of #67 and #89 coarse aggregates
- Substitute 5%, 10% and 15% in volume of coarse aggregate with LWA
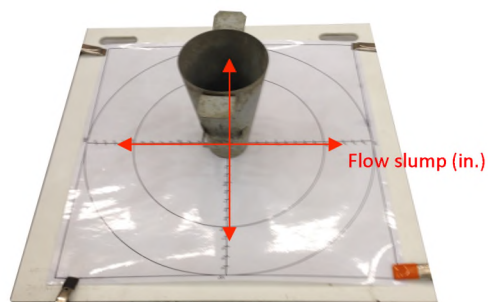
Tuesday, OCTOBER 21, 2014 – Charlotte, NC
Self-Consolidating Concrete Construction for Modular Units

2. Development of SRC Mix Design
Strategies

Mix Component	67M
Cementitious (lb/yd³)	
Cement Type II	617
Fly Ash, Class F	459
Total Powder	*1076*
Water (lb/yd³)	343
w/cm	*0.319*
Coarse Aggregates (lb/yd³)	
# 67	981
# 89	305
Total Coarse	*1286*
Fine Aggregates (lb/yd³)	
Natural sand	679
Manufactured sand	679
Total Fine	*1357*
Total Aggregates	*2796*
Admixures (fl oz./cwt)	
HRWR	0.18
TOT	4063

- Blend of Manufactured and Natural sands
- Improved workability

Tuesday, OCTOBER 21, 2014 – Charlotte, NC
Self-Consolidating Concrete Construction for Modular Units
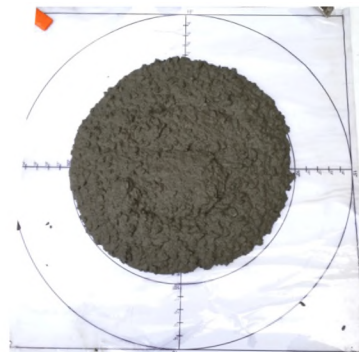
2. Development of SRC Mix Design
Strategies

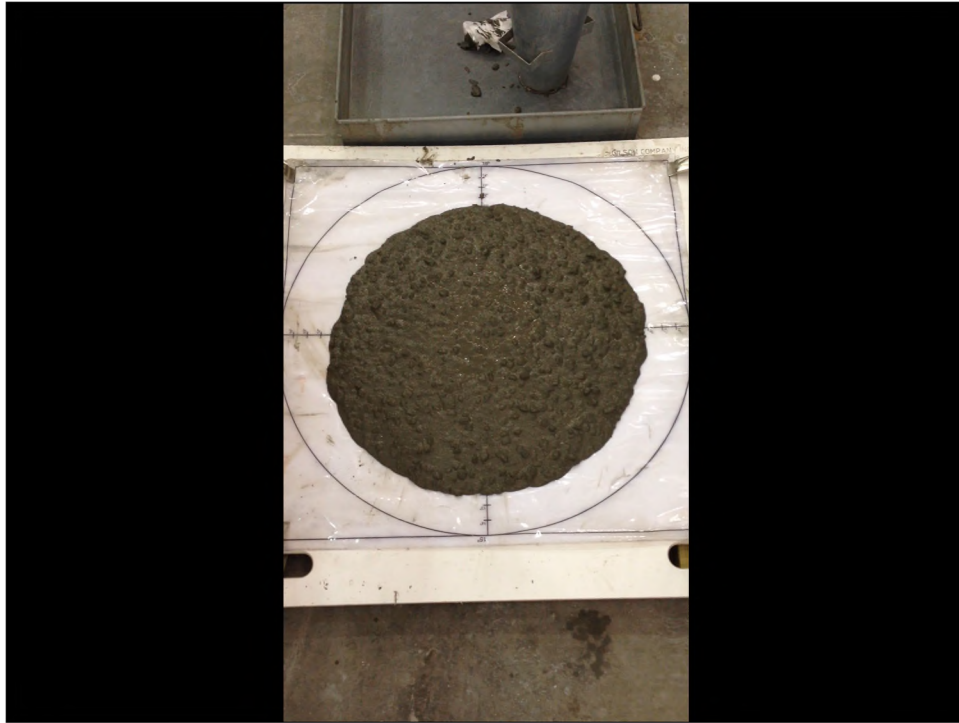| Mix Component	67M
Cementitious (lb/yd^3)	
Cement Type II	617
Fly Ash, Class F	459
Total Powder	*1076*
Water (lb/yd^3)	343
w/cm	*0.319*
Coarse Aggregates (lb/yd^3)	
# 67	981
# 89	305
Total Coarse	*1286*
Fine Aggregates (lb/yd^3)	
Natural sand	679
Manufactured sand	679
Total Fine	*1357*
Total Aggregates	*2796*
Admixures (fl oz./cwt)	
HRWR	0.18
TOT	4063

- High range water reduced (HRWR)
- Decreased w/c ratio

Tuesday, OCTOBER 21, 2014 – Charlotte, NC
Self-Consolidating Concrete Construction for Modular Units

2. Development of SRC Mix Design
Proprieties and tests

Fresh SCC proprieties
- Flowability: flows easily at suitable speed into formwork
- S Groove test
- Hardened Visual Stability Index

Tuesday, OCTOBER 21, 2014 – Charlotte, NC
Self-Consolidating Concrete Construction for Modular Units

2. Development of SRC Mix Design
Proprieties and tests

Fresh SCC proprieties
- **Flowability: flows easily at suitable speed into formwork**
- S Groove test
- Hardened Visual Stability Index

T20 (sec)

Slump flow test [ASTM C1611]

Tuesday, OCTOBER 21, 2014 – Charlotte, NC
Self-Consolidating Concrete Construction for Modular Units

2. Development of SRC Mix Design
Proprieties and tests

Fresh SCC proprieties
- **Flowability: flows easily at suitable speed into formwork**
- S Groove test
- Hardened Visual Stability Index

Flow slump (in.)

Slump flow test [ASTM C1611]

Tuesday, OCTOBER 21, 2014 – Charlotte, NC
Self-Consolidating Concrete Construction for Modular Units

2. Development of SRC Mix Design
Proprieties and tests

Fresh SCC proprieties
- Flowability: flows easily at suitable speed into formwork (T20 = 4sec; Flow Slump = 24")
- S Groove test
  Hardened Visual Stability Index

Tuesday, OCTOBER 21, 2014 – Charlotte, NC
Self-Consolidating Concrete Construction for Modular Units

2. Development of SRC Mix Design
Proprieties and tests

Fresh SCC proprieties
- Flowability: flows easily at suitable speed into formwork (T20 = 4sec; Flow Slump = 24")
- **S Groove test**
- Hardened Visual Stability Index

Self-Consolidating Concrete Construction for Modular Units

2. Development of SRC Mix Design
Proprieties and tests

Fresh SCC proprieties
- Flowability: flows easily at suitable speed into formwork (T20 = 4sec; Flow Slump = 24")
- **S Groove test**
- Hardened Visual Stability Index

Good performance

Poor performance

Self-Consolidating Concrete Construction for Modular Units

2. Development of SRC Mix Design
Proprieties and tests

Fresh SCC proprieties
- Flowability: flows easily at suitable speed into formwork (T20 = 4sec; Flow Slump = 24")
- S Groove test (good self-healing ability)
- Hardened Visual Stability Index

Tuesday, OCTOBER 21, 2014 – Charlotte, NC
Self-Consolidating Concrete Construction for Modular Units
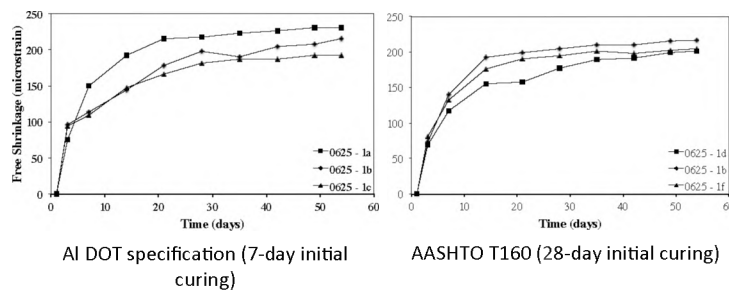
2. Development of SRC Mix Design
Proprieties and tests

Fresh SCC proprieties
- Flowability: flows easily at suitable speed into formwork (T20 = 4sec; Flow Slump = 24")
- S Groove test (good self-healing ability)
- **Hardened Visual Stability Index (VSI = 0)**

Rating	Number	Criteria
Highly Stable	0	No evidence of slump segregation
	0.5	Very slight evidence of bleed and air popping
Stable	1	No mortar halo No aggregate pile-up Slight bleed and air popping
	1.5	Just noticeable mortar halo and aggregate pile- up
Unstable	2	Slight mortar halo, less than 0.4 in. (10mm) Slight aggregate pile-up Noticeable bleed
Highly Unstable	3	Large mortar halo greater than 0.4 in. (10mm)

Tuesday, OCTOBER 21, 2014 – Charlotte, NC
Self-Consolidating Concrete Construction for Modular Units

---

2. Development of SRC Mix Design
Proprieties and tests

Fresh SCC proprieties
- Flowability: flows easily at suitable speed into formwork (T20 = 4sec; Flow Slump = 24")
- S Groove test (good self-healing ability)
- Hardened Visual Stability Index (VSI = 0)

Moving from SCC to SRC

Self-Consolidating Concrete

Self-Roughening Concrete

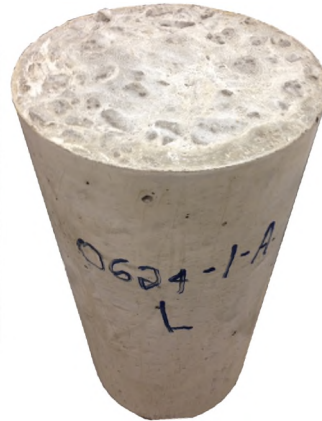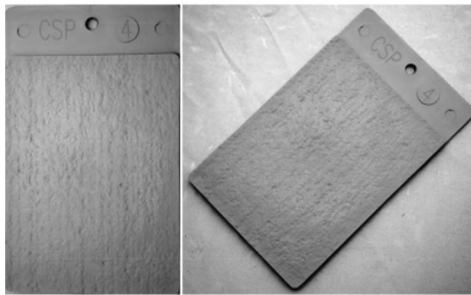Tuesday, OCTOBER 21, 2014 – Charlotte, NC
Self-Consolidating Concrete Construction for Modular Units

2. Development of SRC Mix Design
Proprieties and tests

Fresh SCC proprieties
- Flowability: flows easily at suitable speed into formwork (T20 = 4sec; Flow Slump = 24")
- S Groove test (optimal self-healing ability)
- Hardened Visual Stability Index (VSI = 0)

Hardened SRC proprieties
- Compressive strength
- Shrinkage

---

2. Development of SRC Mix Design
Proprieties and tests

Fresh SCC proprieties
- Flowability: flows easily at suitable speed into formwork (T20 = 4sec; Flow Slump = 24")
- S Groove test (optimal self-healing ability)
- Hardened Visual Stability Index (VSI = 0)

Hardened SRC proprieties
- Compressive strength: 9-10ksi
- Shrinkage

Mix Component	05 30 - 2	06 05 – 3	06 10 - 1	06 23 - 1	06 24 - 1	06 25 - 1	07 08 - 1	07 23 - 1	07 23 - 2
Compression (psi)	8682	9208	9602	9942	11347	9755	9834	10575	9186
Std. dev.	352	305	818	671	396	689	1035	1076	672

ASTM C39/39M – 14a

2. Development of SRC Mix Design
Proprieties and tests

Fresh SCC proprieties
- Flowability: flows easily at suitable speed into formwork (T20 = 4sec; Flow Slump = 24")
- S Groove test (optimal self-healing ability)
- Hardened Visual Stability Index (VSI = 0)

Hardened SRC proprieties
- Shrinkage: <250 με

| Al DOT specification (7-day initial curing) | AASHTO T160 (28-day initial curing) |

Tuesday, OCTOBER 21, 2014 – Charlotte, NC
Self-Consolidating Concrete Construction for Modular Units

---

2. Development of SRC Mix Design
Future work

Tuesday, OCTOBER 21, 2014 – Charlotte, NC
Self-Consolidating Concrete Construction for Modular Units

2. Development of SRC Mix Design
Measurements of Roughness

2. Development of SRC Mix Design
Measurements of Roughness

ACI 318-11 (11.6.9):
"...when concrete is placed against previously hardened concrete, the interface for shear transfer shall be clean and free of laitance. If µ is assumed equal to **1.0λ**, interface shall be roughened to a full amplitude of approximately 1/4 in."

2. Development of SRC Mix Design
Roughness

ICRI's CSPs

Tuesday, OCTOBER 21, 2014 – Charlotte, NC
Self-Consolidating Concrete Construction for Modular Units

2. Development of SRC Mix Design
Roughness
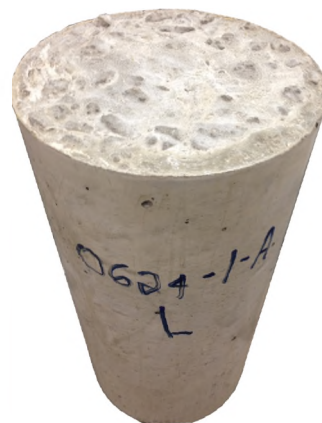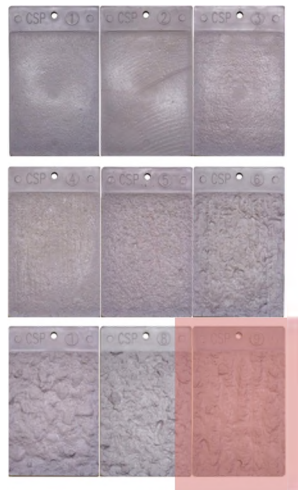
Tuesday, OCTOBER 21, 2014 – Charlotte, NC
Self-Consolidating Concrete Construction for Modular Units

2. Development of SRC Mix Design
Surface quantitative characterization
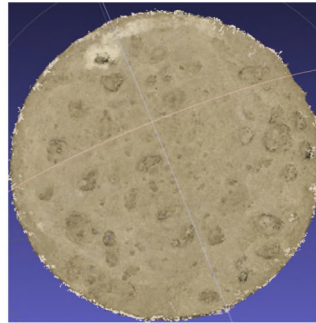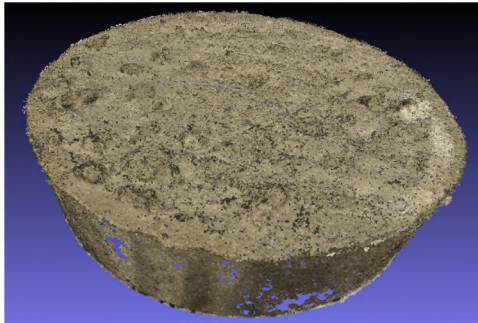
Construction Engineering Group:
- Yong K. Cho, Associate Professor
- Chao Wang, PhD

Tuesday, OCTOBER 21, 2014 – Charlotte, NC
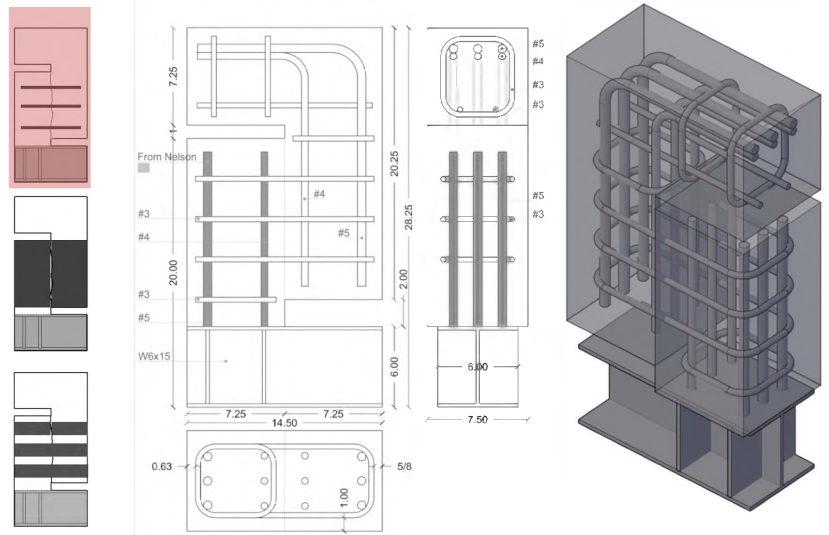Self-Consolidating Concrete Construction for Modular Units

---

Tuesday, OCTOBER 21, 2014 – Charlotte, NC
Self-Consolidating Concrete Construction for Modular Units
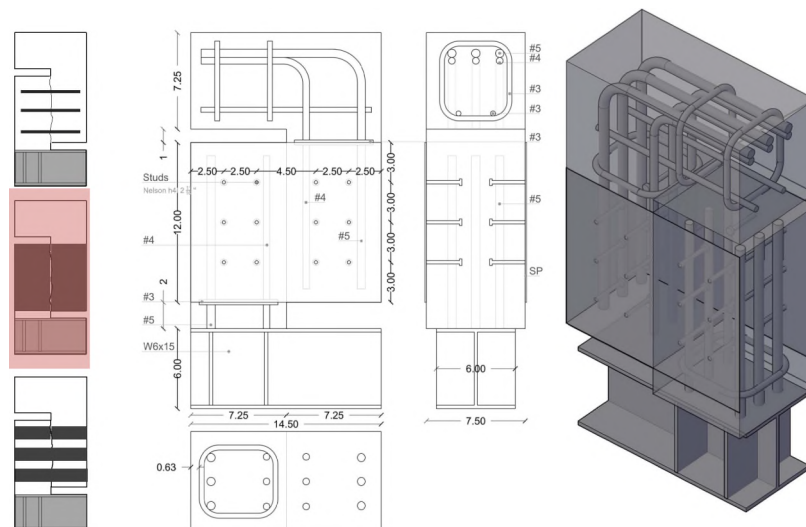
3. Assessment of Cold Joint Shear Friction Capacity
Previous research

Laboratory test

Kahn, L., Mitchell, A. D. (2002) "Shear friction test with high-strength concrete" ACI Structural Journal, 99 (1).

Wood formwork

Hot rolled structural steel channels

Cold Joint

Cold Joint
Wall Section
When wet concrete is cast up to dry concrete.

Tuesday, OCTOBER 21, 2014 – Charlotte, NC
Self-Consolidating Concrete Construction for Modular Units

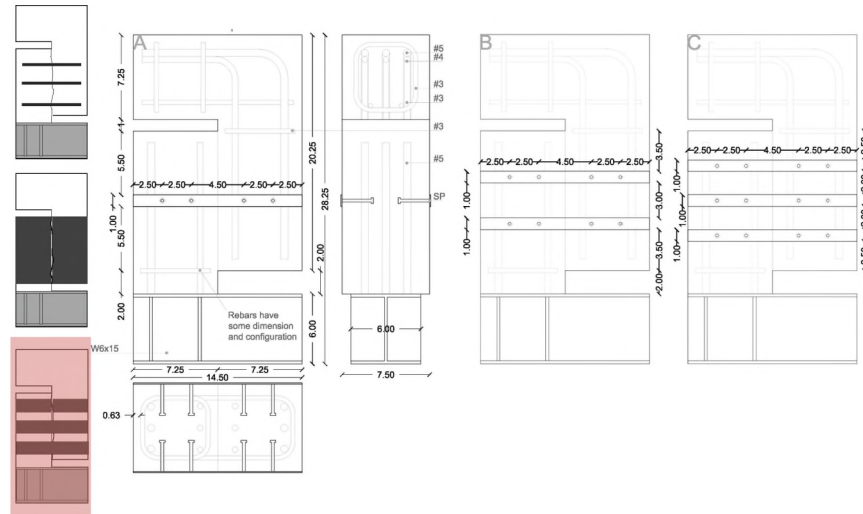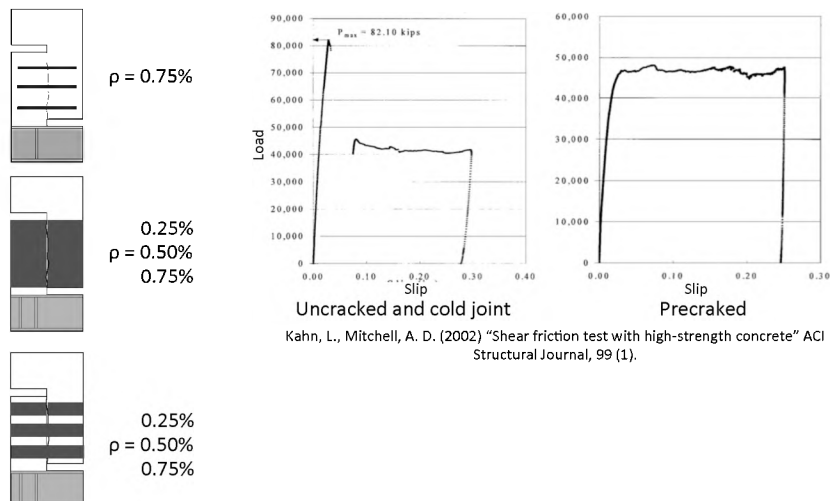# 3. Assessment of Cold Joint Shear Friction Capacity
Mechanical tests for shear friction characterization

Tuesday, OCTOBER 21, 2014 – Charlotte, NC
Self-Consolidating Concrete Construction for Modular Units

3. Assessment of Cold Joint Shear Friction Capacity
Mechanical tests for shear friction characterization

Tuesday, OCTOBER 21, 2014 – Charlotte, NC
Self-Consolidating Concrete Construction for Modular Units

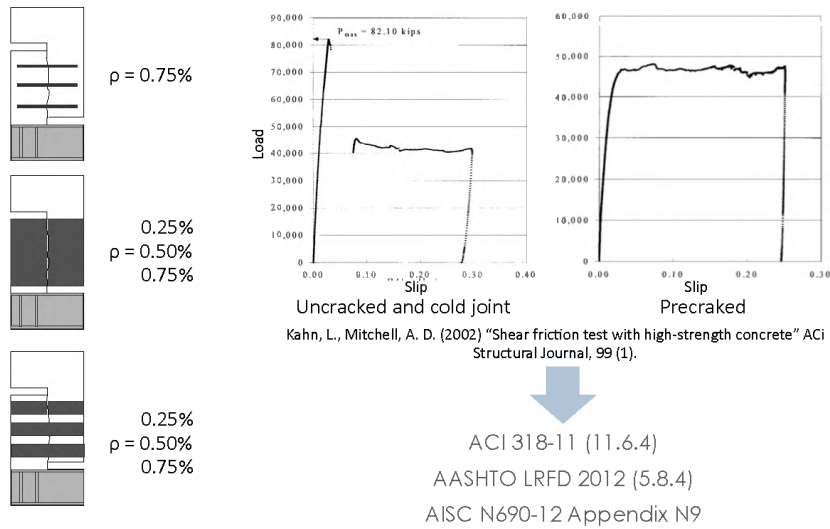3. Assessment of Cold Joint Shear Friction Capacity
Mechanical tests for shear friction characterization

Tuesday, OCTOBER 21, 2014 – Charlotte, NC
Self-Consolidating Concrete Construction for Modular Units

3. Assessment of Cold Joint Shear Friction Capacity
Mechanical tests for shear friction characterization

Tuesday, OCTOBER 21, 2014 – Charlotte, NC
Self-Consolidating Concrete Construction for Modular Units

3. Assessment of Cold Joint Shear Friction Capacity
Mechanical tests for shear friction characterization

ρ = 0.75%

0.25%
ρ = 0.50%
0.75%

0.25%
ρ = 0.50%
0.75%

Uncracked and cold joint

Precraked

Kahn, L., Mitchell, A. D. (2002) "Shear friction test with high-strength concrete" ACI Structural Journal, 99 (1).

Tuesday, OCTOBER 21, 2014 – Charlotte, NC
Self-Consolidating Concrete Construction for Modular Units

3. Assessment of Cold Joint Shear Friction Capacity
Mechanical tests for shear friction characterization

ρ = 0.75%

0.25%
ρ = 0.50%
0.75%

0.25%
ρ = 0.50%
0.75%

Uncracked and cold joint

Precraked

Kahn, L., Mitchell, A. D. (2002) "Shear friction test with high-strength concrete" ACi Structural Journal, 99 (1).

ACI 318-11 (11.6.4)

AASHTO LRFD 2012 (5.8.4)

AISC N690-12 Appendix N9

Tuesday, OCTOBER 21, 2014 – Charlotte, NC
Self-Consolidating Concrete Construction for Modular Units

---

3. Assessment of Cold Joint Shear Friction Capacity
Future work

Tuesday, OCTOBER 21, 2014 – Charlotte, NC
Self-Consolidating Concrete Construction for Modular Units

3. Assessment of Cold Joint Shear Friction Capacity
Future work

Tuesday, OCTOBER 21, 2014 – Charlotte, NC
Self-Consolidating Concrete Construction for Modular Units

3. Assessment of Cold Joint Shear Friction Capacity
Future work

Tuesday, OCTOBER 21, 2014 – Charlotte, NC
Self-Consolidating Concrete Construction for Modular Units

1. Intro

2. Task 1 – Development of Self-Roughening Concrete (SRC) Mix Design

3. Task 2 – Assessment of Cold Joint Shear Friction Capacity

4. Preliminary Conclusions

Tuesday, OCTOBER 21, 2014 – Charlotte, NC
Self-Consolidating Concrete Construction for Modular Units

---

4. Preliminary Conclusions
Highlights

- Development of a new self-consolidating concrete mixtures compatible for steel plate SC modular structures application. SCC fresh and hardned properties monitored along with shrinkage.

- Inclusion of a small fraction of LWA and roughness qualitative analysis.

- SRC capability to produce adequate shear friction between cold joints and assessment of cold joint shear friction capacity.

- Shear friction test matrix, specimen preparation and expected results.

Tuesday, OCTOBER 21, 2014 – Charlotte, NC
Self-Consolidating Concrete Construction for Modular Units

4. Preliminary Conclusions
Future work

	Project Year End		End
2014		2015	
Jan Feb Mar April May June July Aug Sept Oct Nov Dec		Jan Feb Mar April May June July Aug Sept Oct Nov Dec Jan	

Task 1. Developed SCC Mixes

Task 1. Rheology of SCC Mixes

Task 2. Shear Friction Evaluation Across SCC Roughened Cold Joings

Task 3. Measurment of Cold-Joint Effects in Flexure and Shear

Task 4. Upscaling: Experimental assessments of shear friction, pressure, shrinkage/delamination, and strength

Task 5. Model Development

Task 5. Shear Friction Provisions

Tuesday, OCTOBER 21, 2014 – Charlotte, NC
Self-Consolidating Concrete Construction for Modular Units

Questions?

Georgia Institute **of Tech**nology

Self-Consolidating Concrete Construction for Modular Units

Russell Gentry (PI)
Kimberly Kurtis (Co-PI)
Larry Kahn (Co-PI)
Giovanni Loreto (Researcher)
School of Civil and Environmental Engineering (CEE) – Georgia Institute of Technology

Bojan Petrovic (Co-PI)
Nuclear and Radiological Engineering) – Georgia Institute of Technology

Industry partner:
Jurie van Wyk (Westinghouse Electric)
Bernd Laskewitz (Westinghouse Electric)

Tuesday, SEPTEMBER 29, 2015 – Arlington. VA

---

1. Intro

2. Task 1 – Development of Self-Roughening Concrete (SRC) Mix Design

3. Task 2 – Assessment of Cold Joint Shear Friction Capacity

4. Task 3 – Assessment of Shear and Flexural Performances

5. Task 4 – Validation through Full-scale Test and Modeling
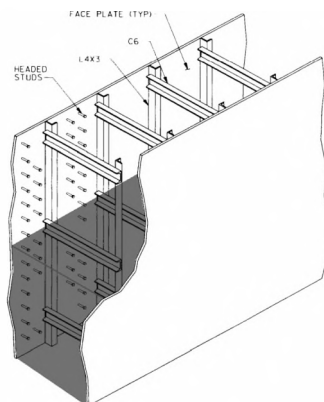
6. Conclusions and Outlooks

Tuesday, SEPTEMBER 29, 2015 – Arlington. VA
Development of a Self-Roughening (SR) Concrete

1. Intro
Objectives and outcomes

- Development of a self-consolidating concrete mixtures so that concrete placement can be made into steel plate composite (SC) modular structures without the need for continuous concrete placement.
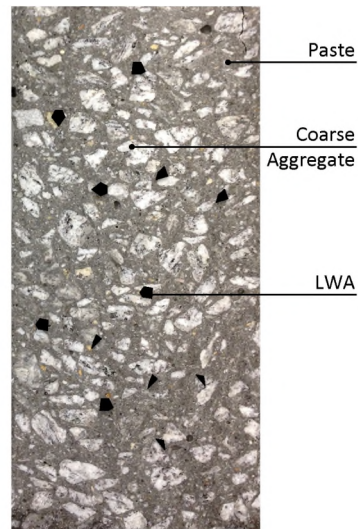*Task 1: Development of SCC with Shear-Friction Capacity for Mass Placement*

- SCC mixtures to ensure sufficient shear capacity across cold- joints (self-roughening), while minimizing shrinkage and temperature increase during curing to enhance concrete bonding with the steel plates.
Task 1: Development of SCC with Shear-Friction Capacity for Mass Placement
Task 2: Assessment of Cold Joint Shear-Friction Capacity

- SCC mixtures featuring a self-roughening capability to produce adequate shear friction between cold joints and to produce draft provisions addressing shear-friction, for consideration in the AISC N690-12 Appendix N9 code used for the design of SC modular structures.
Task 3: Assessment of Shear and Flexural Performance
Task 4: Validation through Full-Scale Testing and Modeling
Task 5: Draft Code Requirement for Shear Friction Design of Cold Joints

Tuesday, SEPTEMBER 29, 2015 – Arlington, VA
Development of a Self-Roughening (SR) Concrete

---

1. Intro
Objectives

- Development of a self-consolidating concrete mixtures so that concrete placement can be made into steel plate composite (SC) modular structures without the need for continuous concrete placement.

Tuesday, SEPTEMBER 29, 2015 – Arlington, VA
Development of a Self-Roughening (SR) Concrete

1. Intro
Objectives

2. Development of SRC Mix Design
Strategies

Mix Component	67M
Cementitious (lb/yd³)	
Cement Type II	617
Fly Ash, Class F	459
Total Powder	*1076*
Water (lb/yd³)	343
w/cm	*0.319*
Coarse Aggregates (lb/yd³)	
# 67	981
# 89	305
Total Coarse	*1286*
Fine Aggregates (lb/yd³)	
Natural sand	679
Manufactured sand	679
Total Fine	*1357*
Total Aggregates	*2796*
Admixures (fl oz./cwt)	
HRWR	0.18
TOT	4063

2. Development of SRC Mix Design
Strategies

Mix Component	67M
Cementitious (lb/yd³)	
Cement Type II	617
Fly Ash, Class F	459
Total Powder	*1076*
Water (lb/yd³)	343
w/cm	*0.319*
Coarse Aggregates (lb/yd³)	
# 67	981
# 89	305
Total Coarse	*1286*
Fine Aggregates (lb/yd³)	
Natural sand	679
Manufactured sand	679
Total Fine	*1357*
Total Aggregates	*2796*
Admixures (fl oz./cwt)	
HRWR	0.18
TOT	4063

- Smaller aggregates and controlled gradation curve
- Use of #67 and #89 coarse aggregates
- Substitute 5%, 10% and 15% in volume of coarse aggregate with LWA

Tuesday, SEPTEMBER 29, 2015 – Arlington, VA
Development of a Self-Roughening (SR) Concrete

2. Development of SRC Mix Design
Proprieties and tests

Self-Consolidating Concrete   Self-Roughening Concrete

Fresh SCC proprieties
- Flowability: flows easily at suitable speed into formwork (T20 = 4-5sec; Flow Slump = 24-26")
- S Groove test (good self-healing ability)
- Hardened Visual Stability Index (VSI = 0)

Hardened SRC proprieties
- Compressive strength: 6-7ksi
- Shrinkage: <250 με

Tuesday, SEPTEMBER 29, 2015 – Arlington, VA
Development of a Self-Roughening (SR) Concrete

2. Development of SRC Mix Design
Measurements of Roughness

Tuesday, SEPTEMBER 29, 2015 – Arlington, VA
Development of a Self-Roughening (SR) Concrete

2. Development of SRC Mix Design
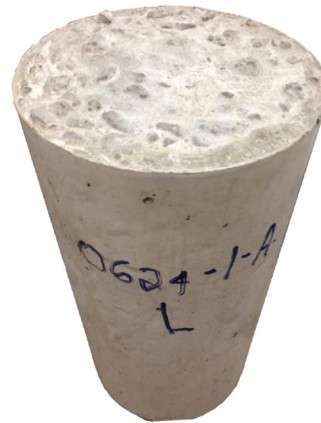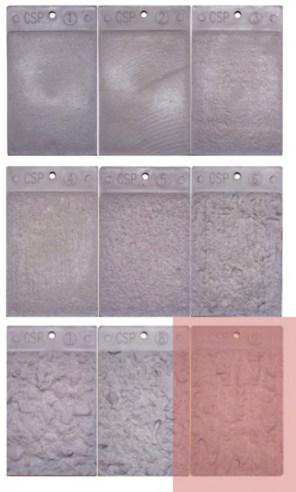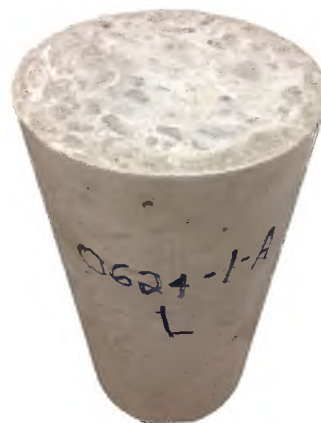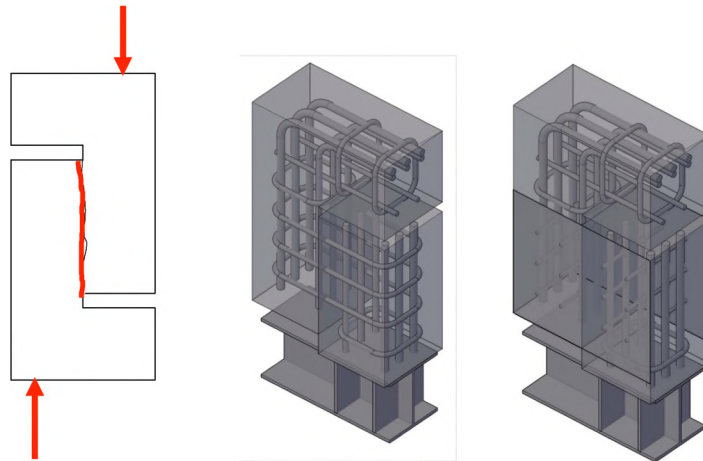Roughness

ICRI's CSPs

Tuesday, SEPTEMBER 29, 2015 – Arlington, VA
Development of a Self-Roughening (SR) Concrete

2. Development of SRC Mix Design
Roughness

2. Development of SRC Mix Design
Measurements of Roughness

ACI 318-11 (11.6.9):
"...when concrete is placed against previously hardened concrete, the interface for shear transfer shall be clean and free of laitance. If μ is assumed equal to 1.0λ, interface shall be roughened to a full amplitude of approximately 1/4 in."

7/27/16

3. Assessment of Cold Joint Shear Friction Capacity
Mechanical tests for shear friction characterization

Laboratory test
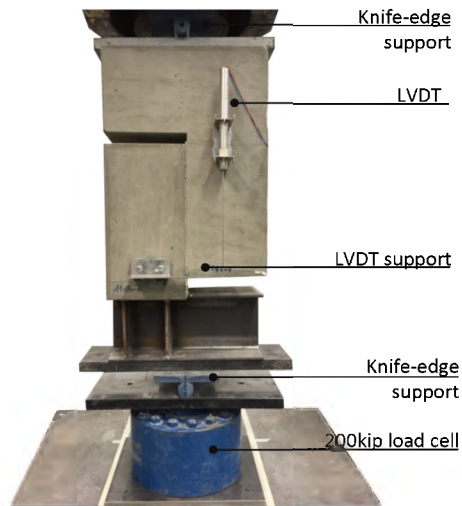Kahn, L., Mitchell, A. D. (2002) "Shear friction test with high-strength concrete" ACI Structural Journal, 99 (1).
Tuesday, SEPTEMBER 29, 2015 – Arlington, VA
Development of a Self-Roughening (SR) Concrete

3. Assessment of Cold Joint Shear Friction Capacity
Mechanical tests for shear friction characterization

Step 1
Step 2
Step 3
Step 4
Step 5

Tuesday, SEPTEMBER 29, 2015 – Arlington, VA
Development of a Self-Roughening (SR) Concrete

7

3. Assessment of Cold Joint Shear Friction Capacity
Mechanical tests for shear friction characterization

- Knife-edge support
- LVDT
- LVDT support
- Knife-edge support
- 200kip load cell

Tuesday, SEPTEMBER 29, 2015 – Arlington, VA
Development of a Self-Roughening (SR) Concrete

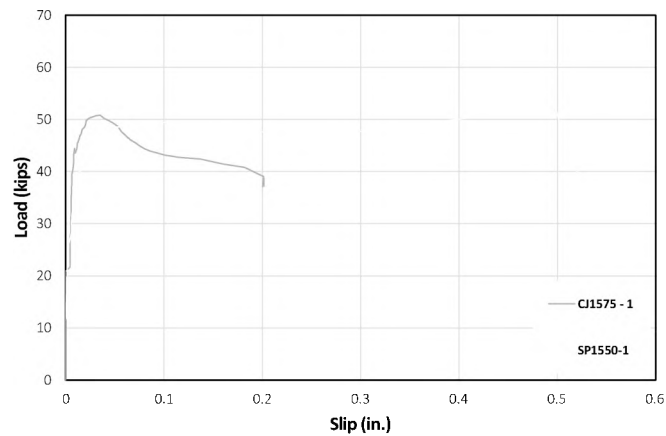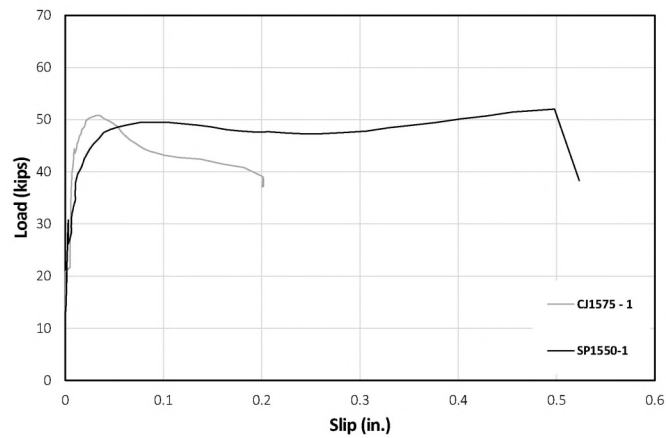## 3. Assessment of Cold Joint Shear Friction Capacity
Failure modes

| Internal Reinforcement p=0.75% | External Steel Plate p=0.25% t=0.031 in. (22 gage) | External Steel Plate p=0.50% t=0.063 in. (16 gage) | External Steel Plate p=0.75% t=0.094 in. (13 gage) | External Steel Strips p=0.75% t=0.375 in. |

Tuesday, SEPTEMBER 29, 2015 – Arlington, VA
Development of a Self-Roughening (SR) Concrete

3. Assessment of Cold Joint Shear Friction Capacity
Test Results – Internal Reinforcement

Tuesday, SEPTEMBER 29, 2015 – Arlington, VA
Development of a Self-Roughening (SR) Concrete
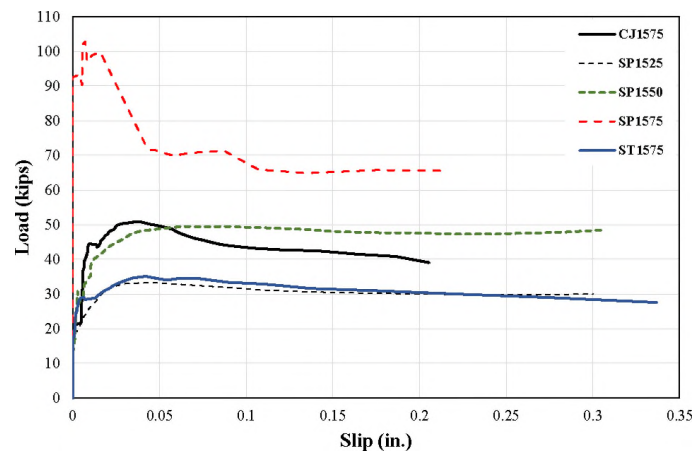

3. Assessment of Cold Joint Shear Friction Capacity
Test Results – External Steel Plate

Tuesday, SEPTEMBER 29, 2015 – Arlington, VA
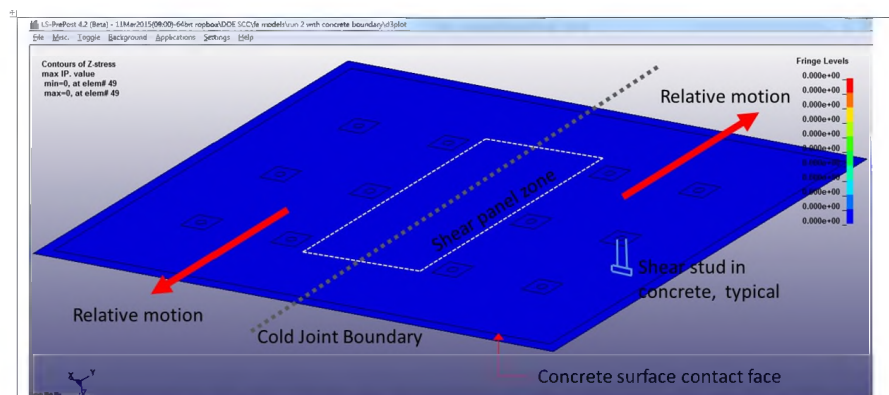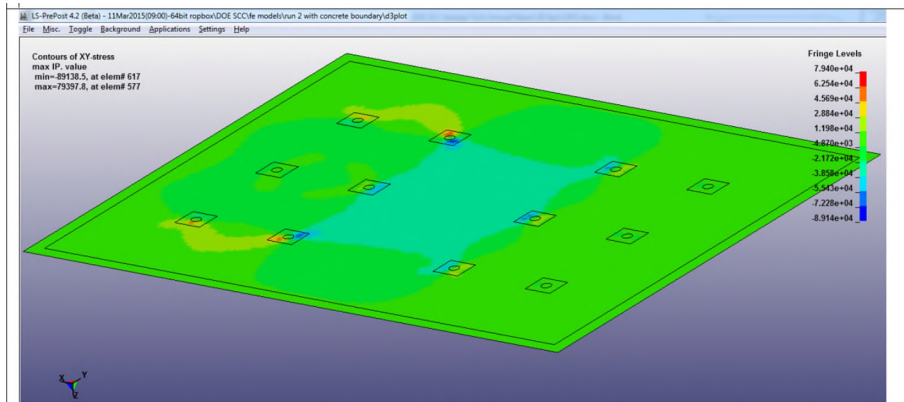Development of a Self-Roughening (SR) Concrete

3. Assessment of Cold Joint Shear Friction Capacity
Test Results – Comparison among sets

(a) Non-linear finite element model in LS-DYNA explicit. This initial model approximate the geometry of specimen SP 15 50-1 but with fewer Nelson studs.
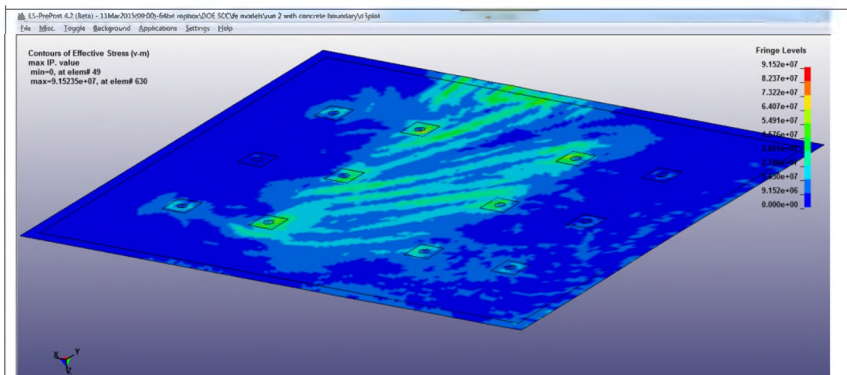
(b) Initital loading. Constant shear in the panel zone. In-plane shear stresses shown (all stresses in Pa).

Tuesday, SEPTEMBER 29, 2015 – Arlington, VA
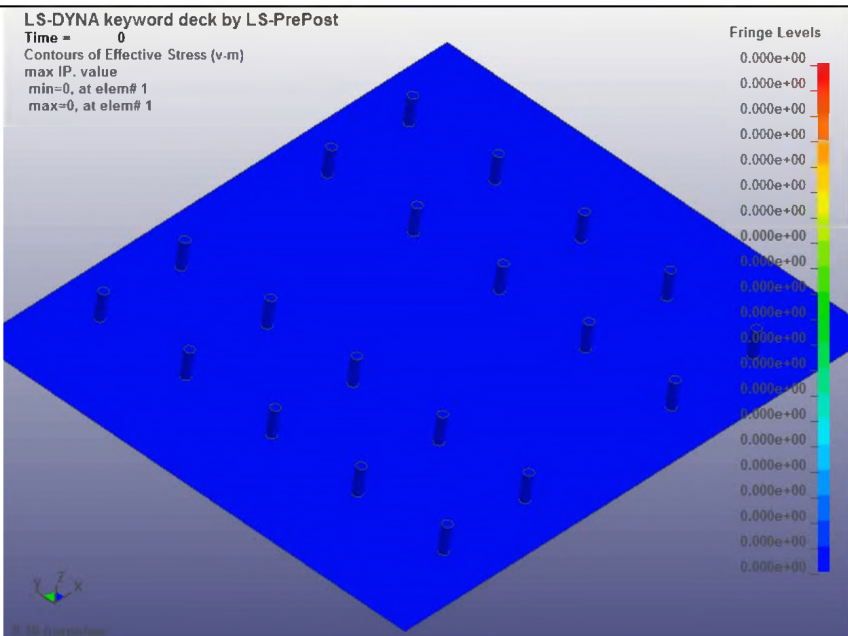Development of a Self-Roughening (SR) Concrete

(d) Onset of buckling. Panel zone shear dramatically reduced. Principle tensile stresses align with buckling of plate steel. Buckling is elastic, that is, steel plate does not yield before the bucking initiates. Model also predicts the lifting of the edge of the steel plate.

Tuesday, SEPTEMBER 29, 2015 – Arlington, VA
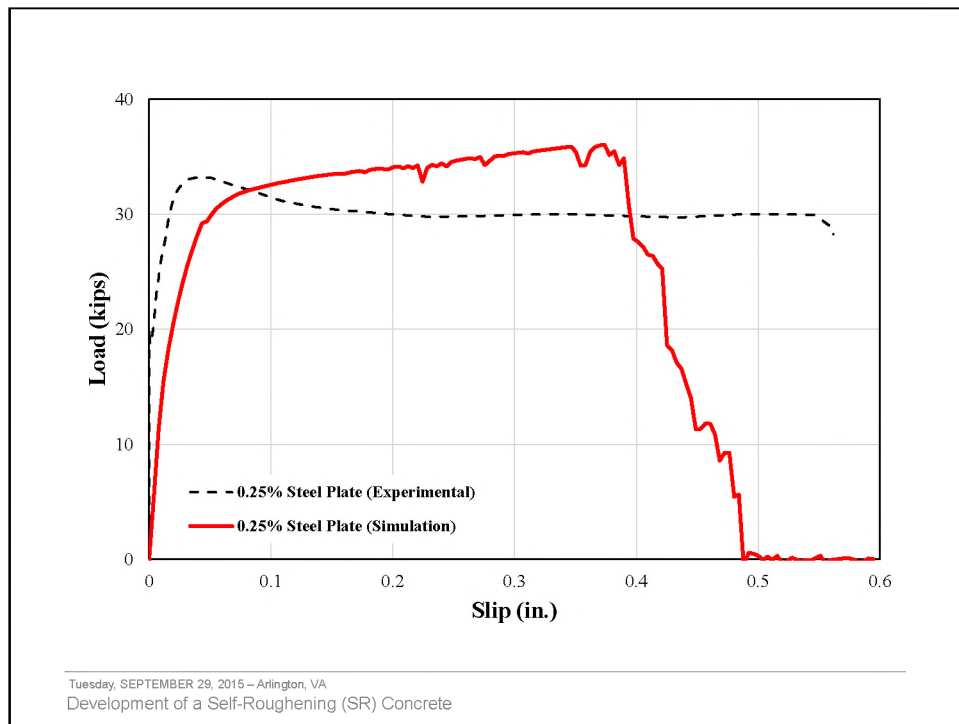Development of a Self-Roughening (SR) Concrete
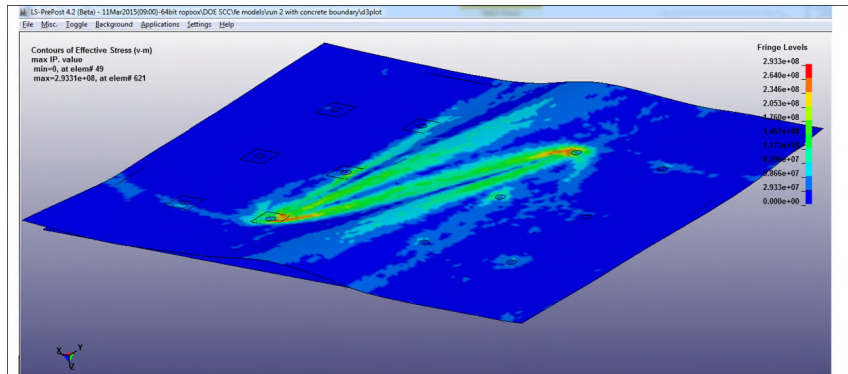
(e) Buckling progresses. Steel plate begins to yield in the vicinity of two studs (see red on stress contour). Buckling distortion as the plate pulls away from the concrete visible.

Tuesday, SEPTEMBER 29, 2015 – Arlington, VA
Development of a Self-Roughening (SR) Concrete

Tuesday, SEPTEMBER 29, 2015 – Arlington, VA
Development of a Self-Roughening (SR) Concrete

Graph: Load (kips) vs Slip (in.)

- - - 0.25% Steel Plate (Experimental)
—— 0.25% Steel Plate (Simulation)

4. Assessment of Shear and Flexural Performances
Specimens preparation
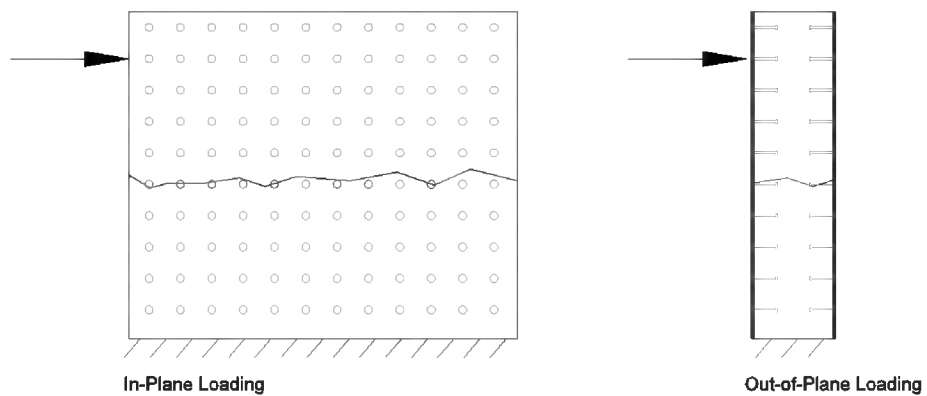
In-Plane Loading

Out-of-Plane Loading

Task 3
A. Control - No cold joint 1 in-plane and 1 out-of-plane

B. Out-of-Plane

C. In-Plane

Tuesday, SEPTEMBER 29, 2015 – Arlington, VA
Development of a Self-Roughening (SR) Concrete

C. In-Plane

First Test   Second Test

2'   7'   2'

Tuesday, SEPTEMBER 29, 2015 – Arlington, VA
Development of a Self-Roughening (SR) Concrete

Tuesday, SEPTEMBER 29, 2015 – Arlington, VA
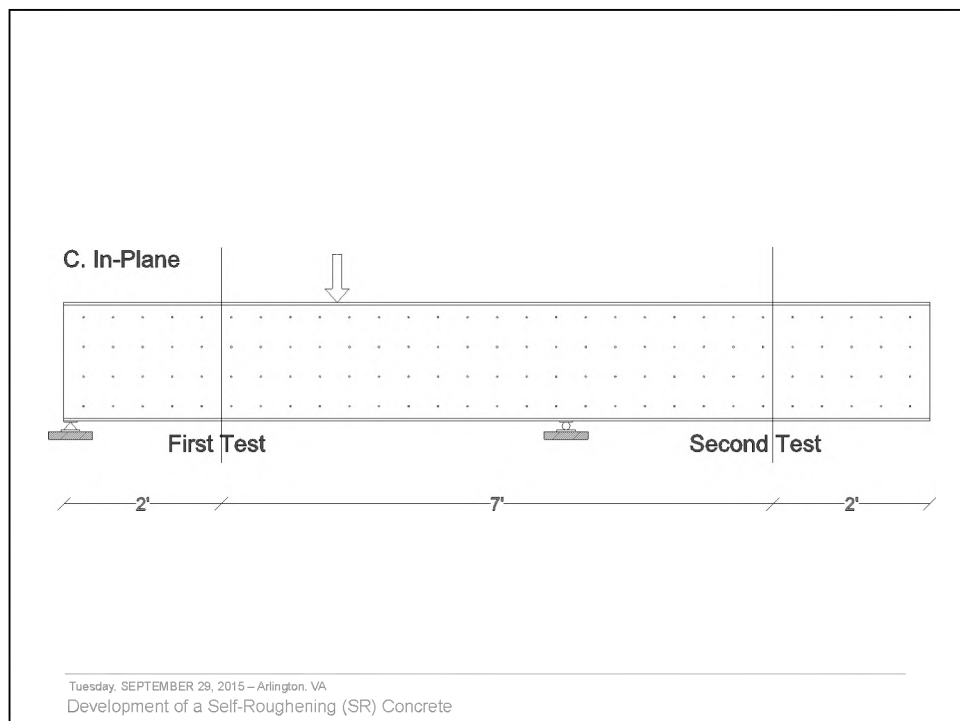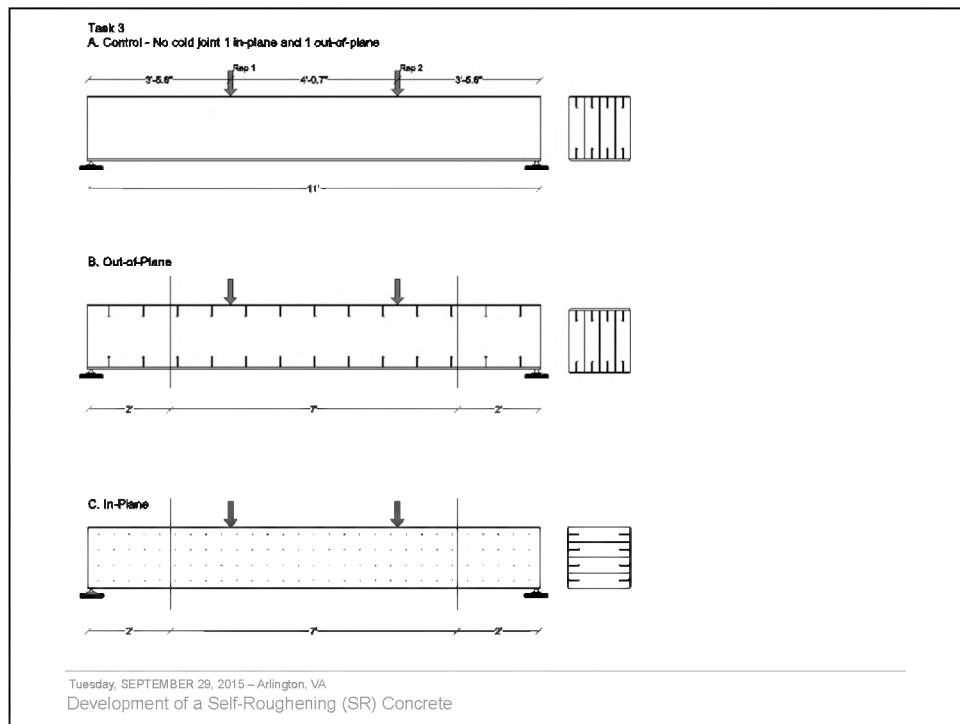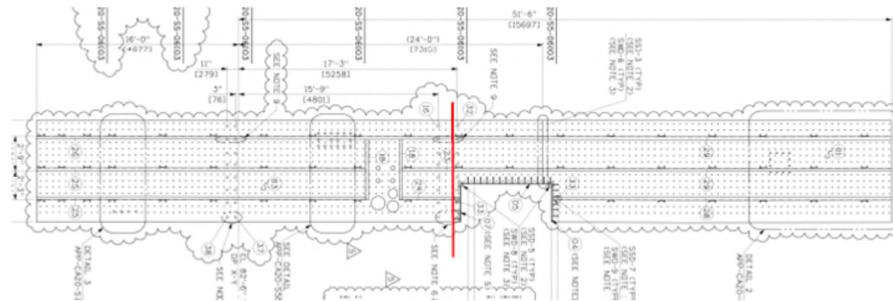Development of a Self-Roughening (SR) Concrete

Tuesday, SEPTEMBER 29, 2015 – Arlington, VA
Development of a Self-Roughening (SR) Concrete

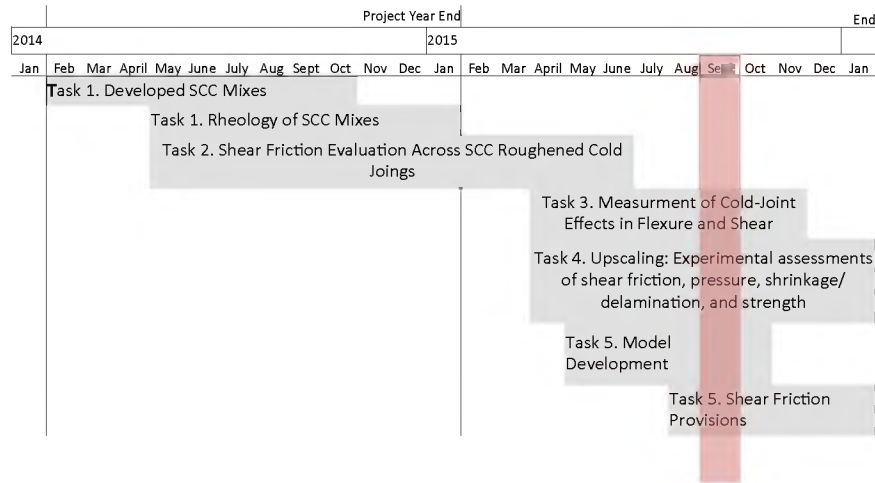## 5. Validation through Full-scale Test and Modeling
Model

6. Conclusions and Outlooks
And future developments

1. Task 2 test results demonstrate the ability of SC construction to transfer in-plane forces across the cold-joint boundaries.
2. Results show that SC construction is more ductile than conventional internally-reinforced concrete.
3. The test results do not conclusively demonstrate the relationship between LWA percentage and cold-joint shear capacity.
4. Non-linear FEA models are promising and may be used for parametric studies of joint behavior – but further calibration is needed.
5. Task 3 specimens will validate in-plane shear behavior and provide better guidance on the out-of-plane behavior of cold-joint behavior in SCC.
6. The Task 4 specimen will be a tremendous challenge and we are working closely with Westinghouse to procure the test article from CBI in a cost-effective and timely manner.

Timeline

| | Project Year End | | End |

| 2014 | 2015 | |

| Jan | Feb | Mar | April | May | June | July | Aug | Sept | Oct | Nov | Dec | Jan | Feb | Mar | April | May | June | July | Aug | Sept | Oct | Nov | Dec | Jan |

Task 1. Developed SCC Mixes

Task 1. Rheology of SCC Mixes

Task 2. Shear Friction Evaluation Across SCC Roughened Cold Joings

Task 3. Measurment of Cold-Joint Effects in Flexure and Shear

Task 4. Upscaling: Experimental assessments of shear friction, pressure, shrinkage/ delamination, and strength

Task 5. Model Development

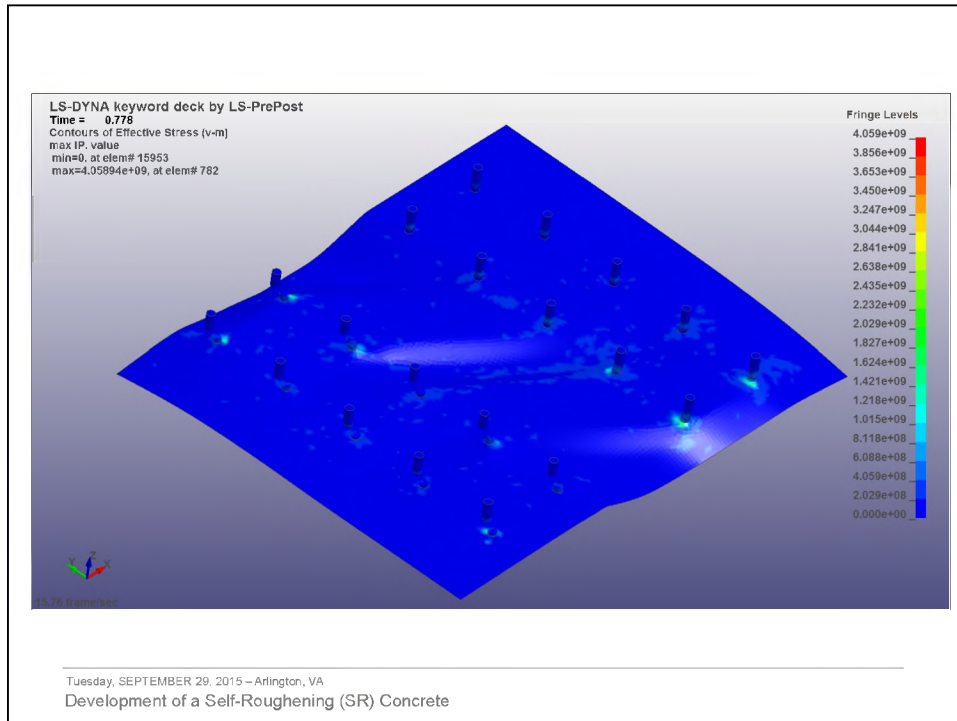Task 5. Shear Friction Provisions

Tuesday, SEPTEMBER 29, 2015 – Arlington, VA

Development of a Self-Roughening (SR) Concrete

"This material is based upon work supported by the Department of Energy [DE-NE0000667 NEET]"

Disclaimer: "This report was prepared as an account of work sponsored by an agency of the United States Government. Neither the United States Government nor any agency thereof, nor any of their employees, makes any warranty, express or implied, or assumes any legal liability or responsibility for the accuracy, completeness, or usefulness of any information, apparatus, product, or process disclosed, or represents that its use would not infringe privately owned rights. Reference herein to any specific commercial product, process, or service by trade name, trademark, manufacturer, or otherwise does not necessarily constitute or imply its endorsement, recommendation, or favoring by the United States Government or any agency thereof. The views and opinions of authors expressed herein do not necessarily state or reflect those of the United States Government or any agency thereof."

Thank you. Questions?

LS-DYNA keyword deck by LS-PrePost
Time =   0.778
Contours of Effective Stress (v-m)
max IP. value
 min=0, at elem# 15953
  max=4.05894e+09, at elem# 782

Fringe Levels

4.059e+09
3.856e+09
3.653e+09
3.450e+09
3.247e+09
3.044e+09
2.841e+09
2.638e+09
2.435e+09
2.232e+09
2.029e+09
1.827e+09
1.624e+09
1.421e+09
1.218e+09
1.015e+09
8.118e+08
6.088e+08
4.059e+08
2.029e+08
0.000e+00

Tuesday, SEPTEMBER 29. 2015 – Arlington, VA
Development of a Self-Roughening (SR) Concrete

Georgia Institute of Technology

Development of a Self-Roughening (SR) Concrete

Russell Gentry (PI)
Kimberly Kurtis (Co-PI)
Larry Kahn (Co-PI)
Giovanni Loreto (Researcher)
School of Civil and Environmental Engineering (CEE) – Georgia Institute of Technology

Bojan Petrovic (Co-PI)
Nuclear and Radiological Engineering) – Georgia Institute of Technology

Industry partner:
Jurie van Wyk (Westinghouse Electric)
Bernd Laskewitz (Westinghouse Electric)

Friday, MAY 19, 2015 – Pocatello, ID

---

1. Intro

2. Task 1 – Development of Self-Roughening Concrete (SRC) Mix Design

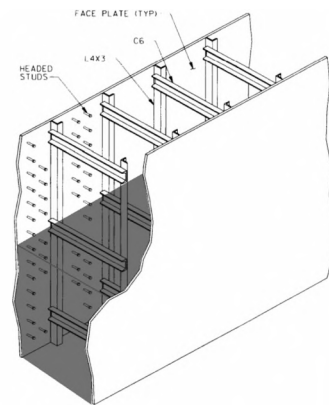3. Task 2 – Assessment of Cold Joint Shear Friction Capacity

4. Future work

Friday, MAY 19, 2015 – Pocatello, ID
Development of a Self-Roughening (SR) Concrete

1. Intro
Objectives

- Development of a self-consolidating concrete mixtures so that concrete placement can be made into steel plate composite (SC) modular structures without the need for continuous concrete placement.
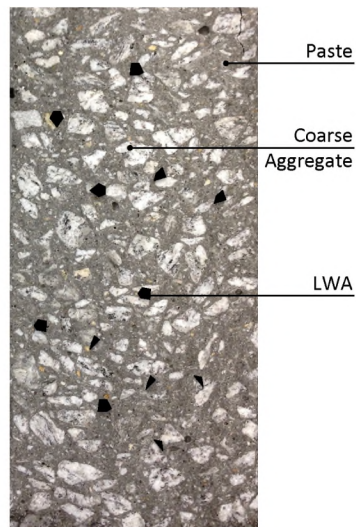

Friday, MAY 19, 2015 – Pocatello, ID
Development of a Self-Roughening (SR) Concrete

1. Intro
Objectives

Friday, MAY 19, 2015 – Pocatello, ID
Development of a Self-Roughening (SR) Concrete

2. Development of SRC Mix Design
Strategies

Mix Component	67M
Cementitious (lb/yd^3)	
Cement Type II	617
Fly Ash, Class F	459
Total Powder	*1076*
Water (lb/yd^3)	343
w/cm	*0.319*
Coarse Aggregates (lb/yd^3)	
# 67	981
# 89	305
Total Coarse	*1286*
Fine Aggregates (lb/yd^3)	
Natural sand	679
Manufactured sand	679
Total Fine	*1357*
Total Aggregates	*2796*
Admixures (fl oz./cwt)	
HRWR	0.18
TOT	4063

Friday, MAY 19, 2015 – Pocatello, ID
Development of a Self-Roughening (SR) Concrete

2. Development of SRC Mix Design
Strategies

Mix Component	67M
Cementitious (lb/yd^3)	
Cement Type II	617
Fly Ash, Class F	459
Total Powder	*1076*
Water (lb/yd^3)	343
w/cm	*0.319*
Coarse Aggregates (lb/yd^3)	
# 67	981
# 89	305
Total Coarse	*1286*
Fine Aggregates (lb/yd^3)	
Natural sand	679
Manufactured sand	679
Total Fine	*1357*
Total Aggregates	*2796*
Admixures (fl oz./cwt)	
HRWR	0.18
TOT	4063

- Smaller aggregates and controlled gradation curve
- Use of #67 and #89 coarse aggregates
- Substitute 5%, 10% and 15% in volume of coarse aggregate with LWA

Friday, MAY 19, 2015 – Pocatello, ID
Development of a Self-Roughening (SR) Concrete

2. Development of SRC Mix Design
Proprieties and tests

Self-Consolidating Concrete   Self-Roughening Concrete

Fresh SCC proprieties
- Flowability: flows easily at suitable speed into formwork (T20 = 4-5sec; Flow Slump = 24-26")
- S Groove test (good self-healing ability)
- Hardened Visual Stability Index (VSI = 0)
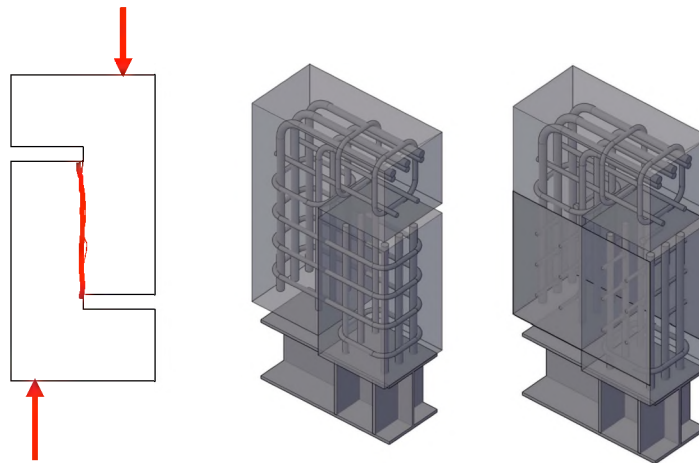
Hardened SRC proprieties
- Compressive strength: 6-7ksi
- Shrinkage: <250 µε

Friday, MAY 19, 2015 – Pocatello, ID
Development of a Self-Roughening (SR) Concrete

3. Assessment of Cold Joint Shear Friction Capacity
Mechanical tests for shear friction characterization

Laboratory test
Kahn, L., Mitchell, A. D. (2002) "Shear friction test with high-strength concrete" ACI Structural Journal, 99 (1).
Friday, MAY 19, 2015 – Pocatello, ID
Development of a Self-Roughening (SR) Concrete

3. Assessment of Cold Joint Shear Friction Capacity
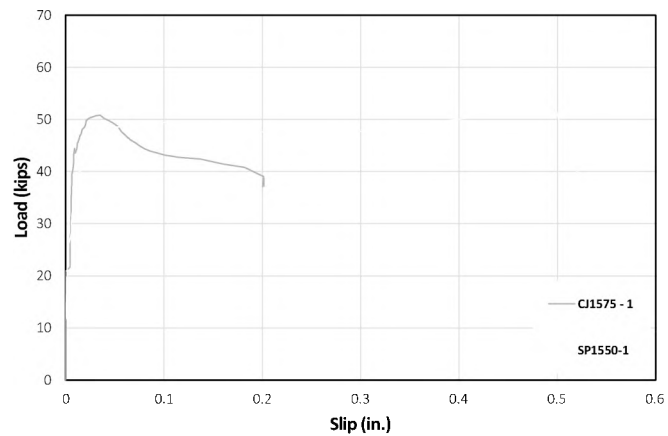Mechanical tests for shear friction characterization

Step 1
Step 2
Step 3
Step 4
Step 5

Friday, MAY 19, 2015 – Pocatello, ID
Development of a Self-Roughening (SR) Concrete

3. Assessment of Cold Joint Shear Friction Capacity
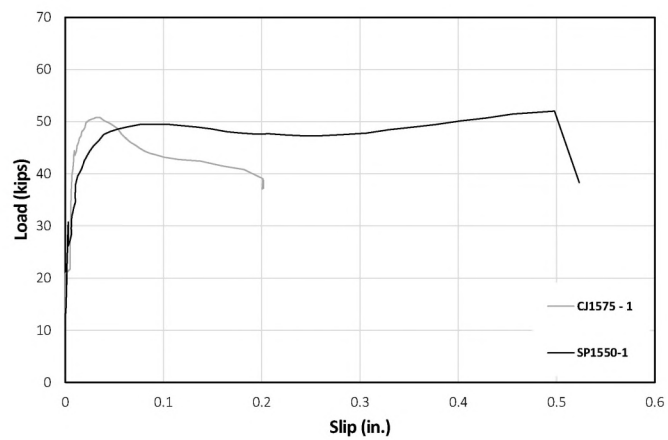Mechanical tests for shear friction characterization

Knife-edge support
LVDT
LVDT support
Knife-edge support
200kip load cell
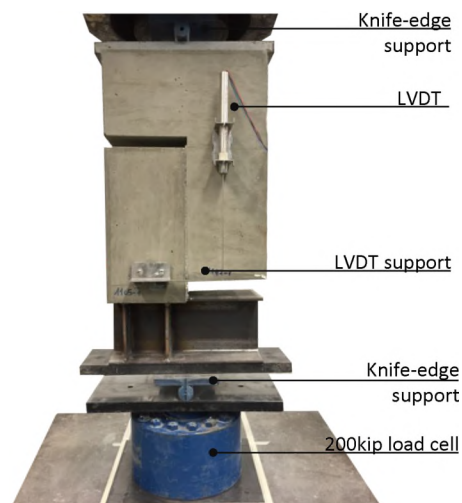
Friday, MAY 19, 2015 – Pocatello, ID
Development of a Self-Roughening (SR) Concrete

4. Conclusions
Question

Are there **New Construction Methods** and Processes that the Nuclear Industry Could Adopt to Increase Quality while **Decreasing Schedule and Cost**?

Friday, MAY 19, 2015 – Pocatello, ID
Development of a Self-Roughening (SR) Concrete

4. Conclusions
And future developments

- Development of a self-consolidating concrete mixtures so that concrete placement can be made into steel plate composite (SC) modular structures without the need for continuous concrete placement.
Task 1: Development of SCC with Shear-Friction Capacity for Mass Placement

- SCC mixtures to ensure sufficient shear capacity across cold- joints (self-roughening), while minimizing shrinkage and temperature increase during curing to enhance concrete bonding with the steel plates.
Task 1: Development of SCC with Shear-Friction Capacity for Mass Placement
Task 2: Assessment of Cold Joint Shear-Friction Capacity

- SCC mixtures featuring a self-roughening capability to produce adequate shear friction between cold joints and to produce draft provisions addressing shear-friction, for consideration in the new AISC N690 Appendix N9 code used for the design of SC modular structures.
Task 3: Assessment of Shear and Flexural Performance
Task 4: Validation through Full-Scale Testing and Modeling
Task 5: Draft Code Requirement for Shear Friction Design of Cold Joints

Friday, MAY 19, 2015 – Pocatello, ID
Development of a Self-Roughening (SR) Concrete

Thank you. Questions?

Self-Consolidating Concrete with Enhanced Shear Friction Capacity for Cold-Joint Applications

Giovanni Loreto[a], Russell Gentry[b], Kimberly Kurtis[a], Larry Kahn[a]

[a] School of Civil, and Env. Engineering, Georgia Institute of Technology, Atlanta, GA
[b] School of Architecture, Georgia Institute of Technology, Atlanta, GA

Abstract. The concept of shear friction in the behavior of reinforced concrete and composite structures describes the ability to transmit shear across a given boundary, typically between two separate placements of concrete – sometimes referred as a cold joint. In order to enhance shear capacity across cold joints, a specific self-consolidating concrete (SCC) mixture was developed by incorporating a small fraction of light-weight coarse aggregate (LWA) so that roughening by raking or other means was not necessary. Key fresh and hardened properties such as slump flow, segregation resistance, shrinkage and temperature increase were evaluated to ensure overall concrete performance. In addition, the roughness of the concrete surfaces was characterized by using a qualitative approach proposed by the International Concrete Repair Institute along with a quantitative approach that complemented the use of existing technology. The test results indicate that the optimized self-consolidating concrete, referred as self-roughening concrete, can successfully increase the shear friction capacity between cold joints showing great potential in real world applications.

Keywords. concrete, self-consolidating concrete, cold joints, walls

1. Mix design and assessment of fresh properties.

A total of thirty-five trial mixes were cast. Table I reports the quantities for a selected mix that passed the qualification protocol, and also included the mixes with 5%, 10% and 15% of LWA. Fresh properties were evaluated by using three different tests: a) slump flow to measure fluidity; b) "S" groove tests and visual stability index (VSI) to assure filling ability and resistance to segregation. To determine the slump flow, an Abrams cone was inverted and filled with fresh concrete. The cone was lifted and the concrete flowed out under its own weight. Two perpendicular measurements of the maximum diameter were taken across the spread of concrete along with the final flow time, from cone removal to flowing completion, and the T50 flow time, which is the time needed by the concrete to spread up to 50 mm (20 in.). After that, using a finger or a tamping rod, an "S" was drawn into the concrete on the slump flow board to assess the stability of the mix. The VSI test was used in conjunction with the slump flow test. The range of values for the VSI is 0 through 3, with zero being a highly stable mix, and 3 designates a highly unstable mix.

Table 1. Mix Design

Mix Component	SCC	SRC 5%	SRC 10%	SRC 15%
Cementitious		kg/m^3 [lb/yd^3]		
Cement Type I/II		366.4 [617]		
Fly Ash, Class F		272.3 [459]		
Water		203.6 [343]		
w/cm		*0.318*		
Coarse Aggregates				
# 67	763.2 [1286]	724.0 [1221]	676.0 [1157]	648.4 [1093]
LWA	-	14.4 [24.5]	29.1 [49.0]	44.1 [74.25]
Fine Aggregates				
Natural sand		402.5 [678.5]		
Manufactured sand		402.5 [678.5]		
Admixtures, ml/100 kg [fl oz./cwt]		425 [6.36]		
Flow Slump mm [in.]		585 – 635 [23 – 25]		
T20 (sec)		4 - 5		
"S" groove (0-5)		0 – 0.5		
VSI (0-3)		0		
Compression, MPa [psi]	53.12 [7705]	52.88 [7670]	52.82 [7661]	52.45 [7608]
Std. dev., MPa [psi]	-	807	275	537
Unit weight kg/m^3 [pcf]	2402 [156.3]	2370 [150.4]	2322 [156.3]	2290 [150.4]
CSP Roughness (1-9)	-	7	8	9
S_a, mm^{-1} [in^{-1}]	-	0.018 [0.448]	0.031 [0.789]	0.042 [1.071]

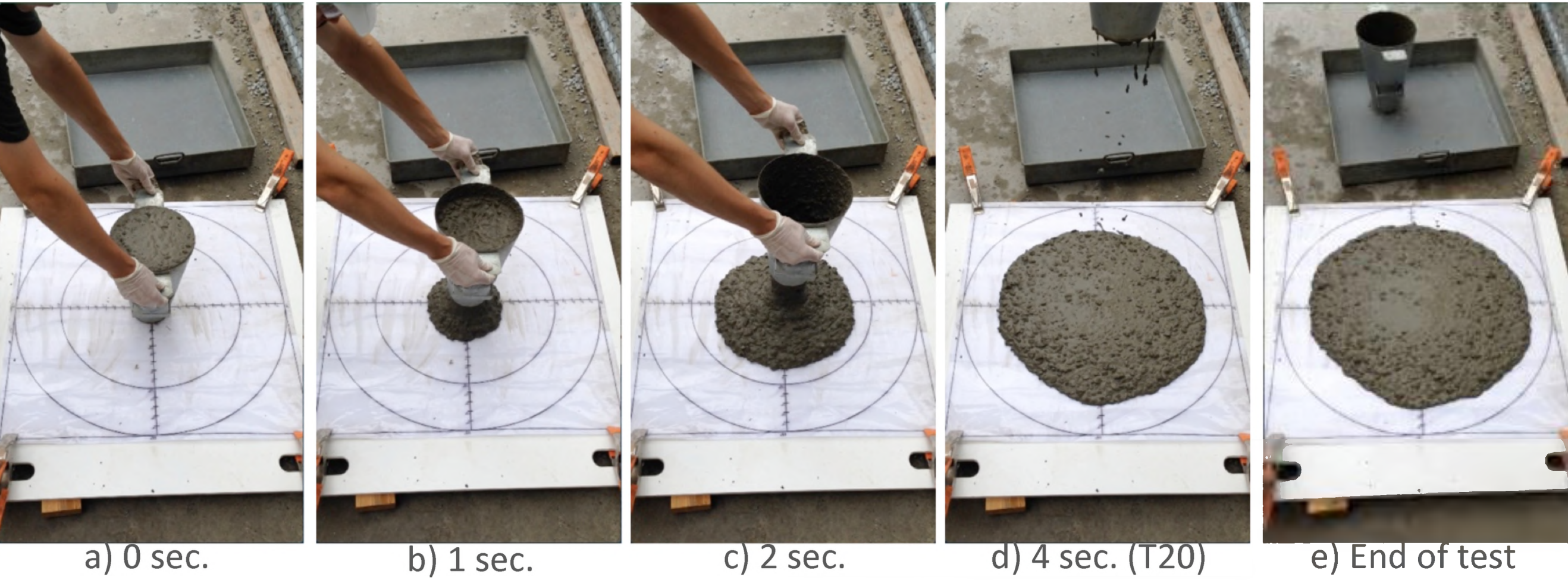a) 0 sec.   b) 1 sec.   c) 2 sec.   d) 4 sec. (T20)   e) End of test

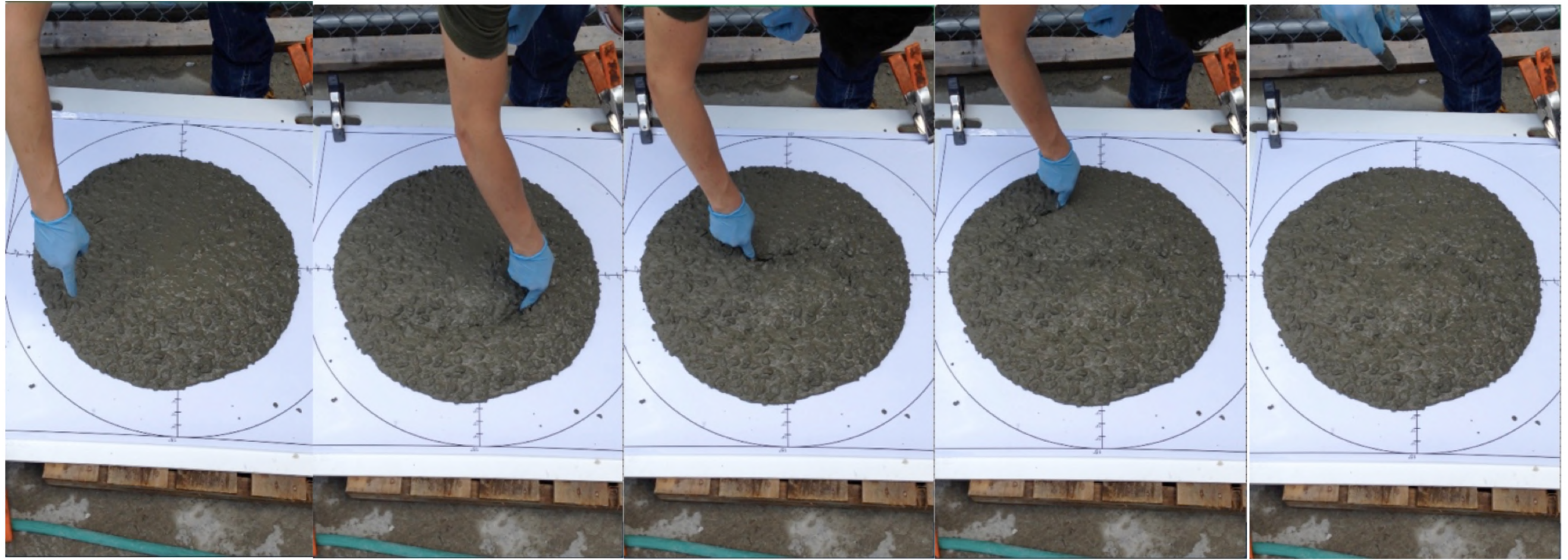**Figure 1.** Performing a flow slump test

Figure 2. Performing "S" groove test

2. Measurement of surface roughness.

One of the main objective in developing the SRC was to generate the appropriate surface roughness essential to facilitate shear interlock between the existing substrate of concrete and the overlay at a cold joint. Surface roughness was measured using: (1) International Concrete Repair Institute's (ICRI's) standard concrete surface profiles (CSPs) (qualitative assessment) and (2) a quantitative assessment.
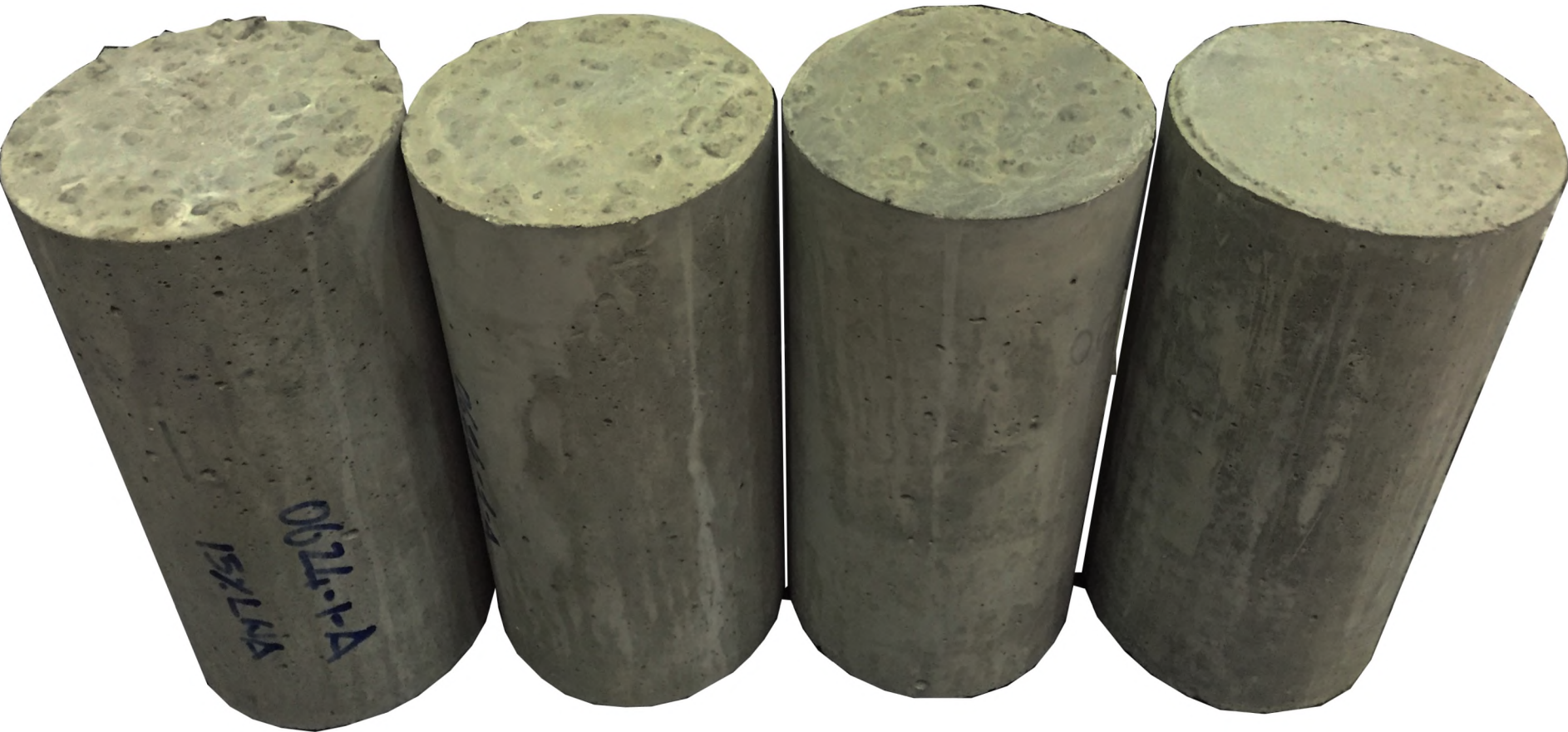

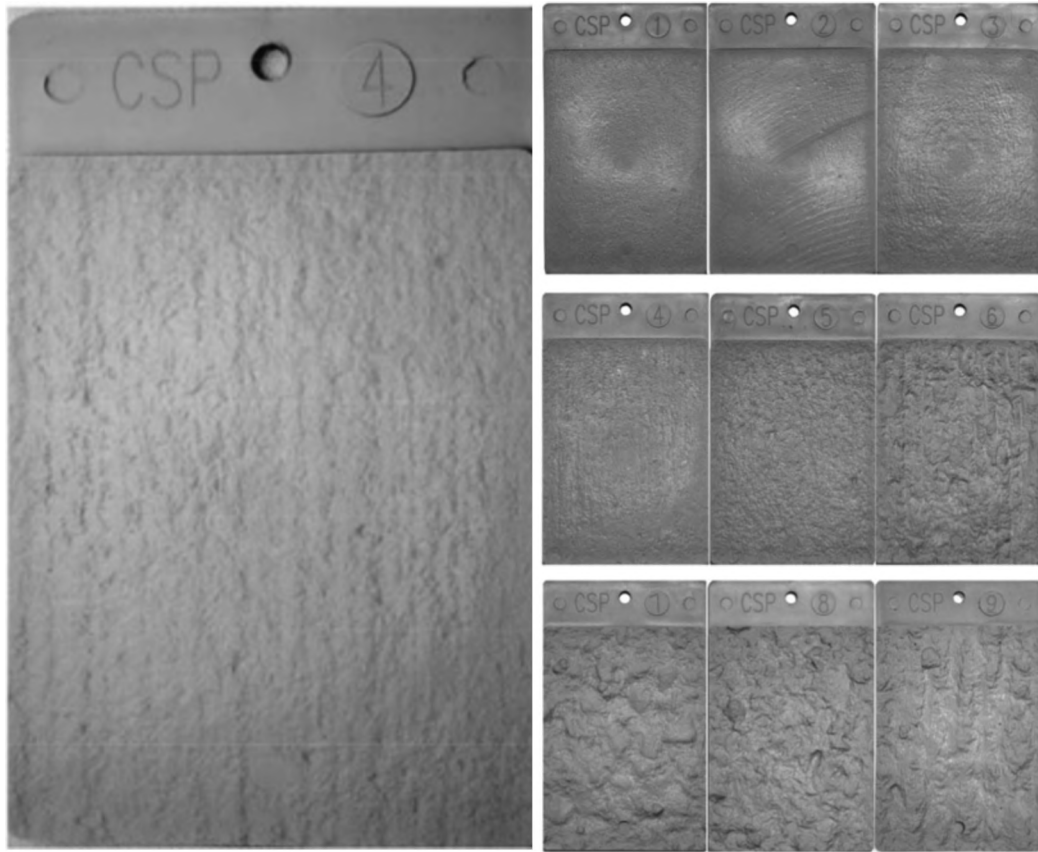**Figure 3:** From left to right, concrete cylinders with 15%, 10%, 5% and no-LWA substitution.

Figure 4. ICRI chips

Figure 5. Roughness quantitative measurements

3. Findings and future directions.

The mixtures demonstrated slump flows between 530 mm to 635 mm (21-25 in.) which satisfy flow and filling ability for an SCC. The mixes demonstrated cohesive properties, so that the mixtures remained in a consistent state during concrete placement while allowing a controlled segregation of the LWA. 3. Because of the high cement fraction in the mixes, early shrinkage of the concrete mix was assessed. High volumes of fly ash used to produce SRC and reduce the early heat of hydration helped to reduce drying shrinkage in the self-roughening SRC mixes with values around 220 με after 54 days.
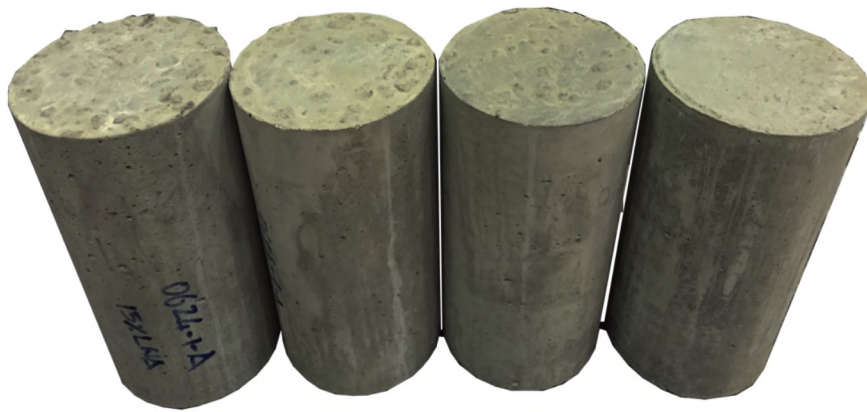
Self-consolidating concrete with enhanced shear friction capacity for cold joint and applications

by

Giovanni Loreto, Russell T. Gentry, Kimberly E. Kurtis and Lawrence F. Kahn

Abstract:

The concept of shear friction in the behavior of reinforced concrete and composite structures describes the ability to transmit shear across a given boundary, typically between two separate placements of concrete – sometimes referred as a cold joint. In order to enhance shear capacity across cold joints, a specific self-consolidating concrete (SCC) mixture was developed by incorporating a small fraction of light-weight coarse aggregate (LWA) so that roughening by raking or other means was not necessary. Key fresh and hardened properties such as slump flow, segregation resistance, shrinkage and temperature increase were evaluated to ensure overall concrete performance. In addition, the roughness of the concrete surfaces was characterized by using a qualitative approach proposed by the International Concrete Repair Institute along with a quantitative approach that complemented the use of existing technology. The test results indicate that the optimized self-consolidating concrete, referred as self-roughening concrete, can successfully increase the shear friction capacity between cold joints showing great potential in real world applications.

Figure: From left to right, concrete cylinders with 15%, 10%, 5% and no-LWA substitution.

Keywords:

Self-Consolidating Concrete (SCC), Light Weight Aggregate (LWA), Cold Joint, Shear Friction, Mass Concrete.

Speaker name, title, organization, and contact information:

Giovanni Loreto, Postdoctoral Associate,

Department of Civil and Environmental Engineering, Georgia Institute of Technology,

790 Atlantic Drive, Room 5139d

Atlanta, GA 30332, USA

Email: giovanni.loreto@ce.gatech.edu

Phone: +1 (305) 773-8896

Presentation:

Poster presentation

Self-Roughening Concrete with Enhance Shear-Friction Capacity for Cold Joint Applications

Giovanni Loreto, T. Russell Gentry, Kimberly E. Kurtis and Lawrence F. Kahn

School of Civil and Environmental Engineering
Georgia Institute of Technology, Atlanta, GA

Abstract: The concept of shear friction in the behavior of reinforced concrete and composite structures describes the ability to transmit shear across a given boundary, typically between two separate placements of concrete – sometimes referred as a cold joint. In order to enhance shear capacity across cold joints, a unique self-consolidating concrete (SCC) mixture was developed by incorporating of a small fraction of light-weight coarse aggregate (LWA) so that roughening by raking or other means was not necessary. Fresh and hardened properties such as slump flow, segregation resistance, shrinkage, and strength were evaluated to ensure overall concrete performance. In addition, the roughness of the concrete surfaces was characterized by using a qualitative approach proposed by the International Concrete Repair Institute along with a quantitative approach that complemented the use of existing technology. The test results indicate that the optimized self-consolidating concrete, referred as self-roughening concrete, can successfully increase the shear friction capacity between cold joints showing great potential in real world applications.

Introduction

Construction joints are necessary in concrete structures when placing concrete in a continuous operation becomes impractical due to unit size, batching and mixing capacity, weather conditions, equipment problems, or the like. When one of these conditions occurs, depending on the time between placements, different surface treatments are used to provide adequate shear capacity between layers of concrete, including manually roughening of the surface.

The concept of shear friction in the behavior of concrete structures describes the ability to transmit shear across a given boundary, typically between two separate placements of concrete – sometimes called a "pour joint" or "cold joint". In conventional reinforced concrete internal reinforcements provides a tension tie that prevents the concrete placements from moving perpendicular to the boundary [1]. The friction of the surface, which is considered by ACI 318 [2] to be a function of the surface roughness, prevents the two placements from moving parallel to the boundary. The normal, clamping force at the interface is provided by the tensile strength of the steel crossing the interface, and the coefficient of friction varies based on the surface roughness, thus "shear friction".

In order to enhance shear friction capacity across as-cast cold joints, a self-consolidating concrete (SCC) mixture was developed by incorporating of a small fraction of light-weight coarse aggregate (LWA), between 5 and 15% by volume of coarse aggregate, so that roughening by raking or other means was not necessary. The purpose of the LWA is to provide an internal source of surface roughening, while still satisfying the requirements for grading (ASTM C33 [3]). Due to its lower specific gravity, the LWA rises to the surface of the concrete shortly after placement.

The attributes of an appropriate SCC mixtures were selected as follows: (1) high spread to facilitate concrete placement in the field without internal vibration, (2) cohesive concrete mixture to prevent segregation of the normal weight aggregates from the cement paste during concrete placement, and (3) low viscosity of the SCC so that the LWA would float. In addition, prior research has demonstrated that high volumes of fly ash, in particular, can be used to produce SCC with reduced drying shrinkage [4]. Therefore, in order to limit shrinkage and heat development associated with cement hydration, improve durability, and to provide the desired self-consolidating behavior [5], the use of relatively high substitution of fly ash (>35%) for cement was included in designing the mixtures.

A SCC mix design that respected all these characteristics was referred as self-roughening concrete (SRC). The following sections discuss the methodology used in designing SRC mixtures: selection of material constituents, optimization of the mixtures, and evaluation of fresh and hardened properties.

Materials and mixture proportioning

Concrete typically contains four main ingredients: coarse aggregate, fine aggregate, cement, and water. Additionally, supplementary cementitious materials (SCM) and chemical admixtures are used to modify the plastic and/or hardened state properties. SCC mixes generally uses a higher volume of fine aggregates and employ super-plasticizers and water-reducers to achieve their increased workability. The SRC mixtures presented in this paper contained coarse and fine aggregates, cement, SCM such as fly ash, water and high-range water reducer as

admixture.

The coarse aggregate was a crushed granite with a maximum size aggregate of 19 mm or #67 (3/4 in.). As a fine aggregate, a blend of 50% manufactured (e.g., fractured granite) sand and 50% alluvial sand was used in order to enhance performances during the fresh state. Gradation curves were generated in accordance to the ASTM C33, which fully respected the upper and lower limits of the ASTM specifications. Density and specific gravity were also determined as per ASTM C29 [6] and ASTM C127 [7], respectively. In addition to the granite, expanded slate aggregate produced using a rotary kiln process was included in the mix design to generate surface roughness.

The cement used for the laboratory mixes was an ASTM C150 [8] Type I/II Portland cement. The only supplementary cementitious material used in combination with cement was fly ash which conformed to ASTM C618 [9] specifications for Class F.

The chemical admixture was a polycarboxylate high range water reducer. For laboratory conditions the recommended dosage was selected between 6 fl. oz. and 8 fl. oz. per 100 lbs. (155-210 ml/100 kg) of cementitious materials. This admixture was added at the end of the batching cycle directly to freshly mixed concrete in the concrete mixer.

Mixture design

All mixes were cast in accordance with ASTM C 192 [10] (standard practice for making and curing concrete test specimens in the laboratory). During the mixing, dry sand was used while coarse aggregates were used in the saturated surface-dry (SSD) condition. LWA were pre-soaked in water for 24 hours and then brought to SSD condition before their use. The design quantities considered in the mix design proportions were:

- Total Cement, kg/m^3 [lb/yd^3]
- Fly Ash, kg/m^3 [lb/yd^3]
- Coarse Aggregate - #67, kg/m^3 [lb/yd^3]
- Coarse LWA - #7 – 5%, 10% and 15% in volume of #67
- Water Cement (w/c) ratio
- Chemical admixtures, ml/m^3 (fl oz/yd^3) (HRWR)

A total of thirty-five trial mixes were cast. Table I reports the quantities for a selected mix that passed the qualification protocol, and also included the mixes with 5%, 10% and 15% of LWA. All trial mixes reported in Table I showed adequate slump flow ranging from 533 – 635 mm (21 in. to 25 in.) and comparable performances using slightly different amount of HRWR.

Table I: Mix design.

Mix Component	SCC	SRC 5%	SRC 10%	SRC 15%
Cementitious	kg/m^3 [lb/yd^3]			
Cement Type I/II	366.4 [617]			
Fly Ash, Class F	272.3 [459]			
Water	203.6 [343]			
w/cm	0.318			
Coarse Aggregates				
# 67	763.2 [1286]	724.0 [1221]	676.0 [1157]	648.4 [1093]
LWA	-	14.4 [24.5]	29.1 [49.0]	44.1 [74.25]
Fine Aggregates				
Natural sand	402.5 [678.5]			
Manufactured sand	402.5 [678.5]			
Admixtures, ml/100 kg [fl oz./cwt]	425 [6.36]			
Flow Slump mm [in.]	585 – 635 [23 – 25]			
T20 (sec)	4 - 5			
"S" groove (0-5)	0 – 0.5			
VSI (0-3)	0			
Compression, MPa [psi]	53.12 [7705]	52.88 [7670]	52.82 [7661]	52.45 [7608]
Std. dev., MPa [psi]	-	807	275	537
Unit weight kg/m^3 [pcf]	2402 [156.3]	2370 [150.4]	2322 [156.3]	2290 [150.4]
CSP Roughness (1-9)	-	7	8	9
S_a, mm^{-1} [in^{-1}]	-	0.018 [0.448]	0.031 [0.789]	0.042 [1.071]

Test Results and Discussion

Fresh properties

Slump flow was used to measure fluidity; the VSI and the "S" groove tests were use to assure filling ability and resistance to segregation.

Slump flow test. To determine the slump flow, an Abrams cone was inverted and placed on a non-absorptive surface and filled with fresh concrete without any tamping. The cone was lifted and the concrete flowed out under its own weight. Two perpendicular measurements of the maximum diameter were taken across the spread of concrete and the average was reported. The final flow time, from cone

removal to flowing completion was recorded, as well as the T50 flow time, which is the time needed by the concrete to spread up to 50 mm (20 in.). Slump flow spread diameter values of 584 ± 51 mm (23 ± 2 in.) were considered satisfactory with test results ranging from 530 mm to 635 mm (21-25 in.). T50 values spanned from 3 sec. to 5 sec., and they were inversely proportionated to the slump flow diameter. Fresh properties are reported in Table I.

"S" groove test. The "S" groove test is a simple and effective method for determining the stability and self-healing ability of fresh SRC. Using a finger or a tamping rod, an "S" is drawn into the concrete on the slump flow board. If the mix is stable, the concrete rapidly fills the 'S' groove and the stability of the concrete is good, otherwise a layer of paste or bleed will fill in the groove, essentially showing the segregation of the coarse aggregate within the mix. An empirical range of values spanning from 0 to 5 was used (0 being highly stable and 5 highly unstable) was associated to the test in order to better characterize the behavior. Numerical data are reported in Table 1.

Visual stability index (VSI) [11]. The VSI test was used in conjunction with the slump flow test. The range of values for the VSI is 0 through 3, with zero being a highly stable mix, and 3 designates a highly unstable mix. The parameters for determining the VSI number of a given mix are mortar halos, bleed, air bubbles, and aggregate pile-up. Table II presents the different criteria for VSI numbers. Mortar halos result from the segregation of the paste from the concrete due to too much water or coarse aggregate in a mix. An unstable mix may contain a mortar halo less than 10 mm (0.4 in.); larger halos result in highly unstable concrete mixes. Slight bleed and few air bubbles surfacing were allowed for stable mixes, but not highly stable. Data are reported in Table I.

Table II: Visual stability index [11].

Rating	Number	Criteria
Highly Stable	*0*	No evidence of slump segregation
	0.5	Very slight evidence of bleed and air popping
Stable	*1*	No mortar halo No aggregate pile-up
	1.5	Slight bleed and air popping Just noticeable mortar halo and aggregate pile- up
Unstable	*2*	Slight mortar halo, less than 0.4 in. (10mm) Slight aggregate pile-up Noticeable bleed
Highly Unstable	*3*	Large mortar halo greater than 0.4 in. (10mm)

In general, the slump flow tests in conjunction with the visual stability index (VSI) were effective in evaluating the workability of the SRC mixtures. The data collected using these tests appeared to be adequate for quantifying the rheological properties of the SCC. In particular, SRC with a slump flow less than 432 mm (17 in.) did not display self-compacting properties; on the other hand SRC with a slump flow over 660 mm (26 in.) experienced severe segregation and bleeding. The inclusion of LWA into the mix led to the formation of a rough surface as showed in Figure 1.
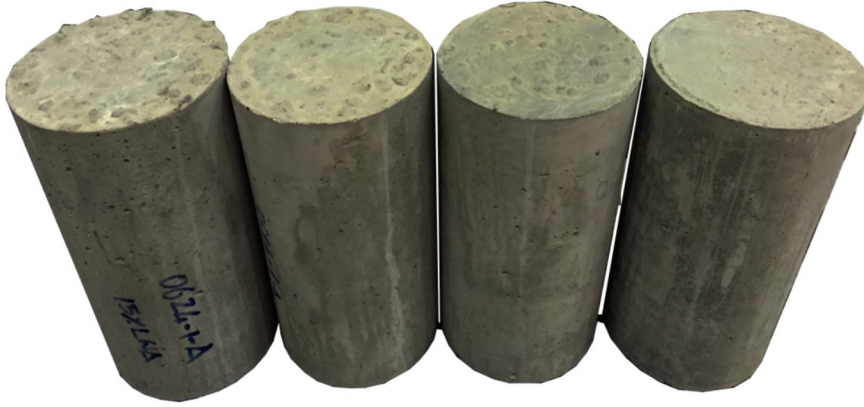
Figure 1: From left to right, concrete cylinders with 15%, 10%, 5% and no-LWA substitution.

Hardened properties

All specimens were cured following the ASTM C192 requirements: specimens were stored in a fog room with temperature of 23 ± 2 °C (73.5 ± 3.5 °F) and humidity > 95%.

Compressive strength. Compression tests were conducted as per ASTM C39 [12] using 100x200 mm (4x8 in.) cylinders. Five cylinders were cast for every mix, demolded after 24 hours and stored in a fog room for 28 days until testing. Results are reported in Table I along with their standard deviations.

Drying shrinkage. Drying shrinkage tests were performed following the AASHTO T160 [13] and Alabama DOT [14] specifications. Two sets of three specimens per each mix were cast in prism molds (75x75x285 mm - 3x3x11.25 in.), coated in advance with an oil-based form release agent, with gage studs inserted into their ends. Concrete specimens were covered with a polyethylene sheet and wet towels to avoid moisture loss during the first 24 hours. They were demolded after one day; initial length and mass were measured; and then they were stored in the fog room until further testing. Following the Alabama DOT specification, the first set of specimens was cured in these conditions for seven days, whereas the remaining

specimens were cured for 28 days in accordance to AASHTO T160. Upon the end of curing duration, the specimens were moved to an environmental chamber with a temperature of $23 \pm 2\,°C$ $(73.5 \pm 3.5\,°F)$ and relative humidity of $50 \pm 4\,\%$. During drying, the length was monitored according to ASTM C 157. The shrinkage measurements were taken at constant intervals from the time the specimens were removed from moist curing. After 54 days, the average shrinkage was equal to $213\,\mu\varepsilon$ with a standard deviation of $16\,\mu\varepsilon$ and $207\,\mu\varepsilon$ with a standard deviation of $17\,\mu\varepsilon$ for specimen with 7-day and 28-day curing time, respectively. Figure 2 compares the difference between 7-day and 28-day shrinkage where each point represents an average of three repetitions. Average measured drying shrinkage was less than $250\,\mu\varepsilon$ in both curing times.
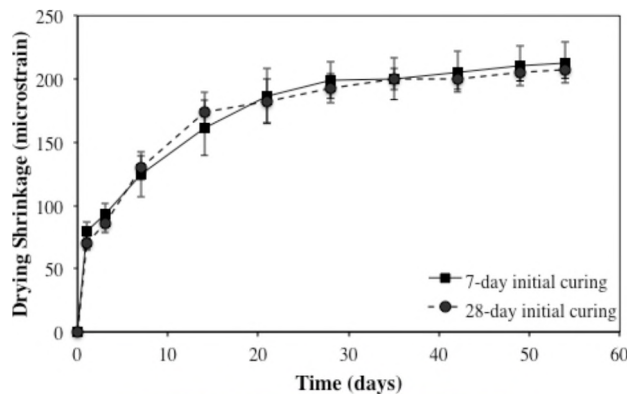
Figure 2: Free Shrinkage test results.

Measurement of surface roughness. One of the main objective in developing the SRC was to generate the appropriate surface roughness essential to facilitate shear interlock between the existing substrate of concrete and the overlay at a cold joint. The ACI 318 shear friction concept is that shear forces are transferred across a joint by friction between the surfaces. The frictional force is a function of the normal force applied and the coefficient of friction, μ, between the surfaces. By incorporating a small fraction of LWA (5%, 10% and 15% in volume,) in the SCC mix designs, the SCC was able to generate a rough surface so that roughening by raking or other means may not be necessary. Surface roughness was measured using two methodologies: (1) International Concrete Repair Institute's (ICRI's) standard concrete surface profiles (CSPs) (qualitative assessment) and (2) a quantitative assessment.

ICRI's CSPs are benchmarks used to establish industry acceptable specifications and represent varying degrees of concrete roughness and texture. Nine rubber profiles represent varying degrees of concrete roughness, with CSP 1 being thought to represent the least rough (smoothest), while CSP 9 being the most rough.

Comparing the concrete surface to the CSPs, a qualitative assessment of the surface roughness was performed by visual inspection.

In addition to the CSP molds, a quantitative assessment of concrete surface condition was also performed. Using 152x559 mm (6x12 in.) concrete cylinders, the amplitude of surface roughness was determined by measuring the distance between the top of the exposed aggregate and its junction with the paste (distance A) using a caliper as shown in Figure 3. A coefficient of surface roughness, S_a, was then calculated considering that roughness is directly proportioned to the number of LWA particles present on the surface and their average amplitude, whereas it is inversely proportional to the surface area. These consideration and the device used for measuring the average amplitude led to the following equation [15]:

$$S_a = \frac{n \cdot \sum_1^n A_n}{S} \tag{1}$$

where: n is the number of LWA particles present on the surface, A_n represents the average amplitude and S is the nominal surface area of the concrete specimen. Results of both methodologies are reported in the last two rows of Table I.

Figure 3: Roughness quantitative measurements.

Conclusions

1. The SRC mixtures demonstrated slump flows between 530 mm to 635 mm (21-25 in.) which satisfy flow and filling ability for an SCC.

2. The SRC mixes demonstrated cohesive properties, so that the mixtures remained in a consistent state during concrete placement while allowing a controlled segregation of the LWA. This was a particular challenge in the SRC because it is necessary that some small fraction of the lightweight aggregate rise through the

mix (and thus segregate) to form the rough surface, but the remaining portion of the mix, including the normal weight aggregates and fines, should remain cohesive.

3. Because of the high cement fraction in the SRC mixes, early shrinkage of the concrete mix was assessed. High volumes of fly ash used to produce SRC and reduce the early heat of hydration helped to reduce drying shrinkage in the self-roughening SRC mixes with values around 220 $\mu\varepsilon$ after 54 days.

Acknowledgements

Reference

[1] Kahn, L. F. and Mitchell, A. D. (2002), *ACI J. Struct.*, vol. 88, n.1, p.98.

[2] ACI Committee 318 (2011) Building Code Requirements for Structural Concrete, American Concrete Institute, Farmington Hills, MI, pp. 503.

[3] ASTM C33/C33M (2013) "Standard Specification for Concrete Aggregates", West Conshohocken, PA.

[4] Kahn, L.F. and Kurtis (2010), *PCI Journal*, vol. 55, n.6, p.79-96.

[5] Gajda, J. (2007) *Mass Concrete for Buildings and Bridges*, PCA, p. 34

[6] ASTM C29 (2009) *Standard Test Method for Bulk Density (Unit Weight) and Voids in Aggregate*, West Conshohocken, PA.

[7] ASTM C127 (2012) *Standard Test Method for Density, Relative Density (Specific Gravity), and Absorption of Coarse Aggregate*, West Conshohocken, PA.

[8] ASTM C150 (2012) *Standard Specification for Portland Cement*, West Conshohocken, PA.

[9] ASTM C618 (2008) *Standard Specification for Coal Fly Ash and Raw or Calcined Natural Pozzolan for Use in Concrete*, West Conshohocken, PA.

[10] ASTM C 192 *Standard Practice for Making and Curing Concrete Test Specimens in the Laboratory*, West Conshohocken, PA.

[11] ASTM C 1611/C 1611M – 05 *Standard Test Method for Slump Flow of Self-Consolidating Concrete*, West Conshohocken, PA.

[12] ASTM C39 (2005) *Standard Test Method for Compressive Strength of Cylindrical Concrete Specimens*, West Conshohocken, PA.

[13] AASHTO T160 (1997) *Length Change of Hardened Hydraulic Cement Mortar and Concrete*.

[14] Alabama DOT (2012) *Standard Specification for Highway Construction*.

[15] Leach, R., *Fundamental Principles of Engineering Nanometrology*, Elsevier Science, Amsterdam, 2010, pp. 352.

Georgia Institute of Technology

Self-Roughening Concrete with Enhance Shear Friction Capacity for Cold Joint Applications

Russell Gentry (PI)
Kimberly Kurtis (Co-PI)
Larry Kahn (Co-PI)
Giovanni Loreto (Researcher)
School of Civil and Environmental Engineering (CEE) – Georgia Institute of Technology

Monday, MAY 16, 2016 – Washington, DC
RILEM Symposium on Self-Compacting Concrete

---

1. Background and research objective

2. Development of Self-Roughening Concrete (SRC) Mix Design

3. Assessment of Cold Joint Shear Friction Capacity

4. Conclusions

Monday, MAY 16, 2016 – RILEM Symposium on Self-Compacting Concrete
Self-Roughening Concrete with Enhanced Shear Friction Capacity for Cold Joint Applications
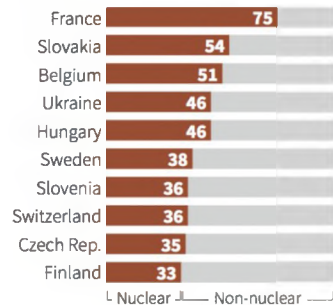
1. Intro

Let's start talking about energy…

1. Intro
Let's talk about energy

- 789 billion kWh in 2014.
- Over 19% of total U.S. electric output.
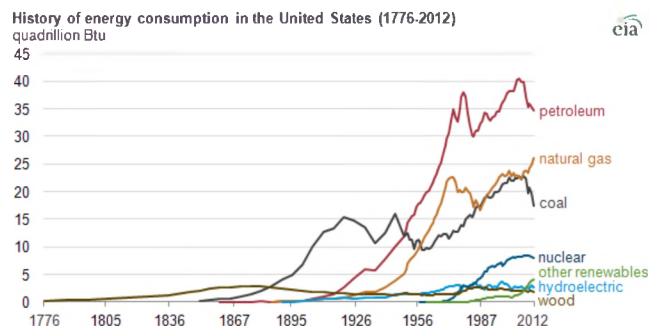
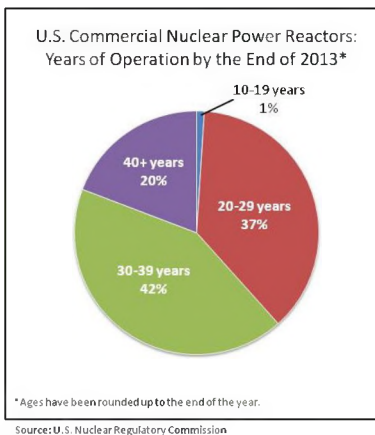History of energy consumption in the United States (1776-2012)
quadrillion Btu

Monday, MAY 16, 2016 – RILEM Symposium on Self-Compacting Concrete
Self-Roughening Concrete with Enhanced Shear Friction Capacity for Cold Joint Applications
www.eia.gov

1. Intro
Let's talk about energy

- 789 billion kWh in 2014.
- Around 20% of total U.S. electric output.
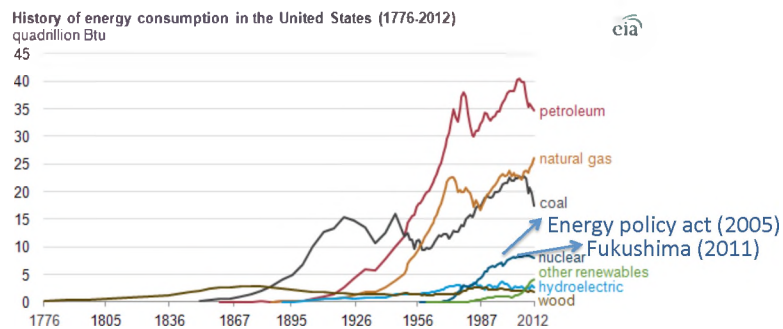
Monday, MAY 16, 2016 – RILEM Symposium on Self-Compacting Concrete
Self-Roughening Concrete with Enhanced Shear Friction Capacity for Cold Joint Applications
www.eia.gov

1. Intro
Facts and Figures

- US produces 30% of worldwide nuclear-generated electricity.
- 99 operating reactors (5 under construction).

Monday, MAY 16, 2016 – RILEM Symposium on Self-Compacting Concrete
Self-Roughening Concrete with Enhanced Shear Friction Capacity for Cold Joint Applications

1. Intro
Let's talk about energy

Nuclear power worldwide

Nuclear power plants provided 12.3 percent of the world's electricity production in 2012. A total of 13 countries relied on nuclear energy to supply at least one-quarter of their total electricity. Here are the top ten nations for:

NUCLEAR SHARE OF ELECTRICITY
In percent

Country	Percent
France	75
Slovakia	54
Belgium	51
Ukraine	46
Hungary	46
Sweden	38
Slovenia	36
Switzerland	36
Czech Rep.	35
Finland	33

└ Nuclear ┘─── Non-nuclear ───┘

NUCLEAR ELECTRICITY PRODUCTION
In terawatt hours (TWh)*

Country	TWh
U.S.	771
France	407
Russia	166
S. Korea	144
Germany	94
China	93
Canada	89
Ukraine	85
UK	64
Sweden	62

* 1 terawatt hour (TWh) =
1 billion kilowatt hours (kWh)
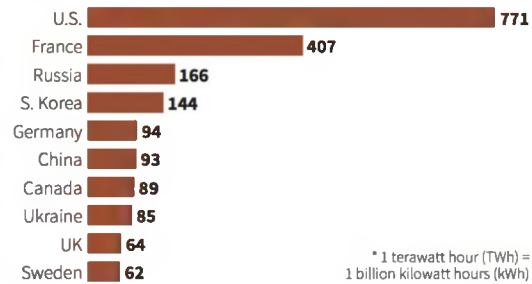
Source: World Nuclear Association

W. Foo, 09/12/2013   REUTERS

Monday, MAY 16, 2016 – RILEM Symposium on Self-Compacting Concrete
Self-Roughening Concrete with Enhanced Shear Friction Capacity for Cold Joint Applications

---

1. Intro
Facts and Figures

- U.S. nuclear energy facilities are licensed to operate for 40 years.
- Can apply for 20 year second license renewal (SLR), to extend the initial 40-year term.
- 30 year period when no new nuclear reactors came on line!

U.S. Commercial Nuclear Power Reactors:
Years of Operation by the End of 2013*

- 10-19 years 1%
- 40+ years 20%
- 20-29 years 37%
- 30-39 years 42%

*Ages have been rounded up to the end of the year.

Source: U.S. Nuclear Regulatory Commission

Monday, MAY 16, 2016 – RILEM Symposium on Self-Compacting Concrete
Self-Roughening Concrete with Enhanced Shear Friction Capacity for Cold Joint Applications

1. Intro
Facts and Figures

Need for improved construction methods!
Faster, more cost-effective and safe

1. Intro
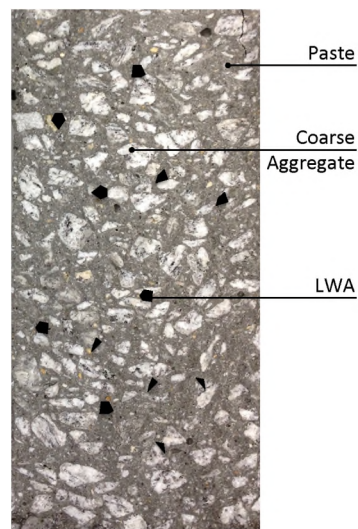Facts and Figures

Do we have a problem?

- Average time for construction for existing NPPs: 9.3 years
- Longest time for construction: 23 years
- Modern construction methods can reduce time, 5-6 years

1. Intro
Facts and Figures

- Average time for construction for existing NPPs: 9.3 years
- Longest time for construction: 23 years
- Modern construction methods can reduce time, 5-6 years

Video: Southern Company, Plant Vogtle construction, 2009-

Monday, MAY 16, 2016 – RILEM Symposium on Self-Compacting Concrete
Self-Roughening Concrete with Enhanced Shear Friction Capacity for Cold Joint Applications

Improved Construction Methods
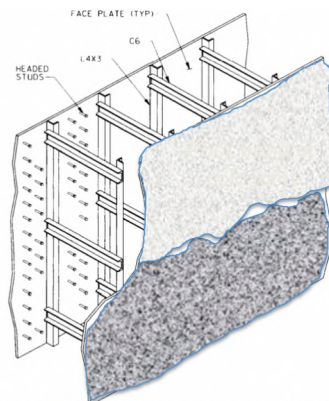
Self-Roughening Concrete with Enhanced Shear Friction Capacity for Cold Joint Applications

1. Intro
Objectives

- In third generation modular (steel composite) construction of containment structures, concrete is placed between two steel plates, tied together
- To avoid cold joints, requires *continuous concrete placement* → 1200 trucks!
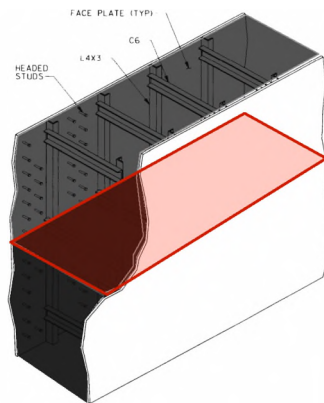
Monday, MAY 16, 2016 – RILEM Symposium on Self-Compacting Concrete
Self-Roughening Concrete with Enhanced Shear Friction Capacity for Cold Joint Applications

1. Intro
Objectives

1) Development of a self-consolidating concrete mixtures so that concrete placement can be made into steel plate composite (SC) modular structures without the need for continuous concrete placement (cold joint) .

Monday, MAY 16, 2016 – RILEM Symposium on Self-Compacting Concrete
Self-Roughening Concrete with Enhanced Shear Friction Capacity for Cold Joint Applications

1. Intro
Objectives

1) Development of a self-consolidating concrete mixtures so that concrete placement can be made into steel plate composite (SC) modular structures without the need for continuous concrete placement (cold joint) .

2) SCC mixtures to ensure sufficient shear capacity across cold- joints (self-roughening), while minimizing shrinkage and temperature increase during curing to enhance concrete bonding with the steel plates.

Monday, MAY 16, 2016 – RILEM Symposium on Self-Compacting Concrete
Self-Roughening Concrete with Enhanced Shear Friction Capacity for Cold Joint Applications

1. Intro
Objectives

Paste

Coarse
Aggregate

LWA

Monday, MAY 16, 2016 – RILEM Symposium on Self-Compacting Concrete
Self-Roughening Concrete with Enhanced Shear Friction Capacity for Cold Joint Applications

2. Development of SRC Mix Design
Strategies

2. Development of SRC Mix Design
Strategies

Mix Component	67M
Cementitious (lb/yd^3)	
Cement Type II	617
Fly Ash, Class F	459
Total Powder	*1076*
Water (lb/yd^3)	343
w/cm	*0.319*
Coarse Aggregates (lb/yd^3)	
# 67	981
# 89	305
Total Coarse	*1286*
Fine Aggregates (lb/yd^3)	
Natural sand	679
Manufactured sand	679
Total Fine	*1357*
Total Aggregates	*2796*
Admixures (fl oz./cwt)	
HRWR	0.18
TOT	4063

2. Development of SRC Mix Design
Strategies

Mix Component	67M
Cementitious (lb/yd^3)	
Cement Type II	617
Fly Ash, Class F	459
Total Powder	*1076*
Water (lb/yd^3)	343
w/cm	*0.319*
Coarse Aggregates (lb/yd^3)	
# 67	981
# 89	305
Total Coarse	*1286*
Fine Aggregates (lb/yd^3)	
Natural sand	679
Manufactured sand	679
Total Fine	*1357*
Total Aggregates	*2796*
Admixures (fl oz./cwt)	
HRWR	0.18
TOT	4063

- Cement and Fly Ash quantity
- High paste content
- Fresh properties [flowability, segregation resistant]
- Reduced heat generation

Monday, MAY 16, 2016 – RILEM Symposium on Self-Compacting Concrete
Self-Roughening Concrete with Enhanced Shear Friction Capacity for Cold Joint Applications

2. Development of SRC Mix Design
Strategies

Mix Component	67M
Cementitious (lb/yd^3)	
Cement Type II	617
Fly Ash, Class F	459
Total Powder	*1076*
Water (lb/yd^3)	343
w/cm	*0.319*
Coarse Aggregates (lb/yd^3)	
# 67	981
# 89	305
Total Coarse	*1286*
Fine Aggregates (lb/yd^3)	
Natural sand	679
Manufactured sand	679
Total Fine	*1357*
Total Aggregates	*2796*
Admixures (fl oz./cwt)	
HRWR	0.18
TOT	4063

- Cement and Fly Ash quantity
- High paste content
- Fresh properties [flowability, segregation resistant]
- Reduced heat generation

- Blend of Manufactured and Natural sands
- Improved workability

Monday, MAY 16, 2016 – RILEM Symposium on Self-Compacting Concrete
Self-Roughening Concrete with Enhanced Shear Friction Capacity for Cold Joint Applications

2. Development of SRC Mix Design
Strategies

Mix Component	67M
Cementitious (lb/yd³)	
Cement Type II	617
Fly Ash, Class F	459
Total Powder	*1076*
Water (lb/yd³)	343
w/cm	*0.319*
Coarse Aggregates (lb/yd³)	
# 67	981
# 89	305
Total Coarse	*1286*
Fine Aggregates (lb/yd³)	
Natural sand	679
Manufactured sand	679
Total Fine	*1357*
Total Aggregates	*2796*
Admixures (fl oz./cwt)	
HRWR	0.18
TOT	4063

- Cement and Fly Ash quantity
- High paste content
- Fresh properties [flowability, segregation resistant]
- Reduced heat generation

- Blend of Manufactured and Natural sands
- Improved workability

- High range water reduced (HRWR)
- Decreased w/c ratio

Monday, MAY 16, 2016 – RILEM Symposium on Self-Compacting Concrete
Self-Roughening Concrete with Enhanced Shear Friction Capacity for Cold Joint Applications

2. Development of SRC Mix Design
Strategies

Mix Component	67M
Cementitious (lb/yd³)	
Cement Type II	617
Fly Ash, Class F	459
Total Powder	*1076*
Water (lb/yd³)	343
w/cm	*0.319*
Coarse Aggregates (lb/yd³)	
# 67	981
# 89	305
Total Coarse	*1286*
Fine Aggregates (lb/yd³)	
Natural sand	679
Manufactured sand	679
Total Fine	*1357*
Total Aggregates	*2796*
Admixures (fl oz./cwt)	
HRWR	0.18
TOT	4063

- Cement and Fly Ash quantity
- High paste content
- Fresh properties [flowability, segregation resistant]
- Reduced heat generation

- Smaller aggregates and controlled gradation curve
- Use of #67 and #89 coarse aggregates
- Substitute 5%, 10% and 15% in volume of coarse aggregate with LWA

- Blend of Manufactured and Natural sands
- Improved workability

- High range water reduced (HRWR)
- Decreased w/c ratio

Monday, MAY 16, 2016 – RILEM Symposium on Self-Compacting Concrete
Self-Roughening Concrete with Enhanced Shear Friction Capacity for Cold Joint Applications

2. Development of SRC Mix Design
Proprieties and tests

Self-Consolidating Concrete   Self-Roughening Concrete

Fresh SCC proprieties
- Flowability: flows easily at suitable speed into formwork (T20 = 4-5sec; Flow Slump = 24-26")
- S Groove test (good self-healing ability)
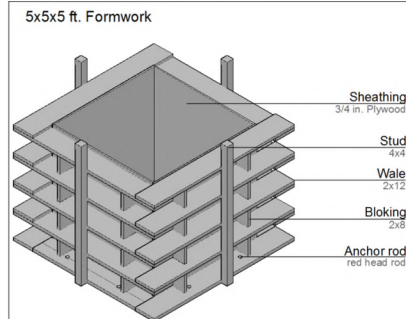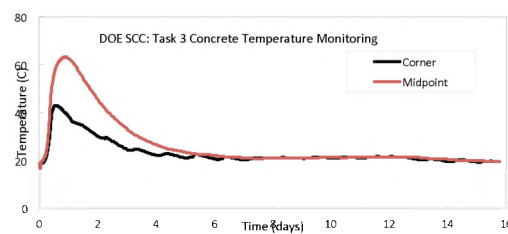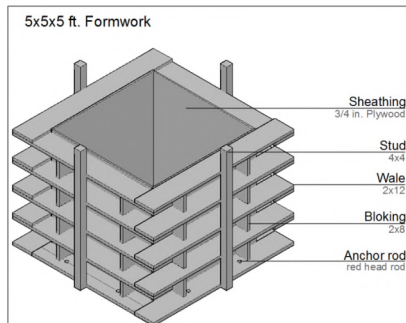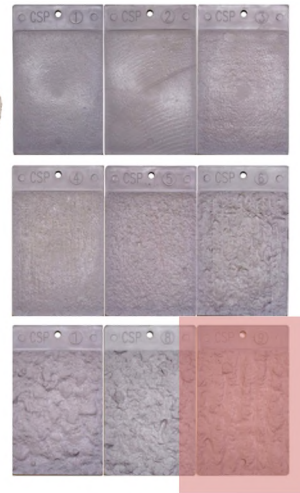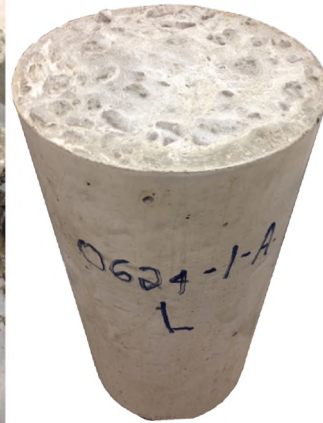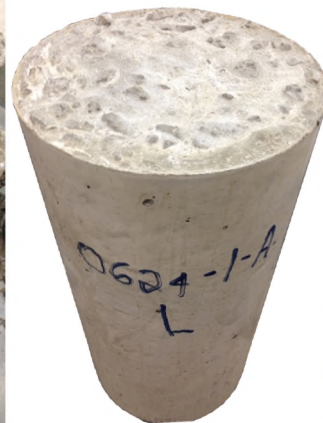- Hardened Visual Stability Index (VSI = 0)

Hardened SRC proprieties
- Compressive strength: 6-7ksi
- Shrinkage: <250 $\mu\varepsilon$

Monday, MAY 16, 2016 – RILEM Symposium on Self-Compacting Concrete
Self-Roughening Concrete with Enhanced Shear Friction Capacity for Cold Joint Applications

2. Development of SRC Mix Design
Measurements of Roughness - Qualitative

Monday, MAY 16, 2016 – RILEM Symposium on Self-Compacting Concrete
Self-Roughening Concrete with Enhanced Shear Friction Capacity for Cold Joint Applications

2. Development of SRC Mix Design
Measurements of Roughness - Quantitative

Monday, MAY 16, 2016 – RILEM Symposium on Self-Compacting Concrete
Self-Roughening Concrete with Enhanced Shear Friction Capacity for Cold Joint Applications

14

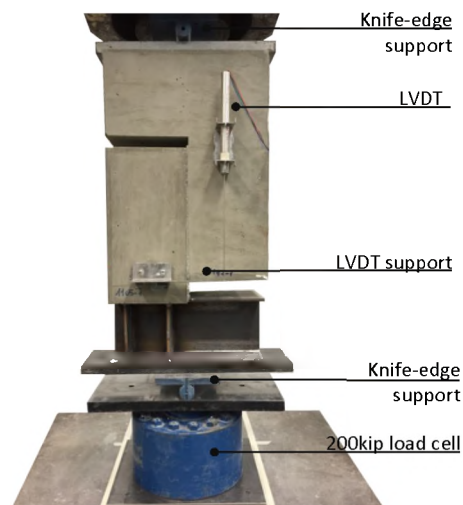## 3. Assessment of Cold Joint Shear Friction Capacity
Mechanical tests for shear friction characterization

ACI 318-11 (11.6.9):

"…when concrete is placed against previously hardened concrete, the interface for shear transfer shall be clean and free of laitance. If μ is assumed equal … interface shall be roughened to a full amplitude of approximately 1/4 in."

Wall Elevation

Formwork

Hot rolled structural steel channels

Cold Joint

Wall Section

Monday, MAY 16, 2016 – RILEM Symposium on Self-Compacting Concrete
Self-Roughening Concrete with Enhanced Shear Friction Capacity for Cold Joint Applications
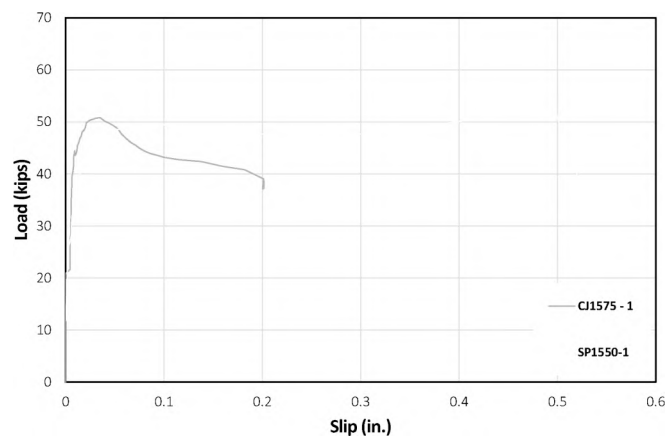

3. Assessment of Cold Joint Shear Friction Capacity
Mechanical tests for shear friction characterization

Formwork

Hot rolled structural steel channels
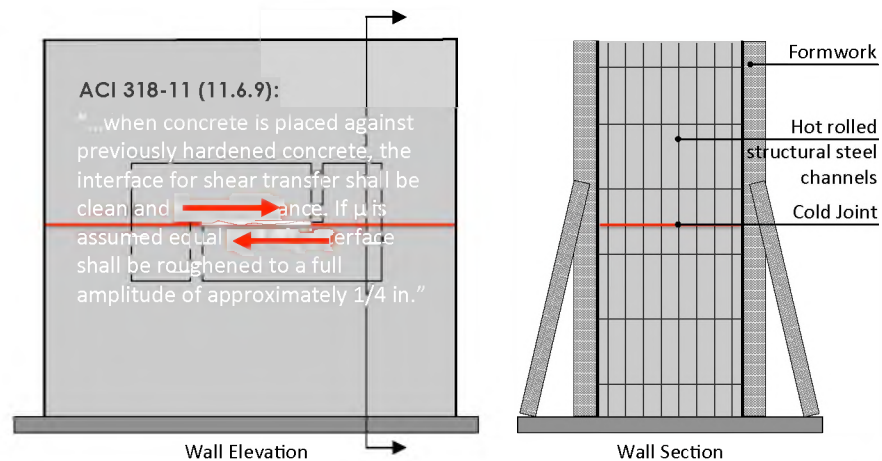
Cold Joint

Wall Section

Cold Joint
When wet concrete is cast up to dry concrete.

Monday, MAY 16, 2016 – RILEM Symposium on Self-Compacting Concrete
Self-Roughening Concrete with Enhanced Shear Friction Capacity for Cold Joint Applications
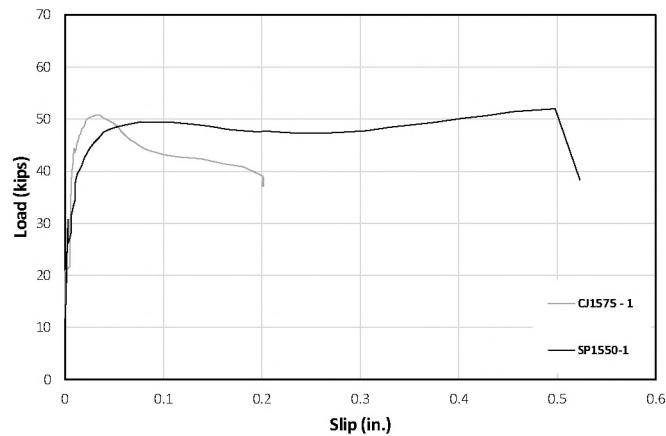
3. Assessment of Cold Joint Shear Friction Capacity
Mechanical tests for shear friction characterization

Step 1 Step 2 Step 3 Step 4 Step 5

Monday, MAY 16, 2016 – RILEM Symposium on Self-Compacting Concrete
Self-Roughening Concrete with Enhanced Shear Friction Capacity for Cold Joint Applications

3. Assessment of Cold Joint Shear Friction Capacity
Mechanical tests for shear friction characterization

Knife-edge support
LVDT
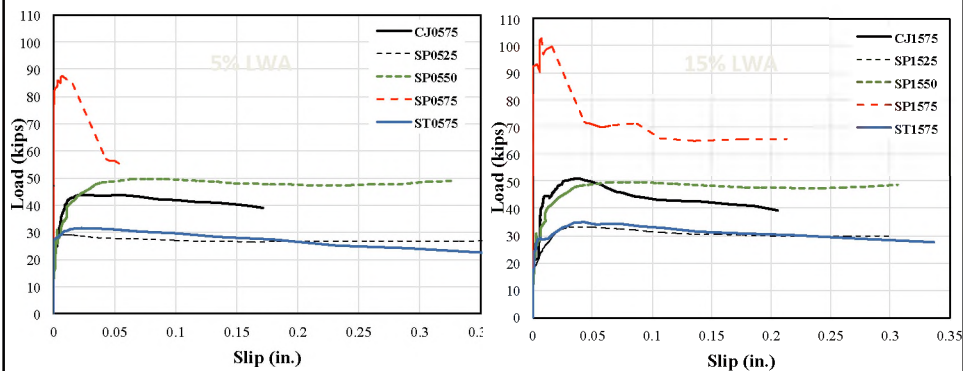LVDT support
Knife-edge support
200kip load cell
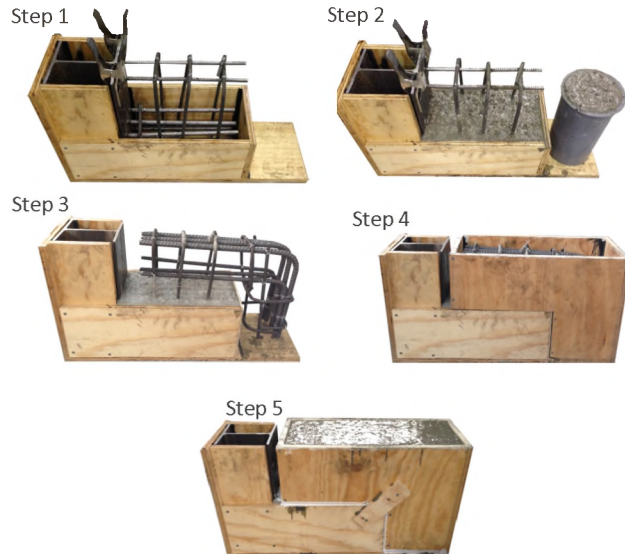
Monday, MAY 16, 2016 – RILEM Symposium on Self-Compacting Concrete
Self-Roughening Concrete with Enhanced Shear Friction Capacity for Cold Joint Applications

3. Assessment of Cold Joint Shear Friction Capacity
Mechanical tests for shear friction characterization

Monday, MAY 16, 2016 – RILEM Symposium on Self-Compacting Concrete
Self-Roughening Concrete with Enhanced Shear Friction Capacity for Cold Joint Applications

3. Assessment of Cold Joint Shear Friction Capacity
Behavior at cold joint with internal reinforcement

Monday, MAY 16, 2016 – RILEM Symposium on Self-Compacting Concrete
Self-Roughening Concrete with Enhanced Shear Friction Capacity for Cold Joint Applications

3. Assessment of Cold Joint Shear Friction Capacity
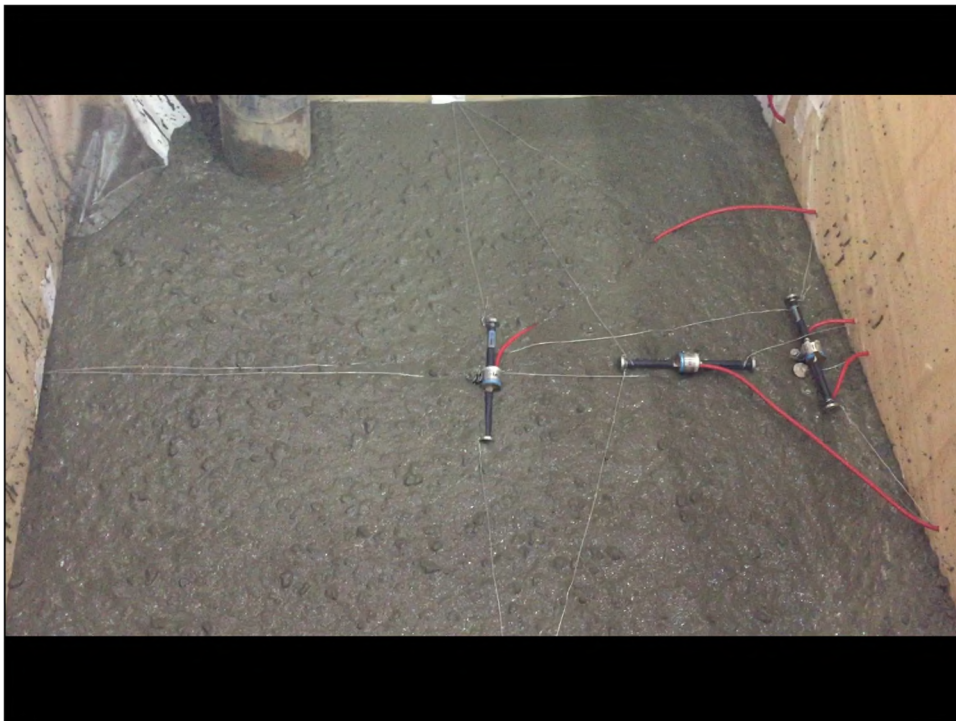Behavior at cold joint comparing internal and external reinforcement.

Monday, MAY 16, 2016 – RILEM Symposium on Self-Compacting Concrete
Self-Roughening Concrete with Enhanced Shear Friction Capacity for Cold Joint Applications

3. Assessment of Cold Joint Shear Friction Capacity
Behavior at cold joint comparing internal and external reinforcement.

- Self-roughening concrete carries higher load.
- Higher load with greater fraction of LWA.

Monday, MAY 16, 2016 – RILEM Symposium on Self-Compacting Concrete
Self-Roughening Concrete with Enhanced Shear Friction Capacity for Cold Joint Applications

4. Conclusions
And future developments

Concluding…

4. Conclusions
Behavior at cold joint comparing internal and external reinforcement.

- Validation through full-scale testing and modeling
- Considering in-plane and out-of-plane loading

Monday, MAY 16, 2016 – RILEM Symposium on Self-Compacting Concrete
Self-Roughening Concrete with Enhanced Shear Friction Capacity for Cold Joint Applications

19

4. Conclusions

Behavior at cold joint comparing internal and external reinforcement.

Monday, MAY 16, 2016 – RILEM Symposium on Self-Compacting Concrete

Self-Roughening Concrete with Enhanced Shear Friction Capacity for Cold Joint Applications

4. Conclusions
And future developments

- SCC which self-roughens has been developed by replacing small fraction of coarse with lightweight aggregate (LWA) → avoids need for continuous placement
- Achieve improved shear friction capacity, which scales with LWA fraction.
- Additional testing and modeling ongoing
- Meet strength and shrinkage targets, but further assessments on durability and safety needed.

Monday, MAY 16, 2016 – RILEM Symposium on Self-Compacting Concrete
Self-Roughening Concrete with Enhanced Shear Friction Capacity for Cold Joint Applications

Thank you. Questions?